

# **In vitro studies on inflammatory potential of biomaterials with development of anti-inflammatory strategies**

## **Dissertation**

zur Erlangung des  
Doktorgrades der Naturwissenschaften (Dr. rer. nat.)

der  
Naturwissenschaftlichen Fakultät I – Biowissenschaften –

der Martin-Luther-Universität  
Halle-Wittenberg,

vorgelegt

von Frau M.Sc. Guoying Zhou  
geboren am 19.01.1987 in Zibo, China

Gutachter: Prof. Dr. Thomas Groth  
Prof. Dr. Viktoria Weber  
Prof. Dr. Lea Ann Dailey

Tag der öffentlichen Verteidigung: 10.05.2017

To my family

---

**INDEX**

<b>Abbreviations .....</b>	<b>V</b>
<b>Abstract .....</b>	<b>1</b>
<b>Zusammenfassung.....</b>	<b>4</b>
<b>Overview of the thesis .....</b>	<b>6</b>
<b>1 Host responses to implants and the design of anti-inflammatory biomaterials – a review .....</b>	<b>12</b>
1.1 Abstract .....	12
1.2 Introduction.....	12
1.3 Host responses to implants.....	13
1.3.1 Protein adsorption, coagulation and complement activation .....	13
1.3.2 Acute inflammation and role of leukocytes.....	15
1.3.3 Chronic inflammation and foreign body giant cell (FBGC) formation.....	16
1.3.4 Fibrotic encapsulation and fibrosis.....	17
1.4 Cell-based models to investigate host responses to biomaterials .....	18
1.4.1 Inflammatory models based on monocytic cell lines .....	18
1.4.2 Macrophage/fibroblast co-culture models to study host responses .....	19
1.5 Anti-inflammatory strategies .....	21
1.5.1 Modification of the physiochemical properties of biomaterials.....	22
1.5.2 Incorporation of anti-inflammatory agents to biomaterials .....	24
1.6 Summary and future prospects.....	28
1.7 Disclosure.....	29
1.8 Acknowledgements.....	29
1.9 References .....	29
<b>2 A macrophage/fibroblast co-culture system using a cell migration chamber to study inflammatory effects of biomaterials .....</b>	<b>44</b>
2.1 Abstract .....	44
2.2 Introduction.....	45
2.3 Materials and methods.....	47
2.3.1 Preparation of self-assembled monolayers (SAMs) .....	47
2.3.2 Characterization of surface properties of SAMs .....	48
2.3.3 Cell experiments.....	49
2.3.4 Statistics.....	53
2.4 Results and discussion .....	53

---

2.4.1	Surface properties of SAMs .....	53
2.4.2	Adhesion and fusion of macrophages.....	55
2.4.3	Release of pro-inflammatory cytokines .....	59
2.4.4	Macrophage migration studies.....	62
2.5	Conclusion.....	64
2.6	Disclosure.....	65
2.7	Acknowledgements.....	65
2.8	Appendix. Supplementary data.....	65
2.9	References .....	65
<b>3</b>	<b>A fibroblast/macrophage co-culture system to study host responses of model biomaterials .....</b>	<b>73</b>
3.1	Abstract .....	73
3.2	Introduction.....	74
3.3	Materials and Methods.....	76
3.3.1	Preparation of self-assembling monolayers (SAMs) .....	76
3.3.2	Characterization of surface properties of SAMs.....	76
3.3.3	Cell experiments.....	77
3.3.4	Statistics.....	81
3.4	Results and discussion .....	82
3.4.1	Surface properties of SAMs.....	82
3.4.2	HF adhesion, spreading and proliferation .....	83
3.4.3	HF outgrowth studies.....	85
3.4.4	Macrophage fusion studies.....	87
3.4.5	Pro- and anti-inflammatory cytokine production .....	88
3.4.6	ED-A FN and $\alpha$ -SMA expression .....	90
3.5	Conclusion.....	94
3.6	Disclosure.....	95
3.7	Acknowledgement .....	95
3.8	References .....	95
<b>4</b>	<b>Reducing the inflammatory responses of biomaterials by surface modification with glycosaminoglycan multilayers .....</b>	<b>101</b>
4.1	Abstract .....	101
4.2	Introduction.....	102
4.3	Materials and Methods.....	103
4.3.1	Preparation of polyelectrolyte multilayers (PEMs).....	103

---

4.3.2	Characterization of multilayer formation and surface properties.....	104
4.3.3	Cell experiments.....	105
4.3.4	Statistics.....	108
4.4	Results.....	108
4.4.1	Characterization of multilayer formation and surface properties.....	108
4.4.2	Adhesion and fusion of macrophages.....	111
4.4.3	IL-1 $\beta$ cytokine production.....	116
4.5	Discussion.....	117
4.6	Conclusions.....	120
4.7	Disclosure.....	120
4.8	Acknowledgements.....	120
4.9	References.....	121
<b>5</b>	<b>Covalent immobilization of glycosaminoglycans to reduce the inflammatory effects of biomaterials.....</b>	<b>125</b>
5.1	Abstract.....	125
5.2	Introduction.....	126
5.3	Materials and Methods.....	127
5.3.1	Materials.....	127
5.3.2	Preparation of GAGs-modified surfaces.....	128
5.3.3	Characterization of GAGs-modified surfaces.....	128
5.3.4	Cell experiments.....	129
5.3.5	Statistics.....	131
5.4	Results and Discussion.....	132
5.4.1	Characterization of GAGs-modified surfaces.....	132
5.4.2	Adhesion and fusion of macrophages.....	133
5.4.3	IL-1 $\beta$ cytokine production.....	138
5.5	Conclusions.....	141
5.6	Acknowledgements.....	141
5.7	Disclosures.....	141
5.8	References.....	142
<b>6</b>	<b>Summary and outlook.....</b>	<b>145</b>
	<b>List of tables and figures.....</b>	<b>i</b>
	<b>Acknowledgment.....</b>	<b>viii</b>
	<b>Publication list with declaration of self-contribution to research articles.....</b>	<b>x</b>

<b>Curriculum vitae .....</b>	<b>.xiv</b>
<b>Selbstständigkeitserklärung.....</b>	<b>xv</b>

**Abbreviations**

AAS	antibiotic–antimycotic solution
ANOVA	analysis of variance
APTES	3-aminopropyltriethoxysilane
BSA	bovine serum albumin
Chi	chitosan
CLSM	confocal laser scanning microscopy
COL	collagen
CS	chondroitin sulfate
DEX	dexamethasone
DMEM	Dulbecco's modified Eagle's medium
ECM	extracellular matrix
EDC	1-ethyl-3-(3-dimethylaminopropyl) carbodiimide
ELISA	enzyme-linked immunosorbent assay
FBGC	foreign body giant cell
FBR	foreign body response
FBS	fetal bovine serum
FN	fibronectin
FXII	factor XII
GAGs	glycosaminoglycans
GPTMS	glycidoxypropyl trimethoxysilane
HA	hyaluronic acid
HDF	human dermal fibroblasts
Hep	heparin
HF <sub>s</sub>	human fibroblasts
HMW	high molecular weight

---

Hyals	hyaluronidases
IBD	inflammatory bowel disease
IEP	isoelectric point
IL-1 $\beta$	interleukin-1 $\beta$
IL-6	interleukin-6
LBL	layer-by-layer
LMW	low molecular weight
LPS	lipopolysaccharide
MCP-1	monocyte chemoattractant protein-1
MES	2-(N-morpholino)ethanesulfonic acid monohydrate
MIP-1	macrophage-inflammatory protein-1
MMP	matrix metalloproteinase
MUDA	mercaptoundecanoic acid
NF- $\kappa$ B	nuclear factor- $\kappa$ B
NHS	N-hydroxysuccinimide
NSL	nanosphere lithography
ODS	chlorodimethyloctadecylsilane
PEI	poly (ethylene imine)
PEG	polyethylene glycol
PEMs	polyelectrolyte multilayers
PFA	paraformaldehyde
pHEMA	poly(2-hydroxyethyl methacrylate)
PMA	phorbol-12-myristate-13-acetate
PDGF	platelet-derived growth factor
PVDF	polyvinylidene fluoride
PZC	point of zero charge
RFU	relative fluorescence unit
RI	refractive index



---

ROS	reactive oxygen species
RT	room temperature
SAMs	self-assembling monolayers
SD	standard deviations
SPR	surface plasmon resonance
TESPSA	triethoxysilylpropyl succinic anhydride
TF	tissue factor
TGF- $\beta$	transforming growth factor- $\beta$
TLR	toll-like receptor
TNF- $\alpha$	tumour necrosis factor- $\alpha$
VEGF	vascular endothelial growth factor
WCA	water contact angle
$\alpha$ -MSH	alpha melanocyte-stimulating hormone
$\alpha$ -SMA	alpha-smooth muscle actin

## Abstract

Host responses towards implanted biomaterials, in particular chronic inflammation and fibrotic encapsulation, are major hindrances to the functionality and longevity of many implanted biomedical devices. To gain more knowledge about the biomaterial-induced host responses, studies are carried out here with a newly developed *in vitro* macrophage/fibroblast co-culture model to investigate the pro-inflammatory and pro-fibrotic potentials of model biomaterials. The co-culture system is established using a cell migration fence chamber possessing an internal and an external compartment to generate separated and mixed co-cultures before and after removal of the chamber, respectively. The novelty of the system is that it allows not only to mimic autocrine, paracrine and juxtacrine signal exchange in one and the same system, but also to study macrophage migration and fibroblast outgrowth in the presence of the other cell type in a timely and locally controlled manner. Self-assembling monolayers (SAMs) of alkylsilanes on glass substrates with terminal methyl (CH<sub>3</sub>), amine (NH<sub>2</sub>), hydroxyl (OH), and carboxyl (COOH) groups are used here as model surfaces focusing on macrophage as well as fibroblast responses in the co-culture system. The inflammatory reactions on the different SAMs are investigated regarding macrophage adhesion and migration, foreign body giant cell (FBGC) formation,  $\beta$ 1 integrin expression and pro-inflammatory cytokine production in the presence of fibroblasts, while the fibrotic responses are studied in terms of fibroblast attachment, spreading, proliferation, outgrowth, fibroblast to myofibroblast differentiation as well as anti-inflammatory cytokine production within the co-culture system. The results indicate that hydrophobic CH<sub>3</sub> surfaces possess the highest potential of inducing inflammatory responses but evoke only low levels of fibrotic reactions. In contrast, hydrophilic/anionic COOH surfaces result in low levels of both inflammatory and fibrotic responses. In addition, macrophage migration regarding motility and directional movement increase in the presence of fibroblasts, while fibroblast outgrowth on different SAMs is promoted significantly in the presence of macrophages. The obtained relations between surface functionality and host responses are further used for the development of anti-inflammatory strategies. Based on these findings, the second part of the thesis aims to develop anti-inflammatory strategies using glycosaminoglycans (GAGs), which are also hydrophilic and anionic macromolecules due to the presence of carboxyl and/or sulfate groups. In addition, GAGs bind to a wide range of chemokines, cytokines, growth factors as well as enzymes, and thus can modulate events associated with inflammation.

Therefore, three kinds of GAGs, namely hyaluronic acid (HA), chondroitin sulfate (CS), and heparin (Hep) are immobilized here to model material surfaces to reduce the inflammatory responses. They are either physically adsorbed on a primary poly (ethylene imine) (PEI) layer alternately with chitosan (Chi) as multilayers by the layer-by-layer (LBL) technique or covalently immobilized to amino-functionalized substrata via 1-ethyl-3-(3-dimethylaminopropyl) carbodiimide (EDC)/N-hydroxysuccinimide (NHS) cross-linking chemistry. The anti-inflammatory properties of the GAG-modified surfaces are studied focusing on macrophage activation. Here, macrophage adhesion, spreading, fusion, and pro-inflammatory cytokine production are all significantly decreased on each GAG-modified surface at both immobilization techniques in comparison to their respective controls. However, as demonstrated the type of GAGs plays a pivotal role in modulating the inflammation in multilayers, with the Hep-Chi system showing the highest anti-inflammatory potential. The physical adsorption of GAGs during LBL technique probably allows the uptake of Hep molecules by macrophages, which could lead to a reduction of NF- $\kappa$ B nuclear translocation and thus further lowers inflammatory responses. Overall, this thesis not only presents a newly developed, multifunctional co-culture system to elucidate the relation between surface functionality and host responses, but also provides useful clues for future developments of implant materials with anti-inflammatory properties.



## Zusammenfassung

Gewebereaktionen gegenüber implantierten Biomaterialien, insbesondere chronische Entzündungen und fibrotischen Verkapselungen, sind wesentliche Hindernisse für die Funktionalität und Langlebigkeit vieler implantierter biomedizinische Geräte. Um mehr Wissen über Biomaterial-induzierte Wirtsreaktionen zu gewinnen, werden in dieser Arbeit Untersuchungen mit einem neu entwickelten In-vitro-Makrophagen/Fibroblasten-Co-Kultur-Modell durchgeführt, um das Entzündungs-hervorrufende und fibrotische Potenzial von Modellmaterialien zu untersuchen. Das vorgestellte Co-Kultursystem wird über eine Zellmigrationsschranke realisiert, welche die Kulturfläche in eine innere und äußere Kammer separiert und somit getrennte und gemischte Co-Kulturen vor beziehungsweise nach dem Entfernen der Schranke erzeugt. Die Neuheit des Systems besteht darin, nicht nur autokrinen, parakrinen und juxtakrinen Signalaustausch in ein und demselben System zu ermöglichen, sondern auch die Makrophagen-Migration wie auch das Herauswachsen von Fibroblasten in Anwesenheit des jeweils anderen Zelltyps zeitlich und lokal gesteuert zu studieren. Selbstorganisierende Monolagen (SAMs) von Alkylsilanen auf Glassubstraten mit endständigen Methyl- ( $\text{CH}_3$ ), Amino- ( $\text{NH}_2$ ), Hydroxyl- ( $\text{OH}$ ) und Carboxyl- ( $\text{COOH}$ ) -Gruppen dienen hier als Modelloberflächen, um auf die Wechselwirkung von Makrophagen und Fibroblasten im Co-Kultursystem zu fokussieren. Die Entzündungsreaktionen auf den verschiedenen SAMs werden hierbei bezüglich Makrophagenadhäsion und -migration, Fremdkörper-Riesenzell- (FBGC) -Bildung,  $\beta$ 1-Integrin-Expression sowie entzündliche Zytokinproduktion in Gegenwart von Fibroblasten untersucht, während die fibrotischen Reaktionen in Bezug auf Fibroblastenadhäsion, -spreitung, -wachstum, das Herauswachsen aus der Migrationsschranke, die Differenzierung zu Myofibroblasten sowie die entzündungs-hemmende Zytokinproduktion betrachtet werden. Die Ergebnisse zeigen, dass hydrophobe Methyl-Oberflächen das höchste Potential für Entzündungsreaktionen besitzen, aber nur geringe fibrotische Reaktionen hervorrufen. Im Gegensatz dazu führen hydrophile/anionische Carboxyl-Oberflächen nur zu geringen entzündlichen und fibrotischen Reaktionen. Zusätzlich ist die Makrophagenmigration bezüglich Motilität und gerichteter Bewegung in Gegenwart von Fibroblasten erhöht, während das Herauswachsen von Fibroblasten auf den verschiedenen SAMs in Gegenwart von Makrophagen signifikant gefördert wird. Die hier gefundenen Zusammenhänge zwischen Oberflächenfunktionalität und Wirtsreaktionen werden daher für die Entwicklung von weiteren

entzündungshemmenden Strategien verwendet. Auf Basis jener Erkenntnisse konzentriert sich der zweite Teil der Arbeit auf die Verwendung von Glykosaminoglykanen (GAGs), ebenfalls hydrophile und anionische Makromoleküle aufgrund der Anwesenheit von Carboxyl- und/ oder Sulfatgruppen, zur Entwicklung entzündungshemmender Strategien. GAGs können zudem eine Vielzahl von Chemokinen, Zytokinen, Wachstumsfaktoren, sowie Enzyme binden, und hierdurch mit einer Entzündung assoziierte Ereignisse steuern. In dieser Arbeit werden drei Arten von GAGs, Hyaluronsäure (HA), Chondroitinsulfat (CS) und Heparin (Hep), auf Modelloberflächen immobilisiert, um entzündliche Reaktionen zu reduzieren. Sie werden entweder auf einer primären Polyethylenimin- (PEI) -Schicht abwechselnd mit Chitosan (Chi) in Mehrfachsichten durch die Layer-by-Layer- (LBL) -Technik adsorbiert oder kovalent an amino-funktionalisierte Oberflächen über 1-Ethyl-3-(3-dimethylaminopropyl) carbodiimid (EDC)/N-Hydroxysuccinimid (NHS) -Vernetzung gebunden. Die entzündungshemmenden Eigenschaften der GAG-modifizierten Oberflächen fokussieren dabei auf die Makrophagenaktivierung. Hierbei sind Makrophagenadhäsion, -spreitung, -fusion und die entzündliche Zytokinproduktion auf jeder GAG-modifizierten Oberfläche bei beiden Immobilisierungstechniken im Vergleich zu ihren jeweiligen Kontrollen signifikant verringert. Jedoch spielt die Art der GAGs innerhalb der Mehrfachsichten eine zentrale Rolle bei der Entzündungsreaktion, wobei das Hep-Chi-System das höchste entzündungs-hemmende Potential zeigt. Die physikalische Adsorption von GAGs mit der LBL-Technik ermöglicht wahrscheinlich die Aufnahme von Hep-Moleküle durch Makrophagen, was zu einer Verringerung der NF- $\kappa$ B nukleären Translokation führt, was wiederum weitere Entzündungsreaktionen reduziert. Insgesamt stellt diese Arbeit nicht nur ein neu entwickeltes, multifunktionales Co-Kultursystem vor, um die Beziehung zwischen Oberflächenfunktionalität und Wirtsreaktionen aufzuklären, sondern bietet auch nützliche Hinweise für die zukünftige Entwicklung von Implantatmaterialien mit entzündungshemmenden Eigenschaften.

## Overview of the thesis

This cumulative thesis consists of five papers. Out of the five papers, three are published, one is submitted to Biomaterials Science and is currently under revision while the introductory paper is to be submitted to Journal of bioactive and compatible polymers.

The first manuscript is a review which is used as a general introduction to biomaterial-induced host responses and a summary of anti-inflammatory approaches. Firstly, the main issues associated with the host responses towards biomaterial implantation including protein adsorption, leukocyte activation, acute and chronic inflammation as well as the final fibrotic encapsulation and fibrosis were lined out. Thereafter, the recent developments in understanding inflammatory and fibrotic responses with different *in vitro* and *in vivo* cell-based models were summarized. Finally, we outlined the development of several anti-inflammatory strategies, such as the modification of physicochemical surface properties of materials and by incorporation of anti-inflammatory reagents to biomaterials.

The remaining four experimental papers are assembled as chapters 2-5. In the first study (chapter 2), a new macrophage/fibroblast co-culture model was developed to investigate the pro-inflammatory potential of model biomaterials with a focus on macrophage activities, using self-assembling monolayers (SAMs) with terminal methyl (CH<sub>3</sub>), amine (NH<sub>2</sub>), hydroxyl (OH) and carboxyl (COOH) groups as model surfaces. It was indicated that the hydrophobic CH<sub>3</sub> and the hydrophilic/anionic COOH SAMs possessed the highest and lowest potential to induce inflammatory responses, respectively. Furthermore, the co-culture system showed multi-functional properties containing the ability to establish mono-cultures, separated and mixed co-cultures orderly in one and the same model, but also the allowance to study single macrophage migration and fibroblast outgrowth in the presence of the other cell type. In the second study (chapter 3), the chamber-generated fibroblast/macrophage co-culture model as well as the same SAMs were used to study the pro-fibrotic potential of the model materials with a focus on fibroblast activities. The results showed that the hydrophobic CH<sub>3</sub> SAMs possessing the highest potential of inducing inflammatory responses, however a low level of fibrotic responses was observed. By contrast, the hydrophilic/anionic COOH SAMs caused low levels of both inflammatory and fibrotic responses. Therefore, based on the findings that the hydrophilic/anionic groups-functionalized surfaces have the best pro-inflammatory and pro-fibrotic capabilities, the hydrophilic/anionic glycosaminoglycans (GAGs) were immobilized

on model material surfaces in the third (chapter 4) and fourth study (chapter 5) in order to reduce the inflammatory responses of biomaterials. In the third study (chapter 4), three different types of GAGs - hyaluronic acid (HA), chondroitin sulfate (CS), and heparin (Hep), as well as chitosan (Chi) were deposited alternatively on glass substrata to generate polyelectrolyte multilayers (PEMs) through layer-by-layer (LBL) technique. In the fourth study (chapter 5), the same GAGs were covalently immobilized on amino-functionalized substrata by 1-ethyl-3-(3-dimethylaminopropyl) carbodiimide (EDC)/N-hydroxysuccinimide (NHS) crosslinking chemistry. The influence of GAG immobilization on the inflammatory responses by both the two techniques were evaluated in terms of macrophage activation in a mono-culture system, since macrophages are of major importance to inflammatory reactions and before we apply the co-culture system we wanted to learn about the behaviour of macrophages and fibroblasts as single fraction. The results showed that all inflammatory reactions were significantly decreased on GAG-modified surfaces at both covalent immobilized and LBL techniques. However, it was also demonstrated a pivotal role of the type of GAGs in modulating inflammation on GAG-modified surfaces by LBL technique, with Hep-based multilayers showing the best potential in reducing all inflammatory responses. Following are more detailed summaries of the four experimental papers containing the different purposes and the achieved results of each study.

**Summary of Chapter 2 - A macrophage/fibroblast co-culture system using a cell migration chamber to study inflammatory effects of biomaterials:**

The first study was aimed to develop a novel predictive *in vitro* macrophage/fibroblast co-culture model to evaluate the inflammatory potential of implants using model biomaterials, to detect how material surface properties affect the inflammatory responses in the co-culture system. In view of this objective, co-cultures were established using a cell migration fence chamber having an internal and an external channel to establish separated and mixed co-cultures before and after removal of the chamber, respectively. A series of self-assembling monolayers (SAMs) with terminal methyl (CH<sub>3</sub>), amine (NH<sub>2</sub>), hydroxyl (OH) and carboxyl (COOH) groups were prepared by chemisorption of alkylsilanes onto glass surfaces. The physical properties of the SAMs were characterized by water contact angle (WCA) and zeta potential measurements. The results showed that the functionalized SAM surfaces displayed different wetting and surface charge properties, which represent useful models for studying the effect of biomaterial surface properties and functional groups on the inflammatory responses. THP-1 cells were utilized here as a model monocyte and differentiated into



macrophage-like cells by treatment with phorbol-12-myristate-13-acetate (PMA). Subsequently, the inflammatory reactions on different SAMs were investigated in the presence of fibroblasts regarding macrophage adhesion, macrophage migration, foreign body giant cell (FBGC) formation,  $\beta$ 1 integrin expression and pro-inflammatory cytokine production. It was found that all the inflammatory reactions consistently showing the hydrophobic  $\text{CH}_3$  and the hydrophilic/anionic  $\text{COOH}$  SAMs possessed the highest and lowest potential to induce inflammatory responses, indicating low and high biocompatibility of the surfaces, respectively. Furthermore, the macrophage migration results revealed that both macrophage motility and directional movement were increased in the presence of fibroblasts in co-cultures compared to their corresponding mono-cultures. This illustrates one advantage of our co-culture system for allowance the investigation of single cell movement in the presence of the other cell type in a locally controlled manner. Moreover, the presented co-culture system can allow the mimic of autocrine, paracrine and juxtacrine signal exchange in a timely controlled manner between the two cell types during biomaterial contact in one and the same system. Thereupon, a synergistic action was observed by the enhanced release of interleukin-6 (IL-6) production in lipopolysaccharide (LPS)-stimulated macrophage/fibroblast co-cultures, compared to the arithmetic sum of IL-6 release from the corresponding mono-cultures. Overall, the novel macrophage/fibroblast co-culture system can provide a wider range of parameters for testing the inflammatory potential of implants, and shows how biomaterial surface properties can affect the inflammatory responses.

**Summary of Chapter 3 - In vitro study of the host responses to model biomaterials via a fibroblast/macrophage co-culture system:**

In continuation of the previous study that investigated the effects of biomaterial surface properties on the inflammatory responses of macrophages, this work focused on influence of surface chemistry and functional groups on the fibrotic responses with an emphasis on fibroblast activities by using the fence chamber-established fibroblast/macrophage co-culture system, as well as the self-assembling monolayers (SAMs) with terminal methyl ( $\text{CH}_3$ ), amine ( $\text{NH}_2$ ), hydroxyl ( $\text{OH}$ ) and carboxyl ( $\text{COOH}$ ) groups as model biomaterials. The cell migration fence chamber has an internal and an external compartment, which allowed the seeding of fibroblasts and macrophages separately on model biomaterials at the beginning. After 24h-incubation, the fence chambers were removed to allow the exchange of soluble signals such as cytokines, chemokines and growth factors, and at the same time for fibroblast outgrowth, macrophage migration and dynamic interaction between the two cell types. The

fibrotic reactions on different functional group modified-SAMs were then studied with respect to fibroblast attachment, spreading morphology, fibroblast proliferation, outgrowth, as well as pro- (Interleukin-6) and anti- (Interleukin-10) inflammatory cytokine production and expression of two markers for myofibroblasts, namely ED-A fibronectin (FN) and alpha-smooth muscle actin ( $\alpha$ -SMA). The results showed that the hydrophilic/anionic COOH SAMs caused both low levels of inflammatory and fibrotic responses. While, the hydrophobic CH<sub>3</sub> surfaces possessing the highest potential of inducing inflammatory responses, a low level of fibrotic responses was observed. By contrast, the OH SAMs which evoked a low extent of pro-inflammatory responses, revealed a high potential of inducing fibrotic responses. This might reveal that the extent of inflammatory and fibrotic responses is not always consistent. Finally, it was found that macrophages contributed significantly for facilitating fibrotic responses by up-regulation of fibroblast outgrowth, cytokine production as well as ED-A FN and  $\alpha$ -SMA expression. Taken together, the study of surface property effects on fibrotic responses by using the presented fibroblasts/macrophages co-culture model can provide useful clues for the design of biomaterials with triggering appropriate host responses for different biomedical and clinical applications.

***Summary of Chapter 4 - Reducing the inflammatory responses of biomaterials by surface modification with glycosaminoglycan multilayers:***

Glycosaminoglycans (GAGs) are reported to have great anti-inflammatory potential due to their binding of a wide range of chemokines, cytokines, growth factors and enzymes to modulate events associated with inflammation. Hence, the present study was designed to reduce the inflammatory responses to biomaterials by incorporation of three different types of GAGs, namely hyaluronic acid (HA), chondroitin sulfate (CS), and heparin (Hep). Layer-by-layer (LBL) technique, based on the alternate adsorption of oppositely charged molecules onto charged surfaces, was used here to assemble polyelectrolyte multilayers (PEMs) composed of GAGs as polyanion and chitosan (Chi) as polycation on glass surfaces. Physicochemical studies were performed to follow the multilayer formation as well as the resulting surface properties. The exponential growth regimes observed by surface plasmon resonance (SPR) measurements and the resulting water contact angle (WCA) oscillation confirmed the multilayer build-up with alternating deposition of GAGs and Chi layers. In addition, WCA and zeta potential measurements showed significant increases in wettability and negative charges after multilayer deposition, which can be accounted for the abundant negative charges of the GAGs due to the presence of carboxyl and/or sulfate groups.

Subsequently, macrophages resulting from phorbol 12-myristate 13-acetate (PMA)-induced differentiation of human THP-1 monocytic cell line were used here to investigate the anti-inflammatory potential of the GAG-Chi multilayers. The macrophage adhesion and foreign body giant cell (FBGC) formation were visualized by Giemsa staining. The macrophage spreading morphology and  $\beta 1$  integrin expression were determined by immunofluorescence staining. Finally, the release of pro-inflammatory cytokine interleukin-1 $\beta$  (IL-1 $\beta$ ) was examined by enzyme-linked immunosorbent assay (ELISA) measurements. The results showed that all the inflammatory responses were greatly reduced by GAG-Chi multilayers deposition compared to the primary poly (ethylene imine) (PEI) layer, which was used as a stimulatory and pro-inflammatory model surface. Moreover, the type of terminal GAGs played pivotal roles in resisting inflammatory responses to different extent. It was found the Hep-Chi multilayers hindered all the inflammatory responses to a much larger extent compared to HA-Chi and CS-Chi multilayer systems. This might be partly due to the highest wettability and most negatively charged properties of the Hep-Chi multilayers. In addition, the physical adsorption here might allow the uptake of Hep molecules by macrophages, which led to a reduction of NF- $\kappa$ B nuclear translocation, and thus further lowered the inflammatory responses. Therefore, the GAG-Chi multilayers, in particular the Hep-based systems, provide promising applications as anti-inflammatory coatings for biomaterials, to reduce the inflammatory responses.

***Summary of Chapter 5 - Covalent immobilization of glycosaminoglycans to reduce the inflammatory effects of biomaterials:***

In this publication, three different types of glycosaminoglycans (GAGs) - hyaluronic acid (HA), chondroitin sulfate (CS), and heparin (Hep) were covalently immobilized on amino-functionalized substrata by 1-ethyl-3-(3-dimethylaminopropyl) carbodiimide (EDC)/N-hydroxysuccinimide (NHS) crosslinking chemistry for anti-inflammatory targeting. The successful immobilization of GAGs onto the amino-terminated surfaces was confirmed by water contact angle (WCA) and zeta potential measurements, showing significant decrease in water contact angles and zeta potentials on all GAGs-modified surfaces. Among the different GAGs, Hep-modified surface showed the highest wettability and lowest zeta potential, which originate from its high content of sulfate monoesters and sulfamido groups. The inflammatory reactions evoked by the different GAG-modified surfaces were characterized with respect to THP-1-derived macrophage adhesion, spreading, foreign body giant cell (FBGC) formation,  $\beta 1$  integrin expression as well as pro-inflammatory cytokine interleukin-1 $\beta$  (IL-1 $\beta$ ) production.

As a result, all inflammatory responses were significantly decreased on GAGs-modified surfaces in comparison to the initial amino-terminated surface. This can be attributed to both the physiochemical properties of the GAGs-modified surfaces and the physiologic roles of GAGs in regulation of inflammation. Among the distinct GAGs, HA-modified surface expressed a slightly higher reduction of initial macrophage adhesion and spreading compared to CS- and Hep-modified surfaces, possibly due to the higher hydrophilicity and some steric effects of HA compared to CS and Hep. However, no significant differences were found regarding FBGC formation,  $\beta$ 1 integrin expression and IL-1 $\beta$  production among the different types of GAGs. Compared to the previous study where the GAGs were immobilized by layer-by-layer (LbL) technique, we provided here another way for immobilization of GAGs on biomaterial surfaces, namely covalent immobilization approach, which is supposed to be more stable resulting from the chemical bonding vs. physical adsorption. Thereupon, both of the two studies demonstrate the remarkable inflammatory-inhibiting effects of GAGs. Since the two immobilization techniques have their own advantages, we believe that a combination of them, including a first covalently anchored layer and then add-on layers by LbL approach, could provide more promising strategies for long-term *in vivo* applications to reduce adverse biomaterial-induced inflammatory responses.

# 1 Host responses to implants and the design of anti-inflammatory biomaterials – a review

Guoying Zhou, Thomas Groth\*

## 1.1 Abstract

Host responses towards foreign implants that lead to chronic inflammation and fibrosis, may result in failure of implantation. To solve these problems, there are two aspects needed to be addressed. First, an intensive understanding of the biomaterial-induced host reactions including protein adsorption, leukocyte activation, inflammatory and fibrotic responses to biomaterials is required. Second, a better design of biomaterial surfaces to trigger appropriate host responses, causing less inflammatory response and supporting healing process, serves as a promising strategy for improving the implant performance. Based on these clues, the review provides a brief overview of the host responses to implants, as well as the up-to-date findings on inflammatory and fibrotic responses to biomaterials by using various cell-based models. Moreover, the review highlights some anti-inflammatory strategies to improve the biocompatibility of implants, which contain the modification of physicochemical surface properties of materials as well as by incorporation of anti-inflammatory reagents to biomaterials.

**Keywords:** host responses, inflammation, fibrosis, macrophages, foreign body giant cells, fibroblasts, glycosaminoglycans

## 1.2 Introduction

Implantation of biomaterials is intended to diagnose, replace or improve the biological function of the host tissue [1], which is widely used nowadays in a variety of medical applications including glucose biosensors [2], heart valves [3], cardiac pacemakers [4], different implants [5, 6], stents [7], catheters [8] and so on. Nevertheless, all materials introduced to the human body may trigger a series of undesired host responses,

encompassing injury, blood-material interactions, acute inflammation, chronic inflammation, granulation tissue development, foreign body reaction (FBR), and fibrous capsulation [9]. These negative consequences may lead finally to the failure of implantation, largely limiting the functionality and longevity of the biomaterial [10]. Therefore, it is of great importance to gain more fundamental knowledge on the biological responses to biomaterials particularly those elicited by the immune system, but also to be able to design biomaterials with anti-inflammatory properties, which trigger desired tissue responses.

This short review presents a brief background on the host responses induced upon the implantation of biomaterials and summarizes the recent developments in understanding inflammatory and fibrotic responses with distinct *in vitro* and *in vivo* cell-based models. In addition, we outline the development of several anti-inflammatory strategies to generate more biocompatible implants for various medical and tissue engineering applications.

### **1.3 Host responses to implants**

The injury induced by surgical procedure of implantation always initiates a cascade of host responses, starting with protein adsorption and complement activation, and followed by an acute inflammatory phase with neutrophil and monocyte recruitment, which may develop into chronic inflammation and fibrotic encapsulation [11]. The extent and duration of these responses rely on several aspects, such as the injury caused by trauma and surgery, the type of tissue or organ implanted with the biomaterial, the size and surface properties of the implanted biomaterial and so on [9]. The following sections outline the main issues associated with the host responses towards biomaterial implantation and are lined out in some detail in Figure 1.1.

#### **1.3.1 Protein adsorption, coagulation and complement activation**

Upon implantation, host serum proteins like albumin, fibrinogen, fibronectin, immune globulins, vitronectin, and others adsorb immediately onto the biomaterial surfaces (Figure 1.1) [12]. It was documented that the composition of these adsorbed protein layer as well as their conformational changes are related to the activation of coagulation and complement cascade, resulting in the onset of the inflammatory responses [13-15].

Blood coagulation includes the involvement of a cascade of proteolytic reactions leading ultimately to the formation of a fibrin clot [16]. The coagulation cascade possesses two pathways, namely the intrinsic and extrinsic pathway with factor XII (FXII) and tissue factor (TF) as initiators, respectively [17]. Many researchers have reported that biomaterial-induced coagulation is initiated through the intrinsic pathway [18-20]. It was suggested that the adsorbed protein layer on the biomaterial surfaces may act as the negatively charged circumstance necessary for the activation of FXII, and thus initiate the activation of the intrinsic cascade [16]. It was also demonstrated that biomaterials with negatively charged surfaces can promote more the FXII activation by imposing specific arrangements of FXII, kallikrein and high molecular weight kininogen on the surfaces, which represent major components of the intrinsic system [21]. Despite of the important role of FXII activation in coagulation, it was found that the generated thrombin due to FXII activation is limited and cannot induce clot formation, suggesting that contact activation alone is not sufficient for activation of the whole coagulation cascades [22]. Indeed, it has been demonstrated that biomaterial-associated blood coagulation requires the combination of contact activation, platelet adhesion and activation as well as the presence of leukocytes [23, 24].

The complement system consists of a number of proteins that function either as enzymes or binding proteins, which play important roles in host defenses against infection and foreign substances [25]. There are three biochemical pathways that activate the complement system, namely the classical pathway, the alternative pathway, and the lectin pathway [26]. It has been well documented that the complement system can be activated upon contact with biomaterials and the activation is triggered predominantly via the alternative pathway [27, 28]. Furthermore, biomaterials with different surface properties are reported to have distinct complement-activating properties [29]. For instance, biomaterial surfaces with free OH and NH<sub>2</sub> groups are thought to activate the complement system to a larger extent than others like COOH groups due to their essential roles for the covalent binding of complement factor C3b [30]. On the other hand, the complement activation is supposed to be associated with the adsorbed protein layer on biomaterials [31]. The attached proteins such as IgG can promote activation of the classical C3 convertase, resulting in the generation of C3b that binds to the protein layer to generate more C3 convertase [32]. This will lead to the launch of the amplified alternative complement pathway and the onset of the inflammatory responses [16]. Additionally, it should be noted that complement activation can promote platelet activation, which in turn contributes to the coagulation cascades [23, 32]. Thus, the

orchestration of the biomaterial-induced coagulation, complement and platelet activation dictates the following inflammatory cascades.

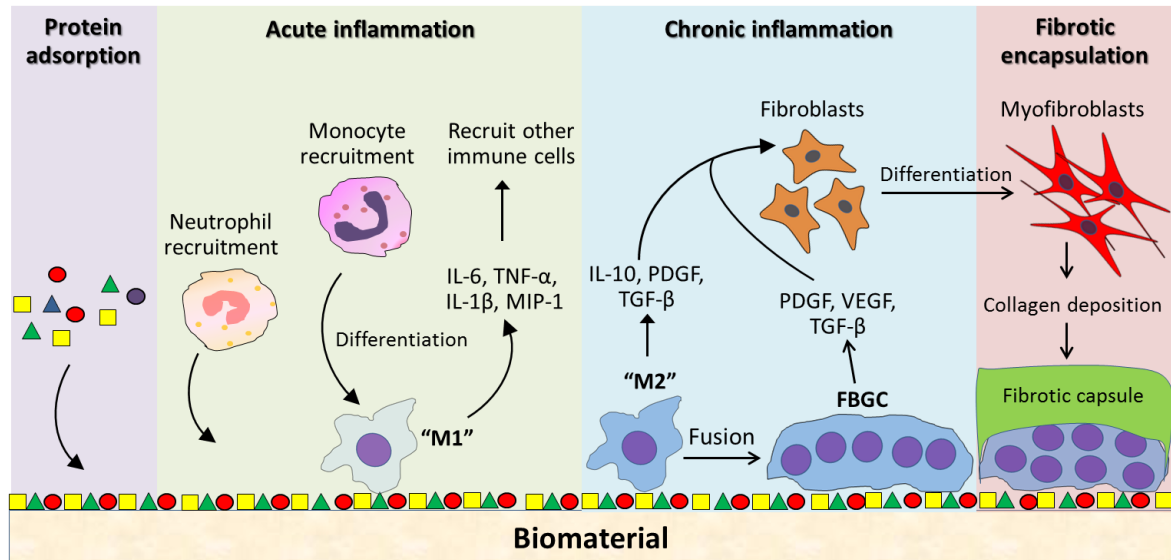


Figure 1.1. Host responses to implanted biomaterials. Serum proteins adsorb onto the biomaterial surface immediately upon implantation. Leukocytes including neutrophils and monocytes are firstly recruited to the implant site, where monocytes differentiate into a "M1" phenotypic macrophages during acute inflammation. During the later chronic inflammatory stage, macrophages polarize towards the "M2" phenotype with pro-healing capacities, but also can fuse to form foreign body giant cells (FBGCs) in order to increase the phagocytic ability. Acting on the pro-fibrotic factors released from the "M2" macrophages and FBGCs, fibroblasts are activated to proliferate, as well as differentiated into myofibroblasts resulting in collagen deposition. Finally, a thick fibrotic capsule is formed around the biomaterial, leading to failure of implantation.

### 1.3.2 Acute inflammation and role of leukocytes

Immediately following injury upon implantation, leukocytes, predominantly neutrophils migrate to the wound site and exudation of fluid occurs, which are the typical characteristics of the acute inflammation (Figure 1.1) [33]. The recruitment and accumulation of neutrophils to implant site are directed by chemoattractants released from activation of complement factors C3 and C5, the formed thrombus, activated platelets, and injured cells [34, 35]. The major role of neutrophils in acute inflammation is acting as the first responders of inflammatory cells to



defend against invading pathogens such as bacteria [36]. However, the neutrophils have very short lifespans of hours to days and then disappear from the exudate, quitting the scene of acute inflammation [37]. At the same time also circulating monocytes are attracted by the released chemotactic agents and migrate to the injured tissues where they differentiate into the so-called classically activated or “M1” macrophages (Figure 1.1) [38, 39]. The M1 phenotypic macrophages can promote inflammatory responses by secreting various pro-inflammatory cytokines and chemokines such as interleukin (IL)-1, IL-6, tumor necrosis factor (TNF)- $\alpha$ , IL-8 and macrophage-inflammatory protein-1 (MIP-1) [40, 41]. These mediators can attribute to additional leukocyte recruitment to the injury area, in an attempt to increase the antimicrobial and phagocytic abilities [42]. However, contrary to microorganism, most of the implanted biomaterials are too large to be engulfed by leukocytes [43]. Thereby the adherent neutrophils and macrophages undergo “frustrated” phagocytosis by releasing potent oxygen and nitrogen radicals, but also proteolytic enzymes in an attempt to degrade the biomaterial [44, 45]. It should be noted that this effect can damage the tissue seriously, because healthy cells in the neighborhood are also getting damaged and even destroyed, which can result in necrosis of tissues [46, 47]. In contrast to neutrophils, macrophages have much longer lifetimes of days to weeks to months and become eventually the predominant cell type in both acute and chronic inflammation, but also during the following wound healing or fibrotic responses [48].

### **1.3.3 Chronic inflammation and foreign body giant cell (FBGC) formation**

Continuous inflammatory stimuli caused by the implantation of biomaterials can give rise to the development of chronic inflammation [49, 50]. This might be caused by the physiochemical properties of the implanted biomaterial, but also the non-sufficient compliance or movement of the biomaterial at the implantation site [10]. Monocyte-derived macrophages are the master regulators of biomaterial-associated chronic inflammation [51]. Apart from their ability to secrete a variety of pro-inflammatory factors like cytokines, chemokines, reactive oxygen species (ROS) and degradative enzymes, single macrophages can coalesce to form foreign body giant cells (FBGCs) in an attempt to increase their phagocytic or degradative capacities (Figure 1.1) [52]. FBGC formation is the hallmark of biomaterial-induced chronic inflammation and subsequent foreign body reaction (FBR) [10]. IL-4 and IL-13 have been considered as the main inducers of FBGC formation on implanted biomaterials [53, 54]. It has been discovered that the surface properties of the biomaterials play important roles during

macrophage fusion [55]. It was found that the surface physicochemical properties dictate the adsorption of proteins like IgG, complement factors and others on the biomaterial surface, which then mediate macrophage adhesion and fusion [56]. It has also been reported that  $\beta 1$  and  $\beta 2$  integrins are important mediators during macrophage adhesion and fusion [57]. Further, it is evident that  $\beta 2$  integrins mediate mainly the initial monocyte adhesion by interactions with a diversity of ligands including fragments of complement C3, fibrinogen, Factor X, and high-molecular weight kininogen [58], while  $\beta 1$  integrins are dominating during macrophage development from monocytes and are strongly expressed in fusing macrophages and FBGCs [59, 60]. Although the mechanism of macrophage fusion into FBGCs on biomaterials is complicated and not completely understood yet, it has been assumed that macrophage fusion might depend on both adhesion density and migration motility [61]. Namely, a certain adhesion density on the surfaces is required to have enough cells for fusion, and on the other hand, the attached macrophages need a moderate motility to migrate to meet each other and then fuse [62].

#### **1.3.4 Fibrotic encapsulation and fibrosis**

The final stage of host responses to implanted biomaterials is normally a fibrous encapsulation or fibrosis, which is orchestrated by the dynamic interactions between macrophages and fibroblasts (Figure 1.1) [63]. During the later stage of healing, macrophages normally polarize towards an alternatively activated or “M2” phenotype by producing pro-fibrotic factors such as platelet-derived growth factor (PDGF) and transforming growth factor- $\beta 1$  (TGF- $\beta 1$ ) to stimulate fibroblasts to proliferate and synthesize collagens and thereby promote wound healing [51, 64]. Additionally, FBGCs are also reported to release PDGF, vascular endothelial growth factor (VEGF) and TGF- $\beta 1$  to activate fibroblasts [65]. Thereupon, activated fibroblasts can be differentiated into myofibroblasts, accompanied by extensive expression of  $\alpha$ -smooth muscle actin ( $\alpha$ -SMA) which can be incorporated into stress fibres and produce contractile forces to promote wound healing, but also scar formation [66]. During normal wound healing, the myofibroblasts are lost by apoptosis or return to a quiescent state and stop releasing collagen after the damaged tissue has been reconstituted [67, 68]. However, a prolonged presence of myofibroblasts due to continuous stimulation from the inflammatory environment will give rise to excessive collagen production and tissue contraction, which will result eventually in fibrosis and scarring [69]. In the case of implantation, fibrous capsules are formed around the biomaterials, in an attempt to isolate the

implant from the host tissues [70]. As a result, the functionality and longevity of many implanted artificial organs [71] and devices such as drug delivery devices [72], various biosensors [73, 74] and tissue-engineering scaffolds [75] are largely impaired.

## **1.4 Cell-based models to investigate host responses to biomaterials**

Since the biomaterials-induced chronic inflammation and fibrotic encapsulation are supposed to be the main reasons leading to implant failure, extensive efforts have been focused on the study of inflammatory and fibrotic responses to various biomaterials by using different *in vitro* and *in vivo* -based models, which have been reviewed by others in much more detail elsewhere [76-80]. We will focus here on example of *in vitro* models.

### **1.4.1 Inflammatory models based on monocytic cell lines**

Due to the crucial roles of monocytes/macrophages involved in the inflammatory responses to foreign materials, different cellular models based on monocytic cell lines are commonly employed to study the mechanistic aspects of acute and chronic inflammation, but also used for testing the pro-inflammatory potential of various biomaterials [61, 77, 81]. Among the several monocytic cell lines, the human leukemic THP-1 cell line cultured from the blood of a one-year-old boy with acute monocytic leukemia has been widely utilized as model monocyte systems [82-84]. In comparison to native human monocytes, the THP-1 cell line has the advantages of uniform genetic background with no donor variation, but also can be more easily obtained from cultures than monocytes isolated from blood [81, 82]. In addition, the THP-1 cells can be induced to differentiate into macrophage-like cells to mimic the monocytes-derived macrophages under the stimulation of phorbol-12-myristate-13-acetate (PMA) [85], but also vitamin D3 [86, 87], retinoic acid [88], or cytokines like TNF- $\alpha$  and interferon (IFN) [89]. Thereupon, the THP-1-derived macrophages can behave either as “M1” phenotype after being exposed to lipopolysaccharides (LPS) and IFN- $\gamma$ , or act as “M2” phenotype in response to Th2 cytokines, such as IL-4 and IL-13 [90]. Hence, the THP-1-derived macrophages provide a valuable model for studying both inflammatory and fibrotic responses to biomaterials [91].

### 1.4.2 Macrophage/fibroblast co-culture models to study host responses

*In vitro* cell models that apply only one cell type can identify only limited inflammatory information due to the lack of synergistic interplay of different cell types [92]. Therefore, cell co-culture systems involving two or more cell types have been employed to mimic more accurately the complexity of the *in vivo* inflammatory situation [93-95]. Because of the essential roles of macrophages and fibroblasts involved in both inflammatory and the final fibrotic reactions, different *in vitro* macrophage/fibroblast co-culture models have been used to study the host responses to biomaterials [96, 97]. Co-cultures of macrophages and fibroblasts were traditionally generated by randomly seeding of the two cell types on the substrates. For example, Pan et al. used a mixed macrophage/fibroblast co-culture system to examine the biocompatibility and the potential to induce inflammatory responses of the electrospun Dextran/PLGA scaffold [93]. These mixed co-cultures allow the study of immediate homotypic and heterotypic cell-cell contact interactions, but cannot mimic the *in vivo* situation with temporal sequence of arrival and spatial arrangement of the two cell types at the implant surface [98]. Another study carried out by Damanik et al. used conditioned medium from one cell type to challenge the other one [99], leading to the lack of in-situ, direct and continuing exchange of soluble signals by paracrine activity. Alternatively, membranes were applied to separate the two different cell types spatially, permitting only the exchange of soluble signaling molecules [94], but no direct cell-cell contact even at later stages, which cannot mimic the complexity of the *in vivo* situations either. To overcome the limitation of the previous models, a novel macrophage/fibroblast co-culture model was developed recently to perform mono-culture, separate and mixed co-cultures in sequence with one and the same system, which should mimic much better the *in vivo* situation [80]. In this model, a cell migration fence chamber that possesses an internal and an external compartment was utilized for seeding the two cell types separately on the substrates at the beginning, which can mimic the corresponding mono-cultures. After the cells were attached, the chambers were removed and a gap of around 500  $\mu\text{m}$  was generated between the two cell populations, allowing the outgrowth and migration of the two cell types towards each other and at the same time exchange of soluble signals between the two cell types, but without immediate direct macrophage-fibroblast contact. At a later stage, the two cell populations are mixed and intertwined, which can thereby mimic the *in vivo* situation with both exchange of soluble signals but also direct cell-cell contacts. By using this novel co-culture model, it is not only able to mimic autocrine, paracrine and juxtacrine signal exchange, but also to study macrophage migration and fibroblast outgrowth in the presence of the other cell type in a

timely and locally controlled manner. Moreover, the co-culture system possesses potent values to study the *in vitro* effects of additional factors like cytokines and other bioactive molecules on the interplay between the two cell types. Therefore, this model system can contribute to a better understanding of the complexity of the *in vivo* inflammatory processes, but also can provide more useful information for the design of novel biomaterials with low pro-inflammatory potential. Figure 1.2 summarized the advantages and disadvantages of the four types of macrophage/fibroblast co-culture systems.

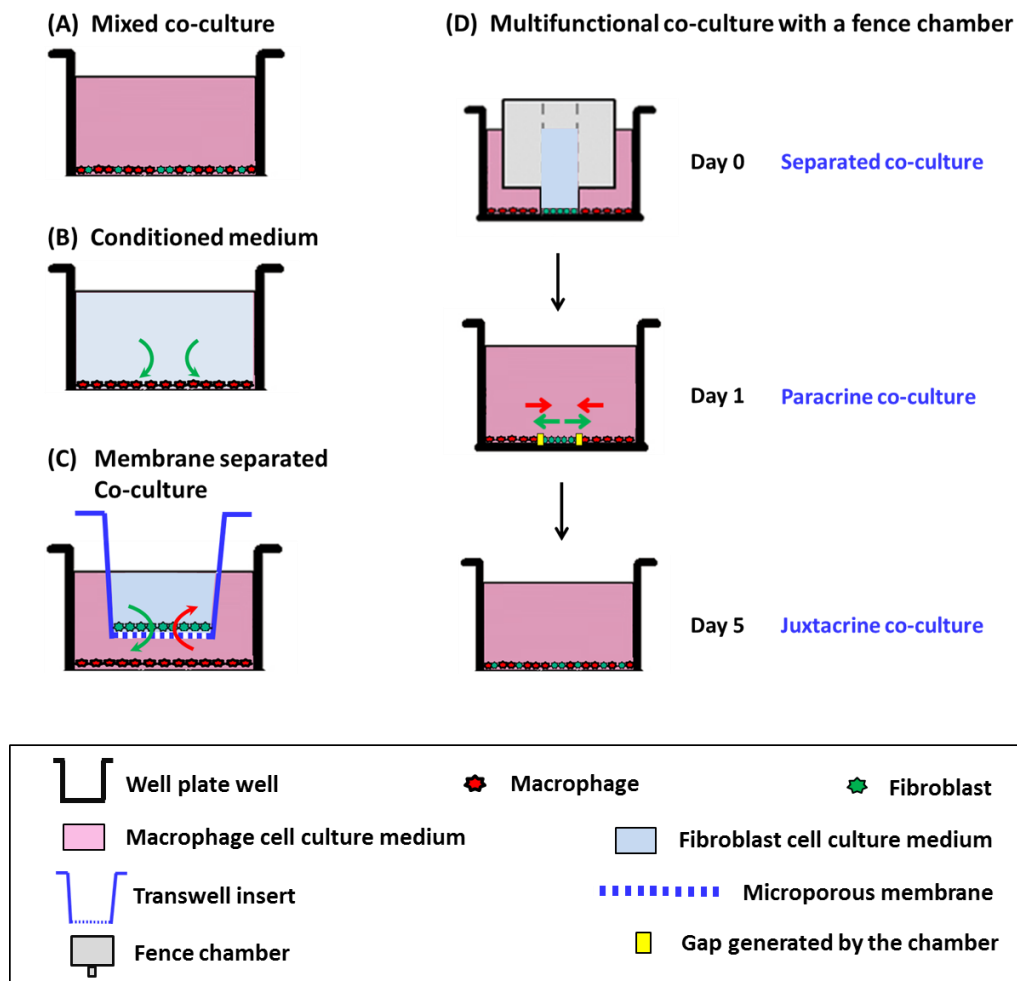


Figure 1.2. Schematic representations of the four types of macrophage/fibroblast co-culture systems. (A) Mixed co-cultures with immediate cell-cell contact. (B) Conditioned medium from fibroblast culture was used to challenge macrophages, but signaling feedback between the two cell types was missed. (C) Membrane separated co-culture with signaling feedback but without cell-cell contact even at later stages. (D) Multifunctional co-culture system using cell

migration fence chambers to mimic separated, paracrine and juxtacrine co-cultures in sequence within one and the same system [80].

## 1.5 Anti-inflammatory strategies

Through many years of research, it has been recognized that the development of strategies to avoid or minimize the adverse biomaterial-induced inflammatory responses to modulate the immune responses for effective biomaterial integration, represents an important direction in the biomaterial field. Recently, significant advances have been achieved in developing various anti-inflammatory strategies. These include both physical and chemical modification of the biomaterials, delivery of anti-inflammatory agents, as well as immunomodulation approaches using bioactive molecules that can directly or indirectly modulate the activity of components of the immune system (Figure 1.3).

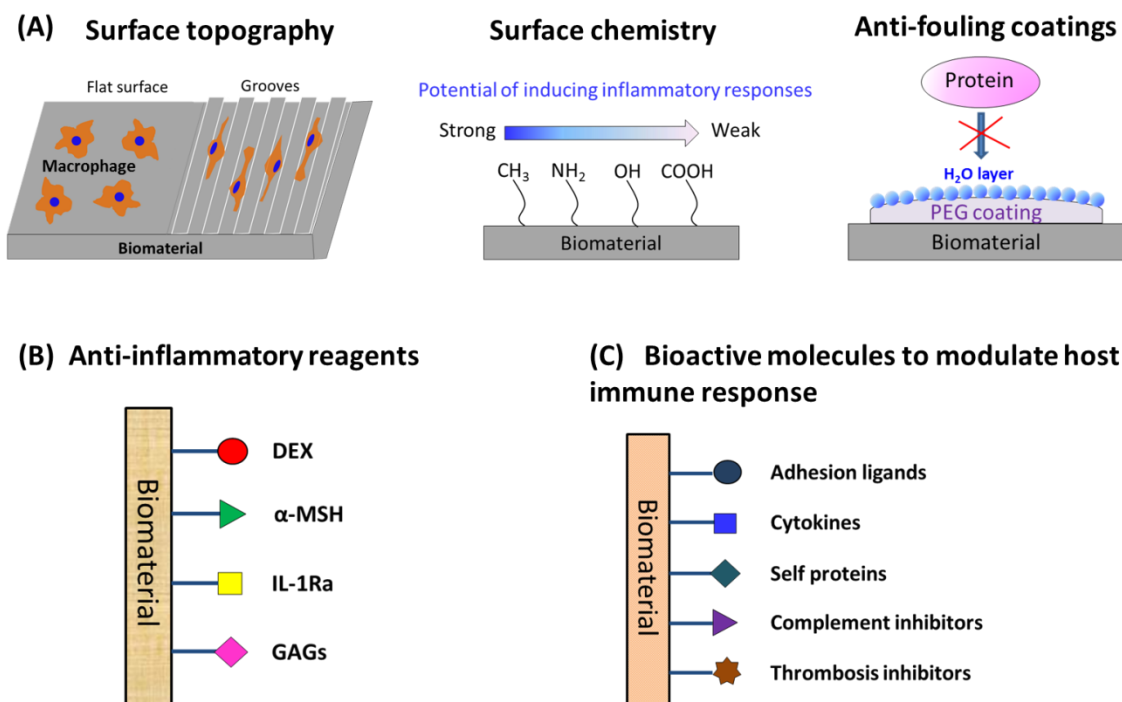


Figure 1.3. Schematic representation of different anti-inflammatory strategies. (A) Physical and chemical modification of the biomaterials by alteration of surface topography, surface chemistry as well as anti-fouling coatings; (B) Incorporation of anti-inflammatory agents to biomaterials; (C) Immunomodulation approaches using bioactive molecules that can directly or indirectly modulate the host immune system. PEG - polyethylene glycol; DEX -

dexamethasone;  $\alpha$ -MSH - alpha melanocyte-stimulating hormone; IL-1Ra - interleukin-1 receptor antagonists; GAGs - glycosaminoglycans.

### 1.5.1 Modification of the physiochemical properties of biomaterials

As it has been lined out in more detail in section 2.1, the physiochemical properties of biomaterials including surface topography, wettability, charge density and surface chemistry play crucial roles in protein adsorption and subsequent cellular behavior. Therefore, adjustment of the surface physiochemical properties of the implanted biomaterials has been explored as an effective approach to generate more biocompatible biomaterials with causing less inflammatory responses.

Physical approaches to alter the surface topography and roughness have been shown to effectively modulate the immune cell behavior [100, 101] (Figure 1.3A). It was found substantial macrophage elongation and align along the grooves with 10  $\mu\text{m}$ -wide and 0.5  $\mu\text{m}$ -deep on poly(methyl methacrylate), compared to flat substrates [78]. The idea of these approaches stems from the natural structure of the extracellular matrix (ECM), where the cells interact with the environment at micro- or nano-meter scale [102]. It has been previously observed by Wójciak-Stothard et al. that microgrooved substrata have a substantial effect on stimulating macrophage spreading, elongation and motile activity [103]. Using different polyvinylidene fluoride (PVDF) surfaces including nanotextured and microstructured surfaces, Paul and colleagues studied the influence of surface topography on the inflammatory response of human macrophages, showing that microstructured, but not nanotextured surfaces significantly affected the macrophage activation by inducing a specific cytokine and gene expression pattern [104]. Similarly, Leong et al. used parallel gratings with 250 nm to 2  $\mu\text{m}$  line width to study the topographical effects on macrophage behavior in a FBR model and found that the topographical cues do affect macrophage morphology and cytokine secretion *in vitro*, as well as macrophage adhesion *in vivo* especially on larger size topography compared to planar controls [78]. Another study carried out by Liu et al. suggested that micropatterned substrates with different wide lines led to different macrophage responses by influencing their shape and cytoskeleton, which modulated then the macrophage phenotype switch to pro-inflammatory (M1) or pro-healing (M2) profiles [105]. A more recent study by Liu et al. demonstrated that the M2 pro-healing phenotype was significantly promoted on intermediate groove sizes ranging from 400 nm to 5  $\mu\text{m}$  in width by using deep-etched titanium surfaces with a wide range of groove sizes from 150 nm to 50  $\mu\text{m}$  [106]. Due to the essential function of

the M2 phenotypic macrophages in the healing processes, such nano- and micro-patterned structures might provide potential insights for resolving inflammation and promoting tissue integration upon implantation [107] .

The modification of the surface chemistry of biomaterials to alter wettability and charge density has long been considered as a promising approach to modulate protein adsorption and the subsequent cellular behavior [108, 109] (Figure 1.3A). In general, it is well accepted that proteins prefer to adsorb at higher amounts and bind more strongly on hydrophobic compared to hydrophilic surfaces [110, 111]. In addition, results of these studies have suggested that the conformation of the adsorbed proteins can change easily on hydrophobic materials due to the hydrophobic interactions between the surfaces and hydrophobic domains of proteins [112]. Such adsorption and conformational change of proteins on surfaces with different chemistries affect their subsequent cellular responses [113]. A large number of studies have shown that hydrophobic surfaces can promote inflammatory reactions with increased leukocyte adhesion, macrophage fusion and pro-inflammatory cytokine release [77, 114]. By contrast, hydrophilic and anionic surfaces promote anti-inflammatory responses with inhibition of leukocyte adhesion, macrophage fusion and pro-inflammatory cytokine production [77, 114]. To determine the roles of surface chemistry in inducing inflammatory and fibrotic responses, we have used an *in vitro* macrophage/fibroblast co-culture model, and a series of self-assembling monolayers (SAMs) bearing different terminal methyl (CH<sub>3</sub>), amine (NH<sub>2</sub>), hydroxyl (OH) and carboxyl (COOH) groups, to investigate their effect on macrophage (adhesion, migration and fusion into FBGCs) and fibroblast (attachment, spreading, proliferation, outgrowth and differentiation into myofibroblasts) cellular responses as well as pro- and anti-inflammatory cytokine production [80, 115]. Our results confirm that the inflammatory and fibrotic responses on different SAMs are highly surface property dependent. Studies on macrophage adhesion, fusion and pro-inflammatory cytokine (IL-6 and TNF- $\alpha$ ) production showed that the hydrophobic CH<sub>3</sub> surface and the hydrophilic/anionic COOH surface caused the highest and lowest level of inflammatory reactions, respectively [80]. Interestingly, the macrophage migration studies revealed that the OH surface provoked the highest macrophage motility, which can be related to the strong complement activation by OH groups via the alternative pathway activation [116]. On the other hand, the fibrotic reaction results indicated that the hydrophilic/anionic COOH surface resulted in low levels of both inflammatory and fibrotic responses, while the hydrophobic CH<sub>3</sub> surface which caused the highest level of inflammatory responses however evoked low levels of fibrotic responses. These results might also reveal that the inflammatory and fibrotic responses are not always



consistent [117]. Therefore, further in-depth inflammation-fibrosis link studies will be helpful for the development of biomaterials that evoked desired tissue reactivity.

Another common approach to modify the surface properties is passivation of biomaterials by surface coating with “anti-fouling” molecules such as polyethylene glycol (PEG) [118] , poly(2-hydroxyethyl methacrylate) (pHEMA) [119] and phosphatidylcholine polymers [120], which can resist protein adsorption by creating strong steric repulsion and hydration forces to hide the material from the host immune system, and eventually limit leukocyte adhesion and host inflammatory responses [121] (Figure 1.3A). However, these molecules cannot completely eliminate protein adsorption, and hence their anti-inflammatory effects were limited [122]. Alternatively, active strategies by incorporation of anti-inflammatory agents have been enabled more wide routes to generate biocompatible materials [11, 123].

### **1.5.2 Incorporation of anti-inflammatory agents to biomaterials**

In recent years, significant progress have been made in the development of active anti-inflammatory strategies by incorporation of various anti-inflammatory agents such as dexamethasone (DEX) [124], superoxide dismutase mimetics [125], alpha melanocyte-stimulating hormone ( $\alpha$ -MSH) [126], as well as receptor antagonists [127] and glycosaminoglycans (GAGs) [128] (Figure 1.3B). While the examples of other anti-inflammatory factors were reported in detail elsewhere [129], the following section will only focus on the anti-inflammatory properties of GAGs and GAG-like polysaccharides.

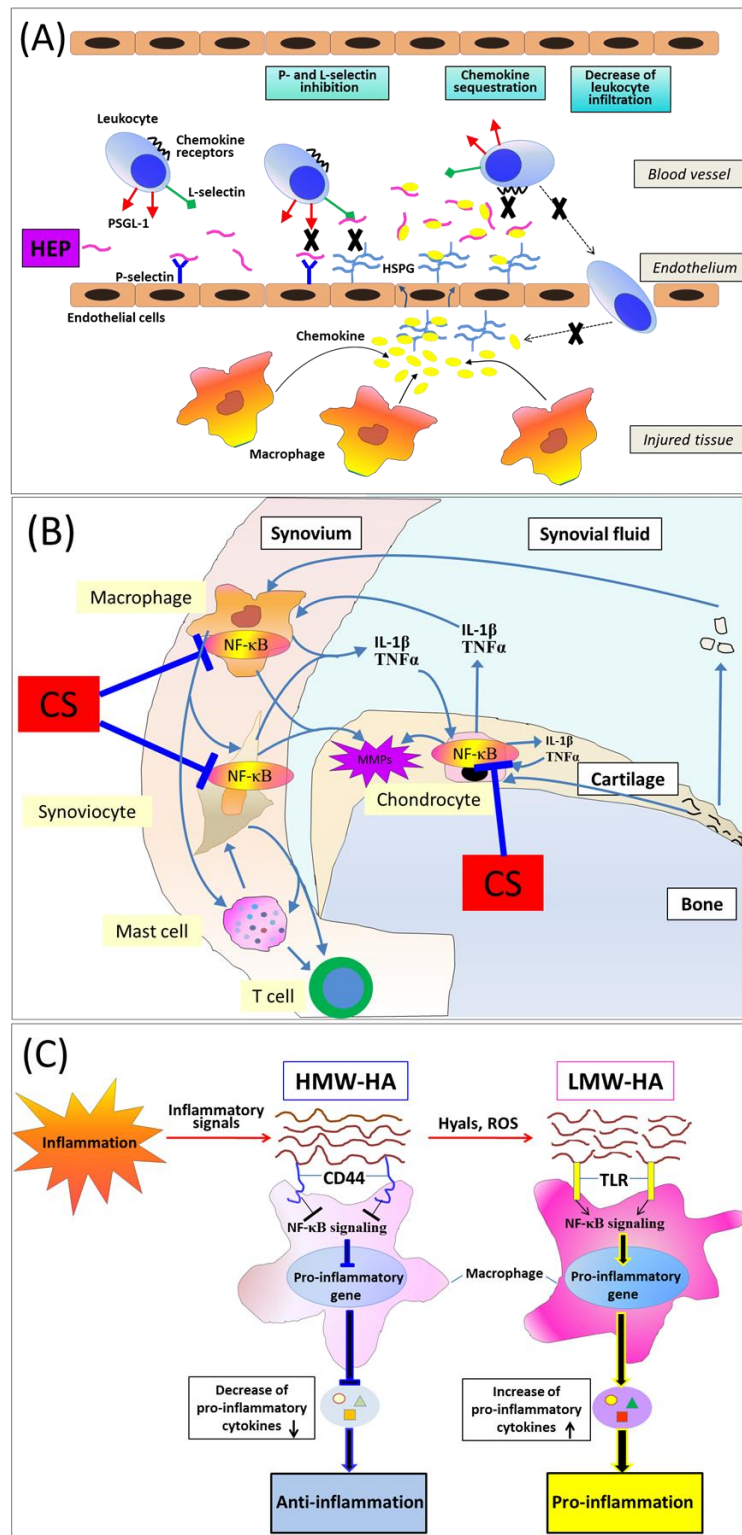


Figure 1.4. Schematic diagrams of anti-inflammatory mechanisms of (A) Heparin (HEP), (B) Chondroitin sulfate (CS) and (C) Hyaluronic acid (HA). HSPG - heparan sulfate proteoglycan; NF-κB - nuclear factor-κB; HMW-HA - high molecular weight HA; LMW-HA - low molecular weight HA; Hyals – hyaluronidases; ROS - reactive oxygen species; TLRs - toll-like receptors (Adapted from [130, 131]).

### 1.5.2.1 Anti-inflammatory activities of glycosaminoglycans (GAGs) and GAG-like polysaccharides

Glycosaminoglycans (GAGs), which represent linear, negatively charged polysaccharides such as heparin (HEP), chondroitin sulfate (CS) and hyaluronic acid (HA) have shown great anti-inflammatory activities as demonstrated in various experimental studies and clinical trials [83, 84, 132-135]. In general, GAGs can interact and bind to a wide range of proteins including ECM adhesive proteins (e.g. collagen, fibronectin, laminin), as well as chemokines, cytokines, growth factors and enzymes that participate in biological processes like cell migration, homing, growth, differentiation, and thus can modulate events associated with inflammation [133, 136]. The respective anti-inflammatory activities of the three types of GAGs - HEP, CS and HA are depicted in Figure 1.4.

HEP, a highly sulfated GAG, although most popular as its anticoagulant activity, has shown also beneficial effects for the treatment of asthma and ulcerative colitis diseases [137, 138]. As shown in Figure 1.4A, in response to inflammatory stimuli, macrophages can produce chemokines that attract more leukocytes to the inflamed tissues. HEP can bind to L- and P-selectin, but also the chemokines, which can impair leukocyte adhesion, activation and transmigration activities. As a consequence, the less activation and infiltration of leukocytes results in attenuation of chemokine and pro-inflammatory cytokine release [139]. Furthermore, it has been suggested that HEP possesses anti-inflammatory effects due to the inhibition of nuclear factor- $\kappa$ B (NF- $\kappa$ B) translocation, which is a crucial transcription factor of many pro-inflammatory mediators, leading to suppression of pro-inflammatory cytokine production [140]. In addition, *in vitro* experiments have shown that the incorporation of HEP to model biomaterial surfaces significantly attenuated the macrophage adhesion, fusion and pro-inflammatory cytokine production [83, 84]. Despite the convincing anti-inflammatory potentials of HEP by clinical and experimental data, the clinical use of HEP as anti-inflammatory drugs is impaired due to its strong anticoagulant activity and haemorrhagic complications [141]. Therefore, the development of heparin analogues with low anticoagulant activity, but preserve the anti-inflammatory activities, has become a promising direction in this regard [142].

Likewise, CS that also belongs to sulfated GAG, exhibits anti-inflammatory activities, which is particularly beneficial for patients with knee and hand osteoarthritis [135]. During osteoarthritis (Figure 1.4B), cartilage fragmentation produces extracellular matrix pieces that

can activate chondrocytes by increasing NF- $\kappa$ B translocation in chondrocytes, synovial macrophages and synoviocytes. These activated cells can release pro-inflammatory cytokines and matrix metalloproteinases (MMPs), exacerbating inflammation and cartilage destruction. It has been confirmed in clinical trials that CS can reduce the pain and improve articular function. Therefore, it has been classified as a symptomatic slow acting drug in osteoarthritis [143, 144]. The anti-inflammatory effects of CS are thought to be achieved through inhibition of the NF- $\kappa$ B translocation, leading to suppression of pro-inflammatory cytokine and MMP production. As a result, the signs and symptoms of osteoarthritis are diminished [130].

By contrast, HA is non-sulfated GAG, which inflammatory modulating activities depend on its molecular weight [145]. As shown in Figure 1.4C, during inflammation, the inflammatory stimuli trigger an increased production of high molecular weight HA (HMW-HA) (MW >  $5 \times 10^5$  Da) [146]. This HMW-HA can bind with CD44 receptor and down-regulate pro-inflammatory cytokine production, exhibiting anti-inflammatory activities [146]. However, during inflammation, this HMW-HA is rapidly catabolized into fragmented low molecular weight HA (LMW-HA) (MW < 200 kDa) due to the activation of matrix degrading enzymes such as hyaluronidases (Hyal) but also reactive oxygen species (ROS) [147]. Thereupon, the LMW-HA promotes inflammatory responses through toll-like receptors (TLRs) on macrophages and regulates pro-inflammatory gene expression [148]. Indeed, an elevated HA production was found in several disease states, including osteoarthritis, rheumatoid arthritis, and scleroderma, which implies also a predictive value of HA on the clinical outcome [149]. For example, the molecular weight (MW) distribution of HA in synovial fluid was shown to be significantly associated with the risk of knee osteoarthritis progression [150]. It was found that a shift in the MW distribution of HA towards higher values is associated with a reduced risk for rapid osteoarthritis progression and baseline pain [150]. Therefore, HMW-HA has been commonly used therapeutically for the treatment of osteoarthritis and rheumatoid arthritis by intra-articular injection [151, 152]. It was shown that the injection of HA with a molecular weight of  $8.4 \times 10^5$  Da to patients with rheumatoid arthritis significantly improves the local clinical symptoms and diminishes pain [152]. However, the mechanism of HA functions *in vivo* after injection has yet to be determined in more detail.

Apart from the use of GAGs as potent anti-inflammatory agents, the development of artificial GAG-like polysaccharides has also been considered as a promising approach to limit inflammation. In this regard, sulfated polysaccharides of marine origin that are isolated from sea organisms, especially algae and invertebrates, have shown great anti-inflammatory

effects. This is achieved mainly by P- and L-selectin blocking, which impairs the interaction of leukocytes with endothelial surface as well as via chemokine sequestration to limit leukocytes activation and infiltration [131]. Additionally, a study by Brito et al. has reported a heparin-like GAG isolated from the shrimp cephalothorax that reduces the influx of inflammatory cells to the injury site and inhibits activity of MMPs secreted from activated human leukocytes in an acute inflammation model [142]. In addition to the great anti-inflammatory potential, this heparin-like compound was found to have a low anticoagulant activity and little hemorrhagic effect compared to mammalian heparin. This indicates that the heparin-like GAG may represent a better alternative than mammalian heparin as anti-inflammatory drug. On the other hand, chemical modification of the cellulose, the most abundant polysaccharide in nature, has also been proved to possess anticoagulant [153] and anti-inflammatory properties [154]. Using a mouse model of inflammatory bowel disease (IBD), Azuma et al. investigated the anti-inflammatory effects of cellulose nanofibers made from adlay chaff and seaweed on colon inflammation [154]. The results showed that the cellulose nanofibers had suppressive effects on colon inflammation by inhibition of NF- $\kappa$ B activation as well as limitation of myeloperoxidase activities of inflammatory cells such as leukocytes. Taken together, several GAG-like polysaccharides obtained from marine organisms or natural plants have not only revealed great anti-inflammatory activities, but also the advantage of being a more abundant source of lower costs compared to mammalian GAGs, and thus might have a wide variety of therapeutic applications for treatment of distinct inflammatory diseases in the future.

## 1.6 Summary and future prospects

Development of biomaterials that do not trigger detrimental immune responses such as chronic inflammation and fibrotic encapsulation is essential for long-term functions of implanted biomedical devices and the overall patient health. To address this issue, considerable efforts have been applied to study the inflammatory and fibrotic responses by using various *in vitro* and *in vivo* cell-based models. Although much progresses in the understanding of interactions between surface functionality and host responses were attained, more efforts to uncover the link between inflammation and fibrosis, as well as the development of more predictive *in vitro* and *in vivo* models are very necessary. On the other hand, significant efforts have focused on developing distinct anti-inflammatory approaches to make materials more biocompatible. The passive approaches to reduce protein adsorption and initial cell adhesion in an attempt to diminish the ensuing host responses, however, did

not work efficiently and led to chronic inflammation and fibrotic encapsulation upon implantation [155]. Alternative active approaches by incorporation of various anti-inflammatory reagents, in particular GAGs and GAG-like polysaccharides have shown more promising anti-inflammatory effects. Furthermore, biomolecule strategies by decoration biomaterials with endogenously expressed proteins to modulate the immune system are gaining considerable interests recently [156]. The bioactive molecules include ECM proteins, cell membrane proteins or cytokines that can directly interact with immune cells, as well as proteins that indirectly modulate immune cells by preventing complement and coagulation activation [157-159] (Figure 1.3C). In addition, these biomolecule decorated biomaterials are closer to the natural environment of the cells and may enable more specific interactions. Last but most importantly, it is our belief that the integration of multiple anti-inflammatory strategies and immunomodulators will be required to help developing novel biomaterials and tissue-engineered constructs with desired tissue responses.

## **1.7 Disclosure**

No conflicts of interests are declared.

## **1.8 Acknowledgements**

G. Zhou thanks the China Scholarship Council for offering the scholarship to work in Germany.

## **1.9 References**

[1] Ratner BD, Hoffman AS, Schoen FJ, Lemons J. Biomaterials science: a multidisciplinary endeavor. *Biomaterials science: an introduction to materials in medicine* 2004:1-9.

[2] Koschwanetz HE, Reichert WM. In vitro, in vivo and post explantation testing of glucose-detecting biosensors: current methods and recommendations. *Biomaterials* 2007;28:3687-703.

[3] Nożyński JK, Religa Z, Wszolek J, Zembala-Nożyńska E, Rozentryt P. Biological heart valve—an alternative to mechanical valve. *Medical Science Monitor Basic Research* 2001;7:RA550-RA62.

[4] Lorenzoni G, Folino F, Soriani N, Iliceto S, Gregori D. Cost-effectiveness of early detection of atrial fibrillation via remote control of implanted devices. *Journal of evaluation in clinical practice* 2014;20:570-7.

[5] Sánchez-Guerrero J, Colditz GA, Karlson EW, Hunter DJ, Speizer FE, Liang MH. Silicone breast implants and the risk of connective-tissue diseases and symptoms. *N Engl J Med* 1995;332:1666-70.

[6] Kosyfaki P, Swain M. Adhesion determination of dental porcelain to zirconia using the Schwickerath test: strength vs. fracture energy approach. *Acta Biomaterialia* 2014;10:4861-9.

[7] van Hooft JE, Bemelman WA, Oldenburg B, Marinelli AW, Holzik MFL, Grubben MJ, Sprangers MA, et al. Colonic stenting versus emergency surgery for acute left-sided malignant colonic obstruction: a multicentre randomised trial. *The lancet oncology* 2011;12:344-52.

[8] O'Neill MD, Jaïs P, Hocini M, Sacher F, Klein GJ, Clémenty J, Haïssaguerre M. Catheter ablation for atrial fibrillation. *Circulation* 2007;116:1515-23.

[9] Anderson JM. In vitro and in vivo monocyte, macrophage, foreign body giant cell, and lymphocyte interactions with biomaterials. *Biological interactions on materials surfaces*: Springer; 2009. p. 225-44.

[10] Anderson JM. Biological responses to materials. *Ann Rev Mater Res* 2001;31:81-110.

[11] Franz S, Rammelt S, Scharnweber D, Simon JC. Immune responses to implants - A review of the implications for the design of immunomodulatory biomaterials. *Biomaterials* 2011;32:6692-709.

[12] Vroman L, Adams A, Fischer G, Munoz P. Interaction of high molecular weight kininogen, factor XII, and fibrinogen in plasma at interfaces. *Blood* 1980;55:156-9.

[13] Markiewski MM, Nilsson B, Ekdahl KN, Mollnes TE, Lambris JD. Complement and coagulation: strangers or partners in crime? *Trends in Immunology* 2007;28:184-92.

[14] Tang LP, Eaton JW. Fibrin(ogen) mediates acute inflammatory responses to biomaterials. *Journal of Experimental Medicine* 1993;178:2147-56.

[15] Jenney CR, Anderson JM. Adsorbed IgG: A potent adhesive substrate for human macrophages. *J Biomed Mater Res* 2000;50:281-90.

[16] Gorbet MB, Sefton MV. Biomaterial-associated thrombosis: roles of coagulation factors, complement, platelets and leukocytes. *Biomaterials* 2004;25:5681-703.

[17] Hanson SR, Harker L. Blood coagulation and blood-materials interactions. *Biomaterials science: an introduction to materials in medicine* 1996:193-200.

[18] Horbett TA. Principles underlying the role of adsorbed plasma proteins in blood interactions with foreign materials. *Cardiovascular Pathology* 1993;2:137-48.

[19] Ziats N, Pankowsky D, Tierney B, Ratnoff O, Anderson J. Adsorption of Hageman factor (factor XII) and other human plasma proteins to biomedical polymers. *The Journal of laboratory and clinical medicine* 1990;116:687-96.

[20] Cornelius RM, Brash JL. Identification of proteins adsorbed to hemodialyser membranes from heparinized plasma. *Journal of Biomaterials Science, Polymer Edition* 1993;4:291-304.

[21] Zhuo R, Siedlecki CA, Vogler EA. Autoactivation of blood factor XII at hydrophilic and hydrophobic surfaces. *Biomaterials* 2006;27:4325-32.

[22] Sperling C, Fischer M, Maitz MF, Werner C. Blood coagulation on biomaterials requires the combination of distinct activation processes. *Biomaterials* 2009;30:4447-56.

[23] Heemskerk JW, Bevers EM, Lindhout T. Platelet activation and blood coagulation. *THROMBOSIS AND HAEMOSTASIS-STUTTGART-2002*;88:186-94.

[24] Hong J, Ekdahl KN, Reynolds H, Larsson R, Nilsson B. A new in vitro model to study interaction between whole blood and biomaterials. *Studies of platelet and coagulation activation and the effect of aspirin. Biomaterials* 1999;20:603-11.

[25] Nilsson B, Ekdahl KN, Mollnes TE, Lambris JD. The role of complement in biomaterial-induced inflammation. *Molecular immunology* 2007;44:82-94.

[26] Sarma JV, Ward PA. The complement system. *Cell and tissue research* 2011;343:227-35.



[27] Lhotta K, Würzner R, Kronenberg F, Oppermann M, König P. Rapid activation of the complement system by cuprophane depends on complement component C4. *Kidney international* 1998;53:1044-51.

[28] Hed J, Johansson M, Lindroth M. Complement activation according to the alternate pathway by glass and plastic surfaces and its role in neutrophil adhesion. *Immunology letters* 1984;8:295-9.

[29] Hakim RM. Complement activation by biomaterials. *Cardiovascular Pathology* 1993;2:187-97.

[30] Chenoweth DE. Complement activation in extracorporeal circuits. *Annals of the New York Academy of Sciences* 1987;516:306-13.

[31] Andersson J, Ekdahl KN, Lambris JD, Nilsson B. Binding of C3 fragments on top of adsorbed plasma proteins during complement activation on a model biomaterial surface. *Biomaterials* 2005;26:1477-85.

[32] Andersson J, Ekdahl KN, Larsson R, Nilsson UR, Nilsson B. C3 adsorbed to a polymer surface can form an initiating alternative pathway convertase. *The Journal of Immunology* 2002;168:5786-91.

[33] Lehrer RI, Ganz T, Selsted ME, Babior BM, Curnutte JT. Neutrophils and host defense. *Ann Intern Med* 1988;109:127-42.

[34] Deuel TF, Senior RM, Chang D, Griffin GL, Heinrikson RL, Kaiser ET. Platelet factor 4 is chemotactic for neutrophils and monocytes. *Proceedings of the National Academy of Sciences* 1981;78:4584-7.

[35] Ghasemzadeh M, Kaplan ZS, Alwis I, Schoenwaelder SM, Ashworth KJ, Westein E, Hosseini E, et al. The CXCR1/2 ligand NAP-2 promotes directed intravascular leukocyte migration through platelet thrombi. *Blood* 2013;121:4555-66.

[36] Wright HL, Moots RJ, Bucknall RC, Edwards SW. Neutrophil function in inflammation and inflammatory diseases. *Rheumatology* 2010;49:1618-31.

[37] Babior BM, Golde DW. Production, distribution, and fate of neutrophils. *Williams Hematology* 2001;5:773-9.

[38] Xia Z, Triffitt JT. A review on macrophage responses to biomaterials. *Biomedical Materials* 2006;1:R1-R9.

[39] Murray PJ, Wynn TA. Protective and pathogenic functions of macrophage subsets. *Nat Rev Immunol* 2011;11:723-37.

[40] Schutte RJ, Parisi-Amon A, Reichert WM. Cytokine profiling using monocytes/macrophages cultured on common biomaterials with a range of surface chemistries. *J Biomed Mater Res Part A* 2009;88A:128-39.

[41] Martin CA, Dorf ME. Interleukin-6 production by murine macrophage cell lines P388D1 and J774A.1: stimulation requirements and kinetics. *Cell Immunol* 1990;128:555-68.

[42] Duque GA, Descoteaux A. Macrophage cytokines: involvement in immunity and infectious diseases. *Secretion of Cytokines and Chemokines by Innate Immune Cells* 2015:6.

[43] Underhill DM, Goodridge HS. Information processing during phagocytosis. *Nat Rev Immunol* 2012;12:492-502.

[44] Labrousse AM, Meunier E, Record J, Labernadie A, Beduer A, Vieu C, Safta TB, et al. Frustrated phagocytosis on micro-patterned immune complexes to characterize lysosome movements in live macrophages. *Frontiers in immunology* 2011;2:51.

[45] Henson P. Mechanisms of exocytosis in phagocytic inflammatory cells. Parke-Davis Award Lecture. *The American journal of pathology* 1980;101:494.

[46] Vatansever F, de Melo WC, Avci P, Vecchio D, Sadasivam M, Gupta A, Chandran R, et al. Antimicrobial strategies centered around reactive oxygen species–bactericidal antibiotics, photodynamic therapy, and beyond. *FEMS microbiology reviews* 2013;37:955-89.

[47] Bhattacharyya A, Chattopadhyay R, Mitra S, Crowe SE. Oxidative stress: an essential factor in the pathogenesis of gastrointestinal mucosal diseases. *Physiological reviews* 2014;94:329-54.

[48] Mosser DM. The many faces of macrophage activation. *Journal of Leukocyte Biology* 2003;73:209-12.

[49] Anderson JM. Biological responses to materials. *Ann Rev Mater Res* 2001;31:81-110.

[50] Tang LP, Eaton JW. Inflammatory responses to biomaterials. *Am J Clin Pathol* 1995;103:466-71.

[51] Wynn TA, Barron L. Macrophages: master regulators of inflammation and fibrosis. *Seminars in Liver Disease: NIH Public Access*; 2010. p. 245.

[52] Xia Z, Triffitt JT. A review on macrophage responses to biomaterials. *Biomedical Materials* 2006;1:R1.

[53] Kao WJ, McNally AK, Hiltner A, Anderson JM. Role for interleukin-4 in foreign-body giant cell formation on a poly (etherurethane urea) in vivo. *J Biomed Mater Res* 1995;29:1267-75.

[54] DeFife KM, Jenney CR, McNally AK, Colton E, Anderson JM. Interleukin-13 induces human monocyte/macrophage fusion and macrophage mannose receptor expression. *The Journal of Immunology* 1997;158:3385-90.

[55] Dadsetan M, Jones JA, Hiltner A, Anderson JM. Surface chemistry mediates adhesive structure, cytoskeletal organization, and fusion of macrophages. *J Biomed Mater Res Part A* 2004;71:439-48.

[56] Collier TO, Thomas CH, Anderson JM, Healy KE. Surface chemistry control of monocyte and macrophage adhesion, morphology, and fusion. *J Biomed Mater Res* 2000;49:141-5.

[57] McNally AK, Anderson JM.  $\beta$ 1 and  $\beta$ 2 integrins mediate adhesion during macrophage fusion and multinucleated foreign body giant cell formation. *The American journal of pathology* 2002;160:621-30.

[58] Berton G, Lowell CA. Integrin signalling in neutrophils and macrophages. *Cellular signalling* 1999;11:621-35.

[59] McNally AK, Anderson JM. beta 1 and beta 2 integrins mediate adhesion during macrophage fusion and multinucleated foreign body giant cell formation. *Am J Pathol* 2002;160:621-30.

[60] McNally AK, MacEwan SR, Anderson JM. alpha subunit partners to beta 1 and beta 2 integrins during IL-4-induced foreign body giant cell formation. *J Biomed Mater Res A* 2007;82A:568-74.

[61] Jenney CR, DeFife KM, Colton E, Anderson JM. Human monocyte/macrophage adhesion, macrophage motility, and IL-4-induced foreign body giant cell formation on silane-modified surfaces in vitro. *J Biomed Mater Res* 1998;41:171-84.

[62] Helming L, Gordon S. Macrophage fusion induced by IL-4 alternative activation is a multistage process involving multiple target molecules. *European journal of immunology* 2007;37:33-42.

[63] Barron L, Wynn TA. Fibrosis is regulated by TH2 and TH17 responses and by dynamic interactions between fibroblasts and macrophages. *American Journal of Physiology-Gastrointestinal and Liver Physiology* 2011;300:G723-G8.

[64] Mantovani A, Sozzani S, Locati M, Allavena P, Sica A. Macrophage polarization: tumor-associated macrophages as a paradigm for polarized M2 mononuclear phagocytes. *Trends in Immunology* 2002;23:549-55.

[65] Ward WK. A review of the foreign-body response to subcutaneously-implanted devices: the role of macrophages and cytokines in biofouling and fibrosis. *Journal of diabetes science and technology* 2008;2:768-77.

[66] Serini G, Bochaton-Piallat ML, Ropraz P, Geinoz A, Borsi L, Zardi L, Gabbiani G. The fibronectin domain ED-A is crucial for myofibroblastic phenotype induction by transforming growth factor-beta 1. *J Cell Biol* 1998;142:873-81.

[67] Diegelmann RF, Evans MC. Wound healing: an overview of acute, fibrotic and delayed healing. *Front Biosci* 2004;9:283-9.

[68] Hinz B. Formation and function of the myofibroblast during tissue repair. *J Invest Dermatol* 2007;127:526-37.

[69] Mutsaers SE, Bishop JE, McGrouther G, Laurent GJ. Mechanisms of tissue repair: From wound healing to fibrosis. *Int J Biochem Cell Biol* 1997;29:5-17.

[70] Williams D. Tissue-biomaterial interactions. *Journal of Materials science* 1987;22:3421-45.

[71] Colton CK. Implantable biohybrid artificial organs. *Cell transplantation* 1995;4:415-36.

[72] Wu P, Grainger DW. Drug/device combinations for local drug therapies and infection prophylaxis. *Biomaterials* 2006;27:2450-67.

[73] Koschwanetz H, Yap F, Klitzman B, Reichert W. In vitro and in vivo characterization of porous poly-L-lactic acid coatings for subcutaneously implanted glucose sensors. *J Biomed Mater Res Part A* 2008;87:792-807.

[74] Klueh U, Dorsky DI, Kreutzer DL. Enhancement of implantable glucose sensor function in vivo using gene transfer-induced neovascularization. *Biomaterials* 2005;26:1155-63.

[75] Drury JL, Mooney DJ. Hydrogels for tissue engineering: scaffold design variables and applications. *Biomaterials* 2003;24:4337-51.

[76] Marques AP, Reis RL, Hunt JA. An in vivo study of the host response to starch-based polymers and composites subcutaneously implanted in rats. *Macromol Biosci* 2005;5:775-85.

[77] Brodbeck WG, Nakayama Y, Matsuda T, Colton E, Ziats NP, Anderson JM. Biomaterial surface chemistry dictates adherent monocyte/macrophage cytokine expression in vitro. *Cytokine* 2002;18:311-9.

[78] Chen S, Jones JA, Xu Y, Low H-Y, Anderson JM, Leong KW. Characterization of topographical effects on macrophage behavior in a foreign body response model. *Biomaterials* 2010;31:3479-91.

[79] Baker DW, Liu X, Weng H, Luo C, Tang L. Fibroblast/Fibrocyte: Surface interaction dictates tissue reactions to micropillar implants. *Biomacromolecules* 2011;12:997-1005.

[80] Zhou G, Loppnow H, Groth T. A macrophage/fibroblast co-culture system using a cell migration chamber to study inflammatory effects of biomaterials. *Acta Biomaterialia* 2015;26:54-63.

[81] Schildberger A, Rossmann E, Eichhorn T, Strassl K, Weber V. Monocytes, peripheral blood mononuclear cells, and THP-1 cells exhibit different cytokine expression patterns following stimulation with lipopolysaccharide. *Mediators of Inflammation* 2013;2013:697972.

[82] Theus SA, Cave MD, Eisenach KD. Activated THP-1 cells: An attractive model for the assessment of intracellular growth rates of *Mycobacterium tuberculosis* isolates. *Infect Immun* 2004;72:1169-73.

[83] Zhou G, Al-Khoury H, Groth T. Covalent immobilization of glycosaminoglycans to reduce the inflammatory effects of biomaterials. *Int J Artif Organs* 2016;39:37-44.

[84] Zhou G, Niepel MS, Saretia S, Groth T. Reducing the inflammatory responses of biomaterials by surface modification with glycosaminoglycan multilayers. *J Biomed Mater Res Part A* 2016;104:493-502.

[85] Park EK, Jung HS, Yang HI, Yoo MC, Kim C, Kim KS. Optimized THP-1 differentiation is required for the detection of responses to weak stimuli. *Inflammation Research* 2007;56:45-50.

[86] Daigneault M, Preston JA, Marriott HM, Whyte MK, Dockrell DH. The identification of markers of macrophage differentiation in PMA-stimulated THP-1 cells and monocyte-derived macrophages. *Plos One* 2010;5:e8668.

[87] Schwende H, Fitzke E, Ambs P, Dieter P. Differences in the state of differentiation of THP-1 cells induced by phorbol ester and 1, 25-dihydroxyvitamin D3. *Journal of Leukocyte Biology* 1996;59:555-61.

[88] Chen Q, Ross AC. Retinoic acid regulates cell cycle progression and cell differentiation in human monocytic THP-1 cells. *Exp Cell Res* 2004;297:68-81.

[89] Hattori T, Pack M, Bougnoux P, Chang Z, Hoffman T. Interferon-induced differentiation of U937 cells. Comparison with other agents that promote differentiation of human myeloid or monocytelike cell lines. *Journal of Clinical Investigation* 1983;72:237.

[90] Tjiu J-W, Chen J-S, Shun C-T, Lin S-J, Liao Y-H, Chu C-Y, Tsai T-F, et al. Tumor-associated macrophage-induced invasion and angiogenesis of human basal cell carcinoma cells by cyclooxygenase-2 induction. *J Invest Dermatol* 2009;129:1016-25.

[91] Qin Z. The use of THP-1 cells as a model for mimicking the function and regulation of monocytes and macrophages in the vasculature. *Atherosclerosis*. 2012;221:2-11..

[92] Miki Y, Ono K, Hata S, Suzuki T, Kumamoto H, Sasano H. The advantages of co-culture over mono cell culture in simulating in vivo environment. *The Journal of steroid biochemistry and molecular biology* 2012;131:68-75.

[93] Pan H, Jiang HL, Kantharia S, Chen WL. A fibroblast/macrophage co-culture model to evaluate the biocompatibility of an electrospun Dextran/PLGA scaffold and its potential to induce inflammatory responses. *Biomedical Materials* 2011;6.

[94] Holt DJ, Chamberlain LM, Grainger DW. Cell-cell signaling in co-cultures of macrophages and fibroblasts. *Biomaterials* 2010;31:9382-94.

[95] Parks AC, Sung K, Wu BM. A three-dimensional in vitro model to quantify inflammatory response to biomaterials. *Acta Biomaterialia* 2014;10:4742-9.

[96] Zeng Q, Chen W. The functional behavior of a macrophage/fibroblast co-culture model derived from normal and diabetic mice with a marine gelatin oxidized alginate hydrogel. *Biomaterials* 2010;31:5772-81.

[97] Swartzlander MD, Lynn AD, Blakney AK, Kyriakides TR, Bryant SJ. Understanding the host response to cell-laden poly(ethylene glycol)-based hydrogels. *Biomaterials* 2013;34:952-64.

[98] Kaji H, Camci-Unal G, Langer R, Khademhosseini A. Engineering systems for the generation of patterned co-cultures for controlling cell-cell interactions. *Biochimica Et Biophysica Acta-General Subjects* 2011;1810:239-50.

[99] Damanik FFR, Rothuizen TC, van Blitterswijk C, Rotmans JI, Moroni L. Towards an in vitro model mimicking the foreign body response: tailoring the surface properties of biomaterials to modulate extracellular matrix. *Scientific Reports* 2014;4.

[100] McNamara LE, Burchmore R, Riehle MO, Herzyk P, Biggs MJ, Wilkinson CD, Curtis AS, et al. The role of microtopography in cellular mechanotransduction. *Biomaterials* 2012;33:2835-47.

[101] McWhorter FY, Davis CT, Liu WF. Physical and mechanical regulation of macrophage phenotype and function. *Cellular and Molecular Life Sciences* 2015;72:1303-16.

[102] Yim EK, Leong KW. Significance of synthetic nanostructures in dictating cellular response. *Nanomedicine: Nanotechnology, biology and medicine* 2005;1:10-21.

[103] Wójciak-Stothard B, Madeja Z, Korohoda W, Curtis A, Wilkinson C. Activation of macrophage-like cells by multiple grooved substrata. *Topographical control of cell behaviour. Cell biology international* 1995;19:485-90.

[104] Paul NE, Skazik C, Harwardt M, Bartneck M, Denecke B, Klee D, Salber J, et al. Topographical control of human macrophages by a regularly microstructured polyvinylidene fluoride surface. *Biomaterials* 2008;29:4056-64.

[105] McWhorter FY, Wang T, Nguyen P, Chung T, Liu WF. Modulation of macrophage phenotype by cell shape. *Proceedings of the National Academy of Sciences* 2013;110:17253-8.

[106] Luu TU, Gott SC, Woo BW, Rao MP, Liu WF. Micro-and Nanopatterned Topographical Cues for Regulating Macrophage Cell Shape and Phenotype. *ACS applied materials & interfaces* 2015;7:28665-72.

[107] KyungáKim Y. Biomolecular strategies to modulate the macrophage response to implanted materials. *J Mat Chem B* 2016.

[108] Thevenot P, Hu W, Tang L. Surface chemistry influence implant biocompatibility. *Current Topics in Medicinal Chemistry* 2008;8:270.

[109] Kamath S, Bhattacharyya D, Padukudru C, Timmons RB, Tang L. Surface chemistry influences implant-mediated host tissue responses. *J Biomed Mater Res Part A* 2008;86A:617-26.

[110] Arima Y, Iwata H. Effect of wettability and surface functional groups on protein adsorption and cell adhesion using well-defined mixed self-assembled monolayers. *Biomaterials* 2007;28:3074-82.

[111] Faucheux N, Schweiss R, Lutzow K, Werner C, Groth T. Self-assembled monolayers with different terminating groups as model substrates for cell adhesion studies. *Biomaterials* 2004;25:2721-30.

[112] Keselowsky BG, Collard DM, Garcia AJ. Surface chemistry modulates fibronectin conformation and directs integrin binding and specificity to control cell adhesion. *J Biomed Mater Res Part A* 2003;66A:247-59.

[113] Groth T, Altankov G, Klosz K. Adhesion of human peripheral blood lymphocytes is dependent on surface wettability and protein preadsorption. *Biomaterials* 1994;15:423-8.

[114] Brodbeck WG, Shive MS, Colton E, Nakayama Y, Matsuda T, Anderson JM. Influence of biomaterial surface chemistry on the apoptosis of adherent cells. *J Biomed Mater Res* 2001;55:661-8.

[115] Zhou G, Groth T. In vitro study of the host responses to model biomaterials via a fibroblast/macrophage co-culture system. *Biomaterials Science*, under revision.

[116] Barbosa JN, Barbosa MA, Aguas AP. Inflammatory responses and cell adhesion to self-assembled monolayers of alkanethiolates on gold. *Biomaterials* 2004;25:2557-63.

[117] Tang LP, Wu YL, Timmons RB. Fibrinogen adsorption and host tissue responses to plasma functionalized surfaces. *J Biomed Mater Res* 1998;42:156-63.

[118] Zhou G, Ma C, Zhang G. Synthesis of polyurethane-g-poly(ethylene glycol) copolymers by macroiniferter and their protein resistance. *Polymer Chemistry* 2011;2:1409-14.

[119] Ananthoji R. Hydrophilic Polymers of Poly (2-Hydroxy Ethyl Methacrylate) with Tunable Properties for Drug Release, Sequestration of Blistering Agent, Preparation of Ultra-Strong Hydrogels & Thermal Stability of Various Organic Azides. 2012.



[120] Groult H, Ruiz-Cabello J, Lechuga-Vieco AV, Mateo J, Benito M, Bilbao I, Martínez-Alcázar MP, et al. Phosphatidylcholine-Coated Iron Oxide Nanomicelles for In Vivo Prolonged Circulation Time with an Antibiofouling Protein Corona. *Chemistry—A European Journal* 2014;20:16662-71.

[121] Swartzlander MD, Barnes CA, Blakney AK, Kaar JL, Kyriakides TR, Bryant SJ. Linking the foreign body response and protein adsorption to PEG-based hydrogels using proteomics. *Biomaterials* 2015;41:26-36.

[122] Park JH, Bae YH. Hydrogels based on poly(ethylene oxide) and poly(tetramethylene oxide) or poly(dimethyl siloxane). III. In vivo biocompatibility and biostability. *J Biomed Mater Res Part A* 2003;64A:309-19.

[123] Boontheekul T, Mooney DJ. Protein-based signaling systems in tissue engineering. *Current Opinion in Biotechnology* 2003;14:559-65.

[124] Zhong Y, Bellamkonda RV. Dexamethasone-coated neural probes elicit attenuated inflammatory response and neuronal loss compared to uncoated neural probes. *Brain research* 2007;1148:15-27.

[125] Udipi K, Ornberg RL, Thurmond KB, Settle SL, Forster D, Riley D. Modification of inflammatory response to implanted biomedical materials in vivo by surface bound superoxide dismutase mimics. *J Biomed Mater Res* 2000;51:549-60.

[126] Schultz P, Vautier D, Richert L, Jessel N, Haikel Y, Schaaf P, Voegel J-C, et al. Polyelectrolyte multilayers functionalized by a synthetic analogue of an anti-inflammatory peptide,  $\alpha$ -MSH, for coating a tracheal prosthesis. *Biomaterials* 2005;26:2621-30.

[127] Kim D-H, Smith JT, Chilkoti A, Reichert WM. The effect of covalently immobilized rhIL-1ra-ELP fusion protein on the inflammatory profile of LPS-stimulated human monocytes. *Biomaterials* 2007;28:3369-77.

[128] Proudfoot AE. Glycosaminoglycan analogs as a novel anti-inflammatory strategy. *Frontiers in immunology* 2012;3:293.

[129] Bridges AW, García AJ. Anti-inflammatory polymeric coatings for implantable biomaterials and devices. *Journal of diabetes science and technology* 2008;2:984-94.

[130] Iovu M, Dumais G, du Souich P. Anti-inflammatory activity of chondroitin sulfate. *Osteoarthritis and cartilage / OARS, Osteoarthritis Research Society* 2008;16 Suppl 3:S14-8.

[131] Pomin VH. Fucanomics and galactanomics: Current status in drug discovery, mechanisms of action and role of the well-defined structures. *Biochimica et Biophysica Acta (BBA)-General Subjects* 2012;1820:1971-9.

[132] Severin IC, Soares A, Hantson J, Teixeira M, Sachs D, Valognes D, Scheer A, et al. Glycosaminoglycan analogs as a novel anti-inflammatory strategy. *Frontiers in immunology* 2012;3:293.

[133] Taylor KR, Gallo RL. Glycosaminoglycans and their proteoglycans: host-associated molecular patterns for initiation and modulation of inflammation. *Faseb J* 2006;20:9-22.

[134] Reichenbach S, Sterchi R, Scherer M, Trelle S, Burgi E, Burgi U, Dieppe PA, et al. Meta-analysis: Chondroitin for osteoarthritis of the knee or hip. *Ann Intern Med* 2007;146:580-U51.

[135] Volpi N. Quality of different chondroitin sulfate preparations in relation to their therapeutic activity. *Journal of pharmacy and pharmacology* 2009;61:1271-80.

[136] Gandhi NS, Mancera RL. The Structure of glycosaminoglycans and their Interactions with Proteins. *Chemical Biology & Drug Design* 2008;72:455-82.

[137] Ahmed T, Garrigo J, Danta I. Preventing bronchoconstriction in exercise-induced asthma with inhaled heparin. *N Engl J Med* 1993;329:90-5.

[138] Torkvist L, Thorlacius H, Sjoqvist U, Bohman L, Lapidus A, Flood L, Agren B, et al. Low molecular weight heparin as adjuvant therapy in active ulcerative colitis. *Aliment Pharmacol Ther* 1999;13:1323-8.

[139] Young E. The anti-inflammatory effects of heparin and related compounds. *Thromb Res* 2008;122:743-52.

[140] Iovu M, Dumais G, du Souich P. Anti-inflammatory activity of chondroitin sulfate. *Osteoarthritis and Cartilage* 2008;16:S14-S8.

[141] Page C. Heparin and related drugs: Beyond anticoagulant activity. *ISRN pharmacology* 2013;2013.

[142] Brito AS, Arimateia DS, Souza LR, Lima MA, Santos VO, Medeiros VP, Ferreira PA, et al. Anti-inflammatory properties of a heparin-like glycosaminoglycan with reduced anti-coagulant activity isolated from a marine shrimp. *Bioorganic & Medicinal Chemistry* 2008;16:9588-95.

[143] Uebelhart D, Malaise M, Marcolongo R, DeVathaire F, Piperno M, Mailleux E, Fioravanti A, et al. Intermittent treatment of knee osteoarthritis with oral chondroitin sulfate: a one-year, randomized, double-blind, multicenter study versus placebo. *Osteoarthritis Cartilage* 2004;12:269-76.

[144] Verbruggen G, Goemaere S, Veys E. Systems to assess the progression of finger joint osteoarthritis and the effects of disease modifying osteoarthritis drugs. *Clin Rheumatol* 2002;21:231-43.

[145] Krejcova D, Pekarova M, Safrankova B, Kubala L. The effect of different molecular weight hyaluronan on macrophage physiology. *Neuroendocrinology Letters*. 2009;30:106.

[146] Ruppert S, Hawn T, Arrigoni A, Wight T, Bollyky P. Tissue integrity signals communicated by high-molecular weight hyaluronan and the resolution of inflammation. *Immunologic Research* 2014;58:186-92.

[147] Stern R, Jedrzejak MJ. Hyaluronidases: their genomics, structures, and mechanisms of action. *Chem Rev* 2006;106:818-39.

[148] Laurent TC, Laurent UB, Fraser JRE. The structure and function of hyaluronan: An overview. *Immunology & Cell Biology* 1996;74.

[149] Moreland LW. Intra-articular hyaluronan (hyaluronic acid) and hylans for the treatment of osteoarthritis: mechanisms of action. *Arthritis Res Ther* 2003;5:1.

[150] Band P, Heeter J, Wisniewski H-G, Liublinska V, Pattanayak C, Karia R, Stabler T, et al. Hyaluronan molecular weight distribution is associated with the risk of knee osteoarthritis progression. *Osteoarthritis Cartilage* 2015;23:70-6.

[151] Gossec L, Dougados M. Intra-articular treatments in osteoarthritis: from the symptomatic to the structure modifying. *Ann Rheum Dis* 2004;63:478-82.

[152] Goto M, Hanyu T, Yoshio T, Matsuno H, Shimizu M, Murata N, Shiozawa S, et al. Intra-articular injection of hyaluronate (SI-6601D) improves joint pain and synovial fluid prostaglandin E2 levels in rheumatoid arthritis: a multicenter clinical trial. *Clin Exp Rheumatol* 2001;19:377-84.

[153] Groth T, Wagenknecht W. Anticoagulant potential of regioselective derivatized cellulose. *Biomaterials* 2001;22:2719-29.

[154] Azuma K, Ifuku S, Osaki T, Arifuku I, Okamoto Y. Anti-inflammatory activities of cellulose nanofibers made from adlay and seaweed in an inflammatory bowel-disease model.

[155] Norton L, Koschwanetz H, Wisniewski N, Klitzman B, Reichert W. Vascular endothelial growth factor and dexamethasone release from nonfouling sensor coatings affect the foreign body response. *J Biomed Mater Res Part A* 2007;81:858-69.

[156] KyungáKim Y. Biomolecular strategies to modulate the macrophage response to implanted materials. *J Mat Chem B* 2016;4:1600-9.

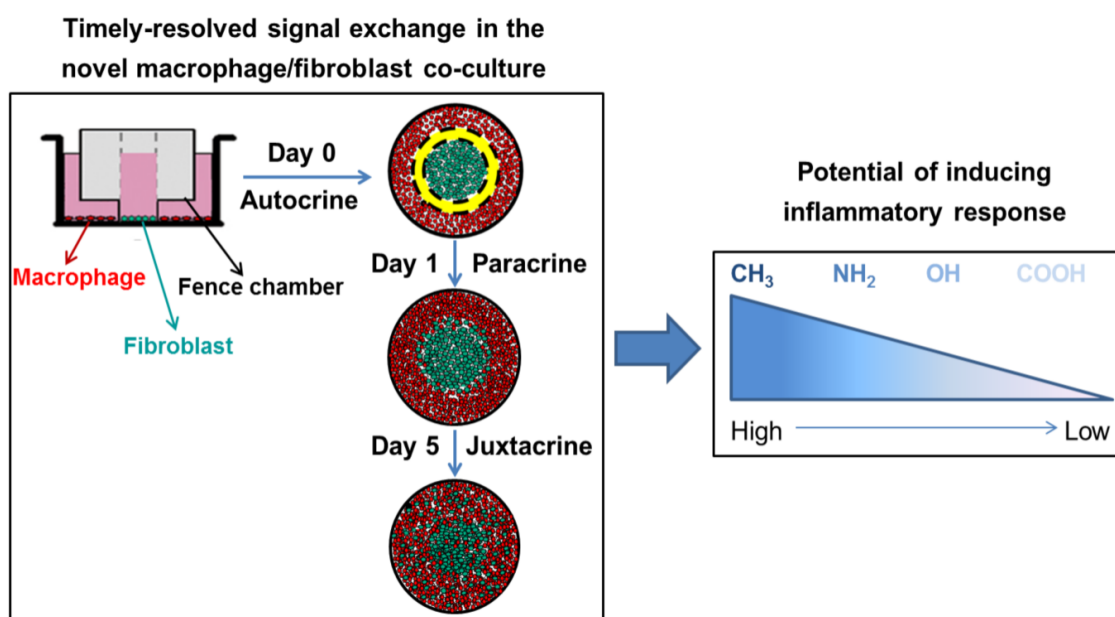
[157] Zaveri TD, Lewis JS, Dolgova NV, Clare-Salzler MJ, Keselowsky BG. Integrin-directed modulation of macrophage responses to biomaterials. *Biomaterials* 2014;35:3504-15.

[158] Gower RM, Boehler RM, Azarin SM, Ricci CF, Leonard JN, Shea LD. Modulation of leukocyte infiltration and phenotype in microporous tissue engineering scaffolds via vector induced IL-10 expression. *Biomaterials* 2014;35:2024-31.

[159] Nakayama Y, Yamaoka S, Nemoto Y, Alexey B, Uchida K. Thermoresponsive heparin bioconjugate as novel aqueous antithrombogenic coating material. *Bioconjugate chemistry* 2011;22:193-9.

## 2 A macrophage/fibroblast co-culture system using a cell migration chamber to study inflammatory effects of biomaterials

Guoying Zhou, Harald Loppnow, Thomas Groth



### 2.1 Abstract

Chronic inflammatory reactions hamper the use of biomaterials after implantation. Thus, the aim of the study was to develop a novel predictive *in vitro* macrophage/fibroblast co-culture model based on cell migration chambers that allows a timely and locally controlled interaction of both cell types to study the inflammatory responses of biomaterials *in vitro*. Here self-assembled monolayers (SAMs) with different wettability and charge properties were used as model biomaterials on which co-cultures were established by use of fence chambers having internal and external compartments. This allowed establishing separated and mixed co-cultures of both cell types before and after removal of the chamber, respectively. The key advantages of this novel co-culture model included not only to establish a timely-resolved study of cytokine release, but also the ability to assess individual macrophage migration in both macrophage mono-cultures and co-cultures. All inflammatory reactions in terms of

macrophage adhesion, macrophage migration, foreign body giant cell (FBGC) formation,  $\beta 1$  integrin expression and pro-inflammatory cytokine production were found strongly surface property dependent. The results show that the hydrophobic  $\text{CH}_3$  surface caused the strongest inflammatory reactions, whereas the hydrophilic/anionic  $\text{COOH}$  surface caused the least inflammatory response, indicating low and high biocompatibility of the surfaces, respectively. Most importantly, we found that both macrophage motility and directional movement were increased in the presence of fibroblasts in co-cultures compared with macrophage mono-cultures. Overall, the novel co-culture system provides access to a range of parameters for studying inflammatory reactions and reveals how material surface properties affect the inflammatory responses.

**Keywords:** inflammation, macrophage, fibroblast, Co-cultures, cytokines

## 2.2 Introduction

Implantation of biomaterials has been widely used nowadays in providing better medical treatment of a large variety of diseases. However, most foreign materials that are implanted into living tissues can trigger a host inflammatory response generally known as foreign body response (FBR) [1-4]. Macrophages and fibroblasts are two major FBR effector cells involved in local implant-associated inflammation, cell recruitment, fibrosis and even implant degradation [5, 6]. Macrophages are recruited rapidly to the implant site and act as the first line of defense, aiming to phagocytose the foreign materials. When macrophages are unable to internalize foreign bodies via phagocytosis due to their large size, they fuse to form foreign body giant cells (FBGC), which is a hallmark of FBR [1, 7]. Besides, in FBR, macrophages and fibroblasts communicate by secreting different mediators including cytokines, chemokines, and growth factors. Secretion of pro-inflammatory cytokines such as interleukin-6 (IL-6) and tumour necrosis factor- $\alpha$  (TNF- $\alpha$ ) by macrophages and fibroblasts is immediately up-regulated in the presence of most foreign materials [8-10]. These soluble signals are recognized by the same cells in an autocrine manner and by neighboring cells in a paracrine manner [11]. Fibroblasts, affected by signals from macrophages can differentiate into myofibroblasts, which produce extracellular matrix (ECM), specifically collagens that finally can lead to implant encapsulation [12]. Since FBR is related to implant failure due to

fibrosis, implant degradation, but also could increase incidence of infection, a better understanding and control of FBR is important for development of biocompatible materials.

*In vitro* cell-based models have been commonly used to study FBR mechanisms. THP-1 cells were often used as model monocyte systems due to their uniform genetic background with no donor variation [13, 14]. Most importantly, THP-1 cells can be differentiated into macrophage-like cells by treatment with phorbol-12-myristate-13-acetate (PMA) [15]. Furthermore, these THP-1-derived macrophages can be further differentiated in a pro-inflammatory M1 phenotype by lipopolysaccharide (LPS) stimulation [7]. Since experimental models applying only one cell type can only identify a limited set of pro-inflammatory signals [16, 17], cell co-culture systems involving two or more types of cells have been employed to mimic more accurately the complexity of the *in vivo* inflammatory situation [11, 18, 19]. So far, different *in vitro* macrophage/fibroblast co-culture models have been used to study inflammatory reactions [18, 20, 21]. However, in most of the previous studies, different cell types were seeded on test materials as mixed cultures, resulting in immediate direct contact of cells [18]. This does not resemble adequately the *in vivo* situation when a time-resolved arrival of cells on the implant surface occurs and a specific spatial and time-dependent release and exchange of signaling molecules occurs. Other experimental settings used membranes to separate the different cell types spatially that no direct contact can occur even at later stages to study the role of released signaling molecules involved in the inflammatory reaction [22].

Material surface properties such as wettability, topography, surface potential and surface chemistry have been proven to affect protein adsorption and cellular behavior on biomaterials [23-27]. Material-dependent monocyte/macrophage adhesion, macrophage fusion into foreign body giant cells (FBGC) and cytokine production have been investigated previously using model biomaterials [28-31]. Most of the studies showed that hydrophobic surfaces promoted pro-inflammatory responses with more monocyte/macrophage adhesion, FBGC formation and pro-inflammatory cytokine production on these surfaces. On the other hand, hydrophilic and anionic surfaces promoted anti-inflammatory response with less monocyte/macrophage adhesion, FBGC formation and pro-inflammatory cytokine production [28, 32]. Self-assembled monolayers (SAMs) of organosilanes are a useful tool to tailor material surfaces to obtain specific surface properties like chemical composition, wettability and surface charge [33-35]. Hence, SAMs have been widely used as a model to study cell-substrate interaction with many kinds of cell types, such as fibroblast, myoblast, endothelial cells, smooth muscle cells, leukocytes and so on [28, 36-38].

To overcome limitations of the previous models, the present study establishes a novel macrophage/fibroblast co-culture system to perform mono-cultures, separate and mixed co-cultures in sequence with one and the same system. This was achieved by the use of migration fence chambers, which possess an internal and an external compartment for seeding macrophages and fibroblast separately on different SAMs, such as methyl (CH<sub>3</sub>), amine (NH<sub>2</sub>), hydroxyl (OH) and carboxyl (COOH) terminated groups. After 24 h-incubation, the fence chambers were removed to allow the exchange of soluble signals, like cytokines between the two cell types, but without direct macrophage-fibroblast contact. Five days later the two cell types have moved towards each other and mixed, which allowed both exchange of soluble signals but also direct cell-cell contacts. In this case, a sequence of studies ranging from mono to separate and mixed co-cultures was performed to mimic autocrine, paracrine and juxtacrine signal transduction between both cell types. The inflammatory reactions on different SAM surfaces were studied in terms of macrophage adhesion, FBGC formation,  $\beta$ 1 integrin expression, pro-inflammatory cytokine production and macrophage migration. Results are reported herein.

## **2.3 Materials and methods**

### **2.3.1 Preparation of self-assembled monolayers (SAMs)**

Glass cover slides (Menzel, Germany) were cleaned by treatment with 0.5 M NaOH in ethanol for 2 h followed by extensive rinsing with double-distilled water (10 × 5 min). Cleaned surfaces were dried with a stream of nitrogen.

The cleaned glass slides were immersed in different silane solutions to prepare self-assembled monolayers (SAMs). Chlorodimethyloctadecylsilane (ODS), 3-aminopropyltriethoxysilane (APTES), glycidoxypropyl trimethoxysilane (GPTMS) and triethoxysilylpropyl succinic anhydride (TESPSA) were obtained from ABCR (Karlsruhe, Germany). The formation of SAMs was performed according to previous studies [39] with slight modifications. CH<sub>3</sub>-terminated SAM were generated by immersion of clean glass in a 5% (v/v) solution of ODS in n-hexane for 16 h at room temperature. Then the surfaces were washed with n-hexane (2 × 5 min), ethanol (2 × 5 min), double-distilled water (6 × 5 min) and dried with a stream of nitrogen. NH<sub>2</sub>-, epoxy- and COOH-terminated surfaces were obtained by immersion of clean glass in 1% (v/v) solution of APTES, GPTMS and TESPSA, respectively, in ethanol for 16 h at room temperature. After that, the surfaces were rinsed extensively with ethanol, washed with double-distilled water (10 × 5 min) and dried with



nitrogen. The epoxy-terminated surfaces were further modified to produce OH-terminated surfaces by immersion in 100 mM HCl at 80 °C for 1 h [39]. Figure 2.1 shows the reaction scheme for the preparation of the SAMs.

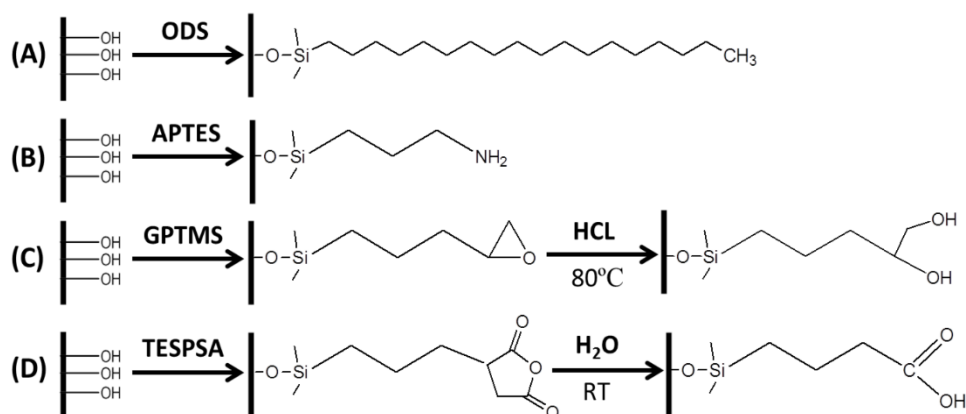


Figure 2.1. Schematic overview of the used SAM surfaces. Four different surfaces (A – D) were prepared. A) ODS, chlorodimethyloctadecylsilane, determined CH<sub>3</sub> in the paper. B) APTES, 3-aminopropyltriethoxysilane, determined NH<sub>2</sub> in the paper. C) GPTMS, glycidoxypropyl trimethoxysilane, determined OH in the paper. D) TESPSA, triethoxysilylpropyl succinic anhydride, determined COOH in the paper. RT, room temperature.

## 2.3.2 Characterization of surface properties of SAMs

### 2.3.2.1 Water contact angle measurements

Dynamic water contact angle (WCA) measurements were done using the sessile drop method at room temperature with OCA 15+ device from Dataphysics (Filderstadt, Germany). The advancing ( $\theta_a$ ) and receding ( $\theta_r$ ) water contact angles were determined by injection and withdrawal of a 5  $\mu$ L ultrapure water droplet with a rate of 0.2  $\mu$ L/s on the SAMs. The means and standard deviations were calculated from two independent experiments, each containing triplicate measurements.

### 2.3.2.2 Zeta potential measurements

Zeta potentials of SAMs were measured with a SurPASS device (Anton Paar, Graz, Austria). Two SAM-coated glass slides were placed oppositely in the SurPASS flow cell. The

width of the flow cell was adjusted to a distance where a flow rate of 100-150 mL/min was achieved at a maximum pressure of 300 mbar. A flow check was performed to achieve a constant flow in both directions. 1 mM potassium chloride (KCl) was used as model electrolyte and 0.1 M hydrochloric acid (HCl) was used for pH titration. The pH value of the electrolyte was adjusted to pH 10.5 using 1 M sodium hydroxide (NaOH) before starting the measurement. Then the measurements were performed by an automated titration program using titration steps of 0.03  $\mu$ L from pH 10.5 to 5.0 and 0.25  $\mu$ L from pH 5.0 to 3.0.

### **2.3.3 Cell experiments**

#### **2.3.3.1 Cell culture**

Cells of the human monocytic cell line THP-1 (DSMZ, Braunschweig, Germany) were cultured in RPMI-1640 medium (Biochrom AG, Berlin, Germany) supplemented with 10% (v/v) fetal bovine serum (FBS, Biochrom AG) and 1% (v/v) antibiotic–antimycotic solution (AAS, Sigma, Deisenhofen, Germany) at 37 °C in a humidified 5% CO<sub>2</sub>/95% air atmosphere using a NUAIRE® DH Autoflow incubator (NuAire Corp., Plymouth, Minnesota, USA). Suspended cells were split by centrifugation. The old medium was removed and the cell pellet was resuspended in fresh medium every second day to obtain a cell density of 0.5-1.0 x 10<sup>6</sup> cells/mL. The THP-1-derived macrophages were obtained by incubation with 200 nM phorbol-12-myristate-13-acetate (PMA, Sigma-Aldrich, Germany) in T75 cell culture flasks (Greiner Bio-One, Frickenhausen, Germany) for 48 h. Then, the PMA-differentiated adherent macrophages were detached by 0.25% trypsin/0.02% EDTA (Biochrom AG) and used for seeding on the SAM surfaces.

Primary human dermal fibroblasts (HF, PromoCell, Heidelberg, Germany,) were grown in Dulbecco's modified Eagle's medium (DMEM, Biochrom AG, Berlin, Germany) supplemented with 10% fetal bovine serum (FBS, Biochrom AG), 1% antibiotic-antimycotic solution (AAS, Sigma-Aldrich, Germany) at 37 °C in a humidified 5% CO<sub>2</sub>/95% air atmosphere. Cells were harvested after confluence by treatment with 0.25% trypsin/0.02% EDTA (Biochrom AG) for 5 min at 37 °C. The fibroblasts were used before passage 10 in this study.

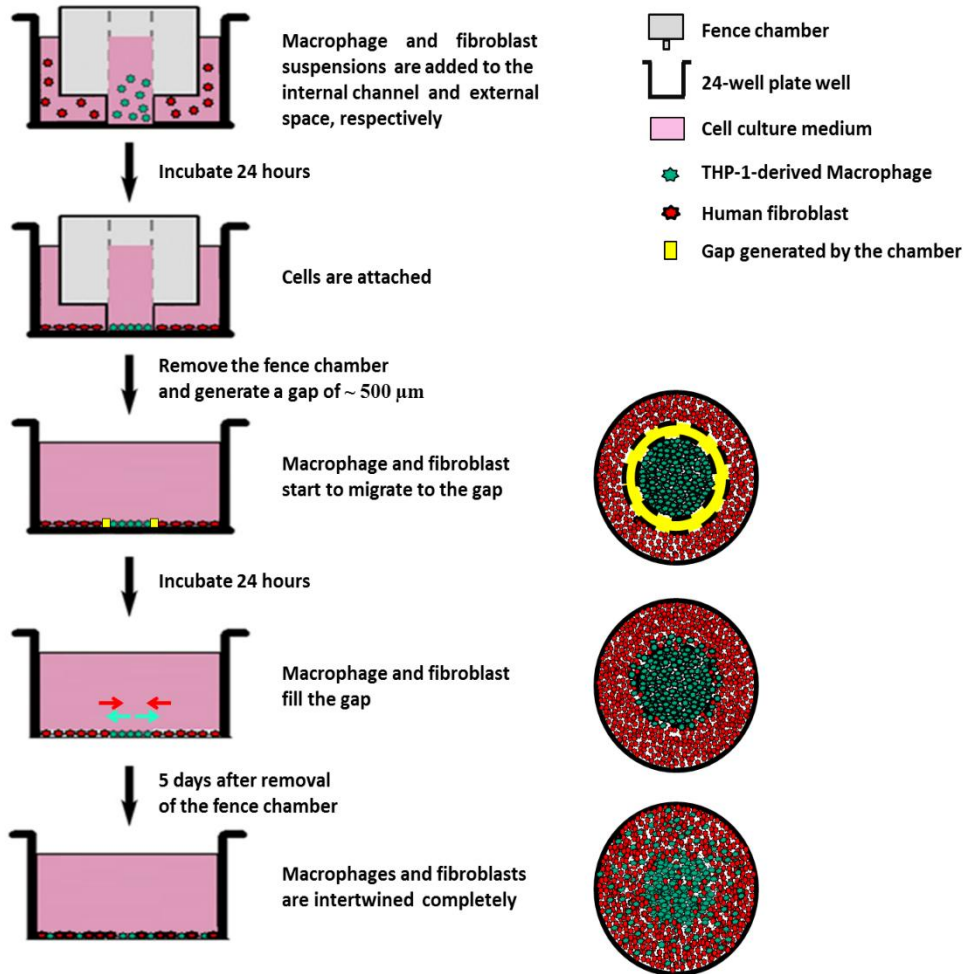


Figure 2.2. Schematic description of the establishment of the macrophage/fibroblast co-culture model using the cell migration fence chamber.

### 2.3.3.2 Establishment of the co-culture model

Cell migration fence chambers (Aix Scientifics, Aachen, Germany) [40], which possess an internal and external compartment, were used to seed macrophages and fibroblasts separately. Figure 2.2 shows the scheme for the establishment of the macrophage/fibroblast co-culture model with the cell migration fence chamber in the 24-well plates. 0.15 mL of a macrophage cell suspension with a cell density of  $5.0 \times 10^5$  cells/mL was seeded into the internal channel, while 0.65 mL of a fibroblast cell suspension with a cell density of  $5.0 \times 10^5$  cells/mL was seeded into the external compartment of the chamber for each well. The macrophage mono-cultures were performed under the same condition but with only 0.65 mL DMEM in the external compartment and vice versa for fibroblast mono-cultures. After incubation for 24 h, the fence chambers were removed, resulting in a gap of approximately

500 µm between the two cell types, allowing the exchange of soluble signals between the two cell types.

#### 2.3.3.3 Cell adhesion studies

THP-1-derived macrophages were seeded on SAM surfaces at a cell density of  $2.5 \times 10^4$  cells/mL. Cultures were incubated at 37 °C in a humidified 5% CO<sub>2</sub>/95% air atmosphere for 24 h. Then, the surfaces were gently washed with PBS once to remove the unbound macrophages. The attached cells were fixed with methanol and stained by 10% (v/v) Giemsa (Merck KGaA, Darmstadt, Germany) solution. The images of adherent macrophages were taken with a light microscope (Axiovert 100, Carl Zeiss MicroImaging GmbH, Germany) equipped with a CCD camera (Sony, MC-3254, AVT-Horn, Aalen, Germany).

#### 2.3.3.4 Foreign body giant cell (FBGC) characterization

The FBGC formation on different surfaces was evaluated 10 days after the removal of the fence chambers. The surfaces were gently washed with PBS once. The adherent cells were fixed with methanol and stained by 10% (v/v) Giemsa solution. Cells were photographed as described above. The area percentage of FBGC on different SAM surfaces was calculated with image analyzing software (ImageJ, version 1.46r).

#### 2.3.3.5 β1 integrin expression

The β1 integrin expression on different surfaces was evaluated 10 days after removal of fence chambers by immunofluorescence staining [41, 42]. The cells were fixed with 4% paraformaldehyde solution and then permeabilized with 0.1% (v/v) Triton X-100 for 10 min. After two times rinsing with PBS, the non-specific binding sites were blocked with 1% (w/v) bovine serum albumin (BSA) for 1 h. Antibodies were diluted in 1% (w/v) BSA in PBS. The cells were firstly incubated with a mouse monoclonal antibody against β1 integrin (1:50, Santa Cruz Biotechnology, Germany) for 30 min at room temperature. Subsequently, after washing the samples twice with PBS, the cells were incubated with the secondary goat-anti-mouse antibody conjugated with Cy2 (1:100, Dianova, Germany) for another 30 min. Then, nuclei were stained by To-Pro-3 (1:500, Invitrogen, Germany) for 30 min. The samples were finally washed with PBS, mounted with Mowiol (Calbiochem, Darmstadt, Germany) and examined with confocal laser scanning microscopy (CLSM, LSM 710, Carl Zeiss, Oberkochen, Germany)

using a 40x oil immersion objective. Images were processed with the ZEN2011 software (Carl Zeiss, Oberkochen, Germany).

#### 2.3.3.6 Pro-inflammatory cytokine production assays

Supernatants from co-cultures were collected on day 0, 1 and 10 after removal of fence chambers to study the cytokine release by cells. In a further set of experiments, 1 µg/mL of lipopolysaccharide (LPS, Sigma-Aldrich, Germany) was added to challenge the cells for 24 h in macrophage mono-, fibroblast mono- and co-culture samples immediately after removal of the chambers. Medium without LPS was used as a negative control. The supernatants of untreated and LPS-challenged samples were collected after additional 24 h incubation after removal of the chambers and used for cytokine release analysis.

Pro-inflammatory cytokine production of IL-6 and TNF-α by cells cultured on SAMs was measured using enzyme-linked immunosorbent assay (ELISA) according to the manufacturer's instructions (BD Biosciences Pharmingen, Heidelberg, Germany). To normalize cytokine production to the quantity of metabolic active cells on different SAMs, the cell viability was determined by Qblue cell viability assay according to manufacturer's instructions (BioChain, Newark, USA). Briefly, after supernatant collection for cytokine measurement, the cells were carefully washed once with sterile PBS and then 500 µL of pre-warmed colorless DMEM with Qblue assay reagent (10:1) were added to each well and incubated at 37 °C for 2 h. Thereafter, 100 µL supernatant from each well was transferred to a black 96-well plate and the relative fluorescence unit (RFU) values were measured at an excitation wavelength of 544 nm and emission wavelength of 590 nm with a plate reader (FLUOstar, BMG LabTech, Offenburg, Germany). The cytokine quantities were then normalized to the RFU values.

#### 2.3.3.7 Macrophage migration studies

0.15 mL of THP-1 cell suspension ( $2.5 \times 10^4$  cells/mL) with 200 nM PMA and 0.65 mL of HF cell suspension ( $2 \times 10^5$  cells/mL) were seeded into the internal and external compartment of the chamber, respectively. The chamber was removed after 48 h and the surfaces were washed once with PBS to remove non-adherent cells. The samples were transferred to a sterile Petri dish and covered by 2.5 mL fresh RPMI with 20 mM HEPES buffer (Biochrom AG, Berlin, Germany). To keep the cells alive, an incubation chamber with temperature control

(PeCon, Germany) was used to maintain the incubation condition at 37 °C with constant supply of carbogen (5% CO<sub>2</sub>/95% air). Macrophage migration was studied with a phase contrast microscope (Axiovert 100, Germany) equipped with CCD camera and software to allow time lapse microscopy. Micrographs were collected every 15 min over a period of 24 h. After collecting the time lapse images, the cell migration behavior such as migration distance and directional movement were evaluated with Gradientech Tracking Tool (Gradientech, Uppsala, Sweden).

#### **2.3.4 Statistics**

All data are represented as mean values ± standard deviations (SD). Statistical analysis was performed using one-way ANOVA followed by post hoc Tukey testing. The number of samples has been indicated in the respective figures. The significance level was set as  $p < 0.05$  and is indicated by an asterisk.

## **2.4 Results and discussion**

### **2.4.1 Surface properties of SAMs**

The wettability of SAMs was determined by advancing ( $\theta_a$ ) and receding ( $\theta_r$ ) contact angles (Figure 2.3). SAMs terminated with  $-\text{CH}_3$  were found to be hydrophobic surfaces with  $\theta_a \sim 106^\circ$ , while SAMs with  $-\text{NH}_2$  [43] and epoxy groups [44] formed moderately wettable surfaces with  $\theta_a \sim 50^\circ$ . SAMs terminated by COOH groups expressed more highly wettable surfaces with  $\theta_a \sim 33^\circ$ , which corresponds well to previous findings [36, 45]. After modification with HCl, the advancing contact angle of the epoxy surfaces decreased from  $54^\circ$  to  $38^\circ$ , which indicated the conversion of epoxy to OH groups according to previous protocols [39] forming a further hydrophilic model surface. Overall, the results of the water contact angle measurements were consistent with previous studies [36, 44-48].

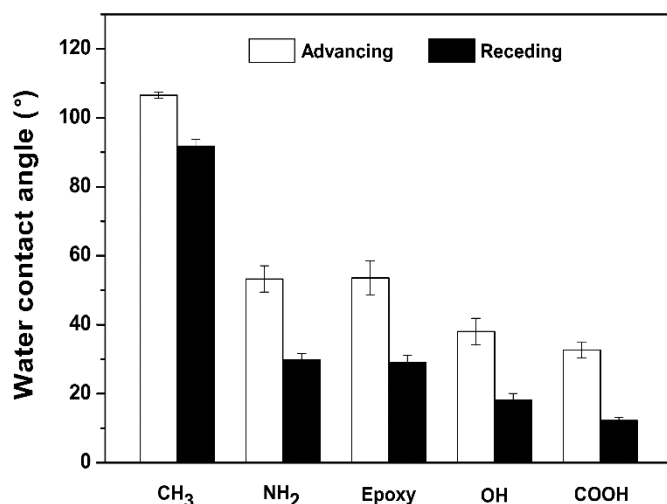


Figure 2.3. Results of dynamic water contact angle measurements of self-assembled monolayers with different terminal groups. The wetting properties were characterised by measuring advancing (white bars) and receding (black bars) water contact angles using the sessile drop method. Data represent mean  $\pm$  SD,  $n = 6$ .

Figure 2.4 shows the zeta potentials of SAMs in dependence on the pH value of the electrolyte solution (1 mM KCl). The bare glass, OH, and COOH SAMs had negative surface potentials throughout the whole measured pH range, while CH<sub>3</sub> and NH<sub>2</sub> surfaces had an isoelectric point (IEP) at pH 3.4 and 4.8, respectively. The comparison of the absolute zeta-potential values of the SAMs at pH 7.4 was: NH<sub>2</sub> (-36 mV) > OH (-47 mV) > COOH (-87 mV) > CH<sub>3</sub> (-94 mV) > Glass (-109 mV). Compared to bare glass, the zeta potential values of all modified SAM surfaces were higher at pH 7.4, indicating the successful immobilization of the organosilanes and formation of SAMs. The highest potential on NH<sub>2</sub> surface at pH 7.4 was due to the partial protonation of amino groups in the low pH region [49]. The neutral OH and CH<sub>3</sub> surfaces had negative zeta potentials at pH 7.4, which are due to a preferential anion adsorption on non-charged surfaces [50, 51]. The COOH surface possessed a negative surface potential from pH 3–10 and a plateau at the basic pH region due to the presence of dissociable acidic groups on this surface [49, 52].

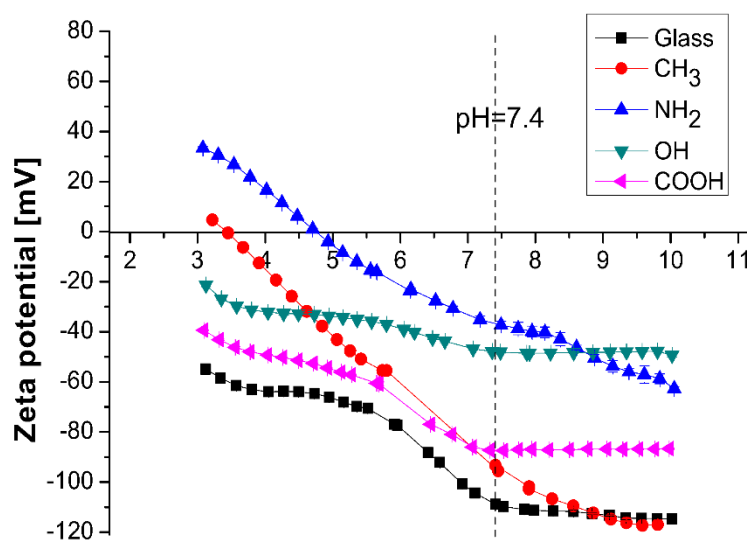


Figure 2.4. The zeta potentials of the SAMs with different terminating groups and glass. Zeta potentials were measured in the pH range 3–10.

The physical characterization studies showed that the functionalized SAM surfaces displayed different wetting and surface charge properties. Therefore, these surfaces were considered as good models to study the effect of surface properties and functional groups on macrophage activation.

#### 2.4.2 Adhesion and fusion of macrophages

Figure 2.5A shows the morphology of macrophages on the different SAM surfaces after 24 h of culture in RPMI medium with 10% serum. It can be seen that the cells on CH<sub>3</sub> and NH<sub>2</sub> surfaces were spreading more (yellow arrows) than cells on OH and COOH surfaces. Even, initial macrophage fusions were observed on CH<sub>3</sub> and NH<sub>2</sub> SAMs (red arrows); while no macrophage fusion was found on the other SAMs. The fusion of macrophages has been related to a lower biocompatibility of biomaterials [1]. The quantitative data of macrophage adhesion on the different surfaces are summarized in Figure 2.5B. The data show that cell adhesion on CH<sub>3</sub> and NH<sub>2</sub> surfaces was significantly higher ( $p < 0.05$ ) than on OH and COOH SAMs. Considering the serum used in the medium, it can be anticipated that CH<sub>3</sub> and NH<sub>2</sub> SAMs bind adhesion promoting proteins like fibronectin and vitronectin from serum [53, 54], which further promoted macrophage adhesion. By contrast, previous studies showed that little serum protein adsorption takes place on OH SAMs [36] while proteins like fibronectin and albumin adsorbed on COOH surface were easily eluted [55], which may explain partly the lower macrophage adhesion than on CH<sub>3</sub> and NH<sub>2</sub> SAMs. On the other hand, complement



activation is believed to be a trigger of inflammatory cells [56, 57]. Barbosa et al. showed previously that the OH surface had higher capacity to activate the complement system than COOH surface [58]. Hence, the results of adhesion studies were consistent with previous findings and showed a ranking of surface chemistries regarding their ability to promote macrophage adhesion: hydrophobic ( $\text{CH}_3$ ) > cationic ( $\text{NH}_2$ ) > hydrophilic (OH) > anionic (COOH) [32].

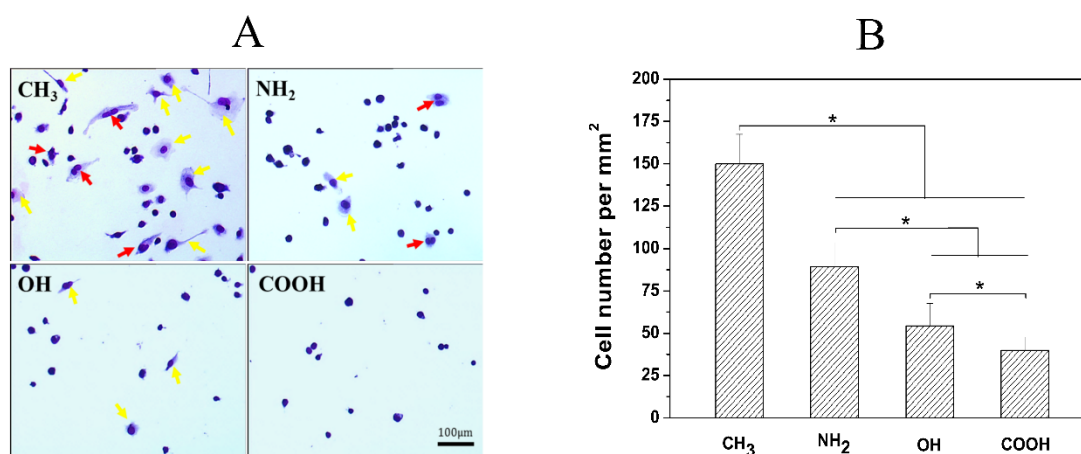


Figure 2.5. (A) Transmitted light microscopic images of macrophage adhesion on different surfaces. THP-1 cells were differentiated into macrophage cells by incubation with 200 nM PMA for 48 h. The THP-1-derived macrophage cells were then detached and seeded on SAMs for 24 h in serum-containing RPMI medium. The attached macrophages on different surfaces were stained by 10% (v/v) Giemsa solution [scale bar: 100  $\mu\text{m}$ ]. The red arrows show the initial fusion of macrophages and the yellow arrows show the spreading cells. (B) Cell numbers of adhering macrophages per area on different SAM surfaces were determined after 24 h incubation in serum-containing medium. Data represent mean  $\pm$  SD,  $n = 4$ , \* $p < 0.05$ .

It is well known that macrophages fuse to form foreign body giant cells (FBGCs) to increase the phagocytosis ability when foreign materials are too large for phagocytosis by a single cell [1, 7]. Hence, the formation of FBGC is a hallmark of foreign body response (FBR) which represents a measure of biocompatibility of materials [59, 60]. Macrophage fusion on SAMs followed a similar trend as observed during macrophage adhesion experiments. Figure 2.6 shows that there was marked macrophage fusion on all the surfaces in macrophage

mono-cultures in terms of more than 2 nuclei in one cell body. Macrophage fusion was detected by a central accumulation of nuclei surrounded by a larger area of cell cytoplasm than in single macrophages. The highest degree of fusion was observed with macrophages cultured on hydrophobic CH<sub>3</sub> SAM, resulting in the formation of large FBGCs with more than 10 nuclei within an extensively spread cell body. In contrast, much less macrophage fusion occurred on anionic COOH SAMs. Figure 2.7 shows the area percentages of FBGCs on SAMs with the order of CH<sub>3</sub> > NH<sub>2</sub> ~ OH > COOH in macrophage mono-cultures. Interestingly, it was found that FBGC formation was greatly reduced in the presence of fibroblasts except for CH<sub>3</sub>, while the differences among NH<sub>2</sub>, OH and COOH surfaces were negligible. So far, the effect of fibroblasts on macrophage fusion is still not well understood. Previous studies reported that MCP-1 production was increased in the presence of fibroblasts in macrophage cultures [61], and MCP-1 probably played a role in promoting FBGC formation [62], which seems contradictory to our findings here. However, the co-culture systems used previously were different from the present study. Here, the two cell types were separated initially. After removal of chambers, the fibroblasts grew from the original region and expanded slowly to the macrophage region. As shown in a later section of this work, presence of fibroblasts promotes motility of macrophages that start to migrate to the fibroblast region. As a result, less macrophages were left for fusion in the original macrophage region. The lower decrease of macrophage fusion on CH<sub>3</sub> SAM in co-cultures compared to the other surfaces is also related to a reduced ability of fibroblasts to colonize this surface [Zhou et al. under preparation].

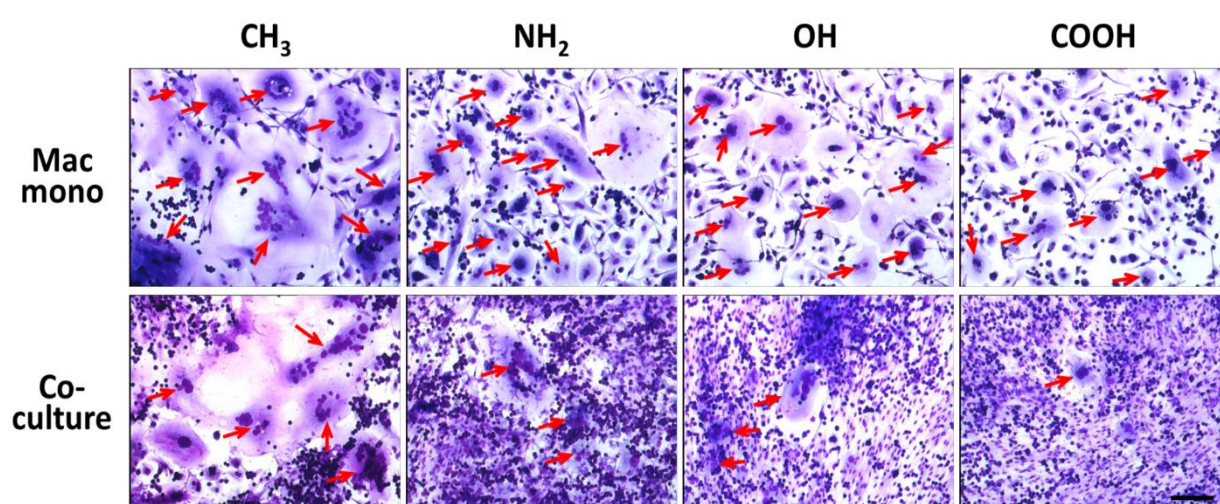


Figure 2.6. Transmitted light microscopic images of Giemsa staining of FBGC in macrophage mono-culture (upper row) and macrophage/fibroblast co-cultures (lower row) on CH<sub>3</sub>, NH<sub>2</sub>,

OH and COOH surfaces for 10 days after removal of fence chambers. The red arrow shows the FBGCs. Bar = 200  $\mu\text{m}$ .

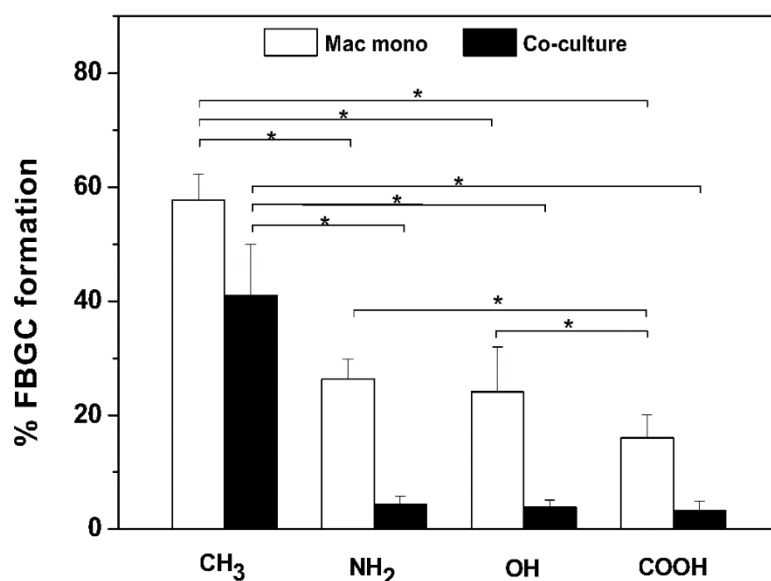


Figure 2.7. The area percentage of FBGCs on SAM surfaces was determined 10 days after removal of fence chambers in macrophage mono-cultures (white bars) and macrophage/fibroblast co-cultures (black bars) by quantitative evaluation of micrographs. Data represent mean  $\pm$  SD,  $n \geq 10$ ,  $*p < 0.05$ .

It has been reported that both  $\beta 1$  and  $\beta 2$  integrins are involved in monocyte/macrophage adhesion [41, 42]. However, it was claimed that  $\beta 2$  integrins mediate mainly the initial monocyte adhesion, while  $\beta 1$  integrins start to dominate during macrophage development from monocytes and are strongly expressed in fusing macrophages and FBGCs [41, 42]. Therefore the focus of this study was on visualization of  $\beta 1$  integrins, to serve as another parameter for the pro-inflammatory activity of biomaterials. Figure 2.8 shows that the  $\beta 1$  integrin expression visualized in green, was mostly located around the nuclei of macrophages, which is in line with previous studies [42]. It was also observed that the expression of  $\beta 1$  integrin was stronger in FBGCs on CH<sub>3</sub> and NH<sub>2</sub> SAMs and much weaker on OH and COOH SAMs. In addition, the cells on the CH<sub>3</sub> and NH<sub>2</sub> SAMs expressed more nuclei per cell body indicating the formation of FBGCs, whereas the cells on the OH and COOH SAMs expressed fewer nuclei. Anderson et al. found previously that  $\beta 1$  integrin is highly expressed during fusion of macrophages and IL-4-induced FBGC formation [42]. Our results further confirmed his findings and revealed that the higher extent of fusion (more nuclei per cell body) was accompanied by a more striking  $\beta 1$  integrin expression.

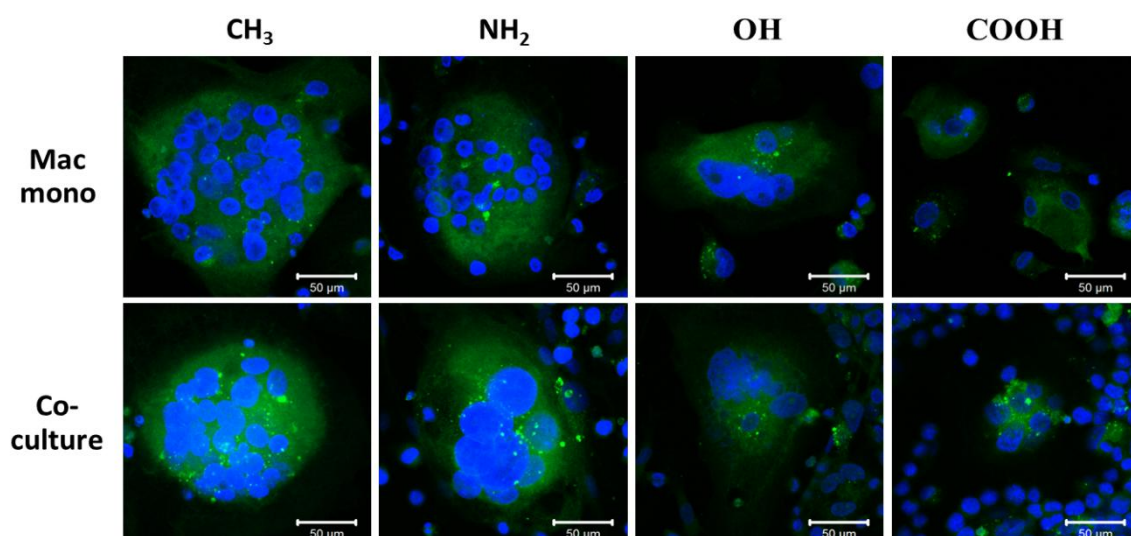


Figure 2.8. Expression of  $\beta 1$  integrin was determined on fusing macrophages/FBGCs in macrophage mono-cultures (upper row) and macrophage/fibroblast co-cultures (lower row) on CH<sub>3</sub>, NH<sub>2</sub>, OH and COOH surfaces 10 days after removal of the fence chambers. Cells were fixed with 4% paraformaldehyde and stained for  $\beta 1$  integrin (green) and nuclei (To-pro-3, blue). Bar in all figures = 50  $\mu$ m.

### 2.4.3 Release of pro-inflammatory cytokines

The production of pro-inflammatory cytokines, such as IL-6 and TNF- $\alpha$ , in the cell cultures may reflect the potential of compounds to induce inflammatory reactions and, therefore, may describe the biocompatibility of a given material [1, 60]. LPS can activate macrophages and up-regulate the pro-inflammatory cytokine release [63, 64]. In addition, injuries, but sometimes also implantation of biomaterials, is complicated by bacterial infections. Hence, LPS was used to challenge the cells in addition to the exposure to SAMs expressing different surface characteristics.

Figure 2.9 shows the IL-6 and TNF- $\alpha$  production by cells on SAMs after an additional 24 h incubation with 1  $\mu$ g/mL (+ LPS) or without LPS (-LPS) after removal of the fence chamber. The production of the pro-inflammatory cytokine IL-6 was up-regulated in all cultures after LPS treatment, indicating that the macrophages expressed a M1 functional phenotype [7]. Macrophage mono-cultures and co-cultures adherent to the hydrophobic CH<sub>3</sub> SAM produced the greatest amounts of IL-6, while the more hydrophilic COOH, OH and NH<sub>2</sub> surfaces caused less IL-6 production. This indicates that the IL-6 release was provoked by the effect of hydrophobicity of CH<sub>3</sub> SAM. The data also show that the IL-6 release from co-cultures on all

surfaces after LPS treatment was much higher than the arithmetic sum of cytokine release on the corresponding macrophage and fibroblast mono-cultures, which indicates a cooperative action of both cell types in the co-cultures [11]. This is in line with previous reports, showing synergistic IL-6 and MCP-1 production in co-cultures of monocytes and vascular smooth muscle cells [65-67]. On the other hand, TNF- $\alpha$  production of LPS-stimulated macrophages was stimulated by CH<sub>3</sub> SAM only but not by the presence of fibroblasts. Furthermore, the TNF- $\alpha$  release in non-stimulated (-LPS) and LPS-stimulated (+LPS) co-cultures was not different. These data suggest that fibroblasts did not produce significant quantities of TNF- $\alpha$ , but reduced TNF- $\alpha$  production of macrophages in the co-culture. Also, in other studies such reduction of TNF- $\alpha$  release by macrophages was found in the presence of fibroblast-released cytokines [11, 68].

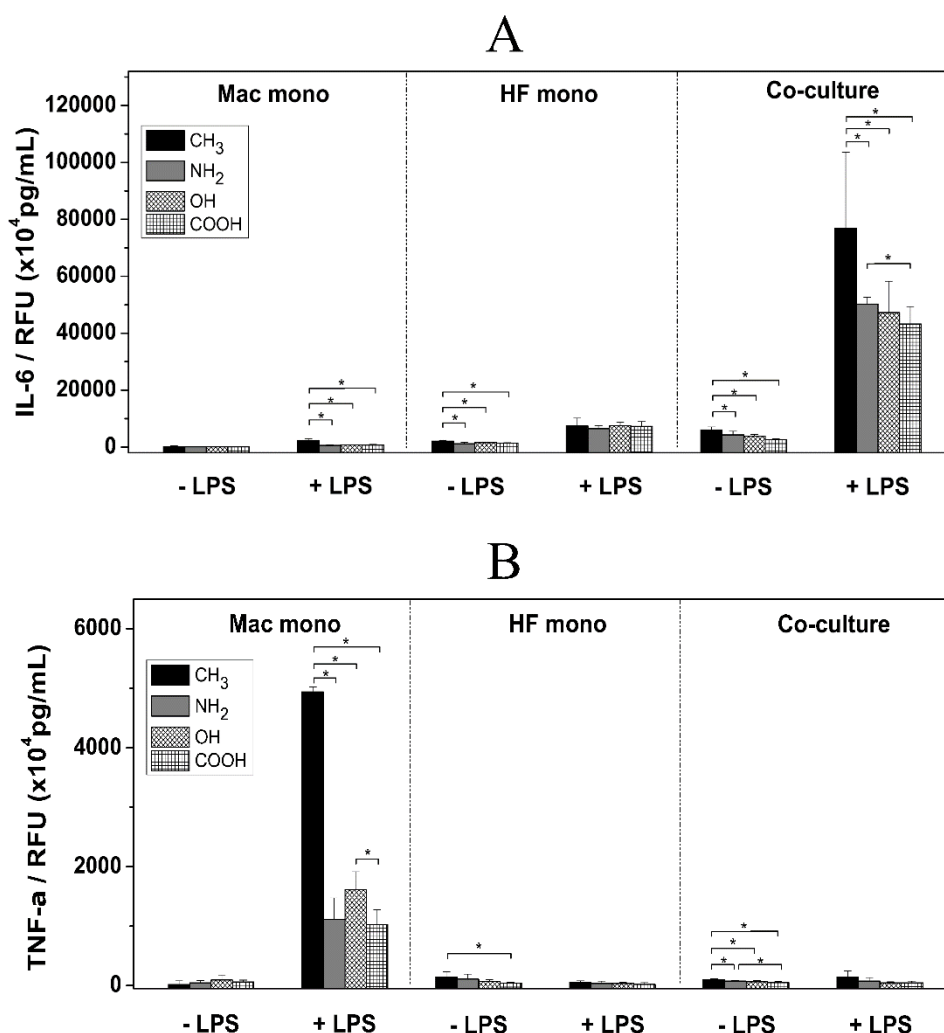


Figure 2.9. IL-6 (A) and TNF- $\alpha$  (B) production of macrophage mono-cultures (Mac mono), fibroblast mono-cultures (HF mono) and macrophage/ fibroblast co-cultures (Co-culture) was

measured after additional 24 h of incubation with (+ LPS) or without 1  $\mu\text{g}/\text{mL}$  LPS (-LPS) after removal of the fence chamber. Data represent mean  $\pm$  SD,  $n = 6$ ,  $*p < 0.05$ .

While the addition of LPS was used to mimic a situation of inflammation resulting from bacterial infection, later a situation of sterile inflammatory response was simulated by a time course study of cytokine release without LPS challenge. Figure 2.10 shows that in the co-cultures both IL-6 and TNF- $\alpha$  production were lowest at day 0 after removal of the chambers because the two cell types were separated without any paracrine/juxtacrine signal exchange. However, the IL-6 and TNF- $\alpha$  production on day 1 increased compared with day 0, which indicates a paracrine effect on the cytokine release in the co-culture. The production of both cytokines at day 10 compared with day 1 was reduced on all surfaces. This may model a wound healing processes at day 10 *in vitro* by suppression of pro-inflammatory cytokine production possibly also due to direct macrophage-fibroblast interactions as discussed previously by other authors [28, 69]. In addition, it was found again that the hydrophobic  $\text{CH}_3$  SAMs produced the highest levels of both IL-6 and TNF- $\alpha$ , especially during the earlier period of the investigated time-scale (day 0 and day 1). This further indicates the higher potential of  $\text{CH}_3$  SAMs to induce pro-inflammatory responses being in line with many other studies.

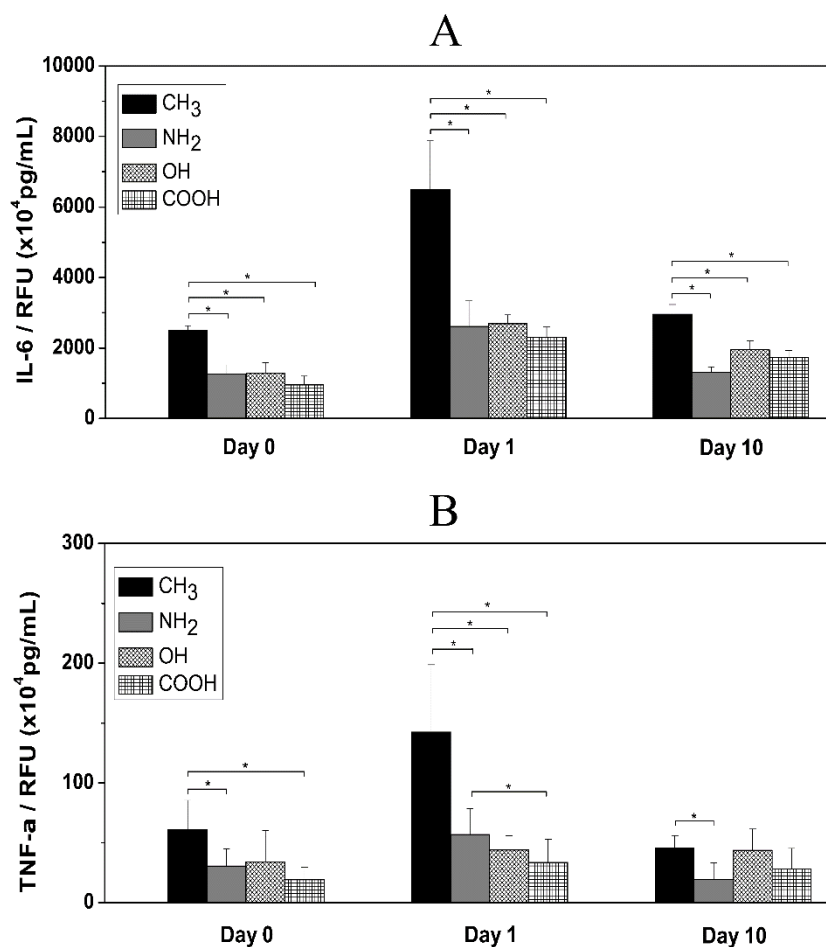


Figure 2.10. The IL-6 (A) and TNF- $\alpha$  (B) production on SAM surfaces in macrophage/fibroblast co-cultures at day 0, 1 and 10 days after removal of the fence chamber was determined. Data represent mean  $\pm$  SD,  $n = 6$ ,  $*p < 0.05$ .

#### 2.4.4 Macrophage migration studies

To investigate the surface effects and fibroblast contribution in co-cultures on macrophage migration, macrophages were viewed by phase contrast microscopy in intervals of 15 min for a 24 h period after removal of the fence chamber in both macrophage mono-cultures and macrophage/fibroblast co-cultures. It was observed in previous studies that there are two kinds of adherent macrophages on biomaterial surfaces defined as motile or stationary fraction [70]. Since the stationary cells have a limited movement and no large overall change in final position, only the motile macrophages were analyzed here.

Figure 2.11A shows the quantitative data of accumulated distance of migrating macrophages during the 24 h period. The highest and lowest macrophage motility was found

on OH (Supplementary Video 1) and COOH (Supplementary Video 2) SAMs, respectively. This was observed in both macrophage mono-cultures and co-cultures, illustrated by their accumulated distance, while macrophages on CH<sub>3</sub> and NH<sub>2</sub> SAMs had intermediate accumulated distances. It was reported elsewhere that OH-functionalized surfaces triggered a higher recruitment of CD11b+ cells and cell infiltration in animal implantation assays [71]. This could be related to the strong complement activation by OH groups via the alternative pathway activation [58] and could explain the higher motility of macrophages in the present study due to the presence of serum. In the case of CH<sub>3</sub> and NH<sub>2</sub> surfaces, probably stronger protein adsorption may lead to stronger adhesion of cells and is also well in line with the finding of macrophage adhesion in this study. The lowest macrophage motility was found on COOH SAMs, which is also consistent with previous studies showing that the COOH surface elicited only a weak inflammatory response [72]. Additionally, it was found that the accumulated distance increased in co-cultures compared with their corresponding mono-cultures, although there was no significant difference on NH<sub>2</sub> and COOH surfaces. This is probably due to the presence of fibroblasts, which can secrete paracrine signals such as chemokines to increase the motility of macrophages [6].

Figure 2.11B shows the percentage of the directional movement of cells which represents macrophages migrating into the direction of fibroblasts across the gap generated by removal of the chamber. It was found that the directional movement percentage was ~50% on all SAM in mono-cultures, indicating that the cells migrated randomly in the absence of fibroblasts. By contrast, the directional movement was increased significantly in co-cultures on CH<sub>3</sub> (Supplementary Videos 3 and 4) and NH<sub>2</sub>, but not on OH and COOH surfaces. The increase of directionality of macrophage migration in co-cultures might be attributed to fibroblasts secreting paracrine signals such as monocyte chemoattractant protein-1 (MCP-1) [73]. Even though we did not investigate MCP-1 production, it is known from the literature that it has the similar trend with IL-6 production [65]. We assume that chemokines secreted by fibroblast were released and sensed by macrophages, which did not only increase the random (accumulated distance) but also directional movement of macrophages. The lack of a significant increase of directional movement of macrophages in co-cultures on OH and COOH SAMs could be related to the lower levels of IL-6 production on these surfaces compared to CH<sub>3</sub> and NH<sub>2</sub> SAMs. On the other hand, it was notable that OH SAMs provoked the highest macrophage motility but no increase in directional movement in co-cultures. This could be explained by the low adhesiveness of this surface, but also by effects of complement activation through hydroxyl groups leading to random movement of macrophages [74].



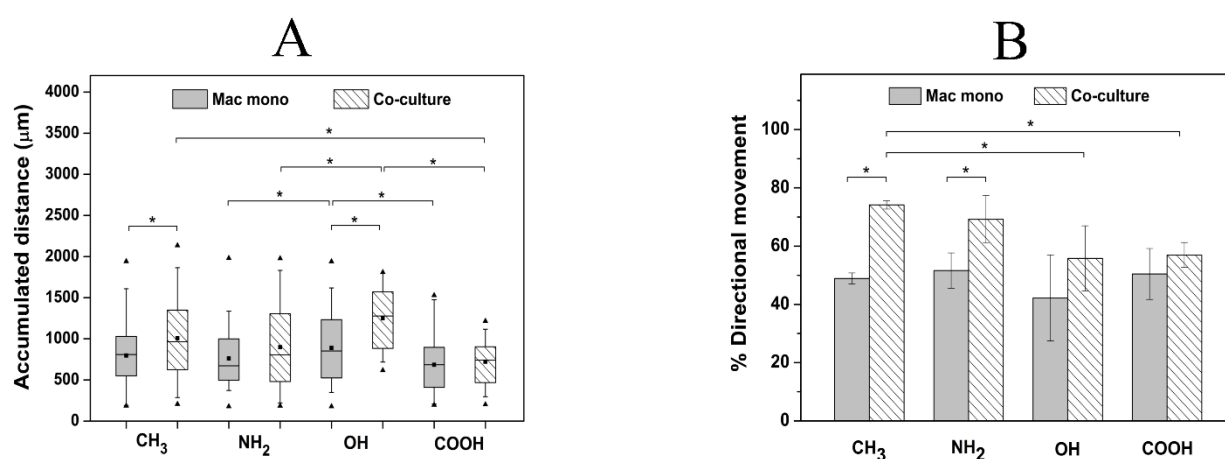


Figure 2.11. (A) The accumulated distance of macrophage migration on different SAM surfaces within a 24 h migration period in macrophage mono-cultures (grey bars) and macrophage/fibroblast co-cultures (white bars). Box-whisker diagrams indicate the 25th and 75th percentile, the median (dash) and mean (black square) values, respectively,  $n \geq 30$ ,  $*p < 0.05$ . (B) The percentage of macrophages that migrate to the direction of the gap generated by the removal of the fence chambers within a 24 h migration period in macrophage mono-cultures (grey bars) and macrophage/fibroblast co-cultures (white bars). Data represent mean  $\pm$  SD,  $n \geq 3$ ,  $*p < 0.05$ .

## 2.5 Conclusion

In this work, a novel macrophage/fibroblast co-culture model was established and used to investigate the effect of material surface properties on regulation of inflammatory responses *in vitro*. Taken together with macrophage adhesion, fusion,  $\beta 1$  integrin expression and pro-inflammatory cytokine production, the data consistently show that the hydrophobic CH<sub>3</sub> and COOH SAMs possessed the highest and lowest potential to induce inflammatory responses, respectively. These findings suggest that the hydrophilic/anionic COOH groups represent a low pro-inflammatory potential, which is also supported by the use of hydrogel-based coatings composed of poly(acrylic acid), developed to modulate events associated with inflammation after implantation [75-78], or hydrophilic/anionic hydrogel coatings that significantly reduced the tissue responses in drug delivery and neural electrode applications [77, 79, 80]. More important, however, is the obvious advantage of the co-culture system of macrophages and fibroblasts presented here to mimic autocrine, paracrine and

juxtacrine signals exchange during biomaterial contact in one system. A further advantage of the systems is the possibility to investigate the macrophage migration behavior in both mono-cultures and co-cultures. In summary, we conclude that the novel co-culture model can provide useful information for a better understanding of the complexity of the *in vivo* inflammatory processes, used to study the inflammatory potential of biomaterials *in vitro* under more adequate co-culture conditions and may also be a useful tool in the design of new biomaterials with low inflammatory potential.

## 2.6 Disclosure

No conflicts of interests are declared.

## 2.7 Acknowledgements

G. Zhou thanks the China Scholarship Council for offering the scholarship to work in Germany. The assistance of Mrs. M. Porobin in zeta potential measurement is gratefully acknowledged. We also thank Mrs. S. Koch and Mrs. C. Pilowski for the technical assistance in the ELISA measurements.

## 2.8 Appendix. Supplementary data

Supplementary data associated with this article can be found, in the online version.

## 2.9 References

- [1] Anderson JM, Rodriguez A, Chang DT. Foreign body reaction to biomaterials. *Semin Immunol* 2008;20:86-100.
- [2] Wynn TA. Cellular and molecular mechanisms of fibrosis. *Journal of Pathology* 2008;214:199-210.
- [3] Lin T-h, et al. Chronic inflammation in biomaterial-induced periprosthetic osteolysis: NF-kappa B as a therapeutic target. *Acta Biomaterialia* 2014;10:1-10.

[4] Dalby MJ, Marshall GE, Johnstone HJH, Affrossman S, Riehle MO. Interactions of human blood and tissue cell types with 95-nm-high nanotopography. *IEEE Trans Nanobiosci* 2002;1:18-23.

[5] Glaros T, Larsen M, Li LW. Macrophages and fibroblasts during inflammation, tissue damage and organ injury. *Front Biosci* 2009;14:3988-93.

[6] Barron L, Wynn TA. Fibrosis is regulated by TH2 and TH17 responses and by dynamic interactions between fibroblasts and macrophages. *American Journal of Physiology-Gastrointestinal and Liver Physiology* 2011;300:G723-G8.

[7] Kou PM, Babensee JE. Macrophage and dendritic cell phenotypic diversity in the context of biomaterials. *J Biomed Mater Res A* 2011;96A:239-60.

[8] Seki E, et al. TLR4 enhances TGF-beta signaling and hepatic fibrosis. *Nature Medicine* 2007;13:1324-32.

[9] Martin CA, Dorf ME. Interleukin-6 production by murine macrophage cell lines P388D1 and J774A.1: stimulation requirements and kinetics. *Cell Immunol* 1990;128:555-68.

[10] Xia Z, Triffitt JT. A review on macrophage responses to biomaterials. *Biomed Mater* 2006;1:R1-R9.

[11] Holt DJ, Chamberlain LM, Grainger DW. Cell-cell signaling in co-cultures of macrophages and fibroblasts. *Biomaterials* 2010;31:9382-94.

[12] Westergren-Thorsson G, et al. Pathological airway remodelling in inflammation. *Clin Respir J* 2010;4:1-8.

[13] Theus SA, Cave MD, Eisenach KD. Activated thp-1 cells: An attractive model for the assessment of intracellular growth rates of mycobacterium tuberculosis isolates. *Infect Immun* 2004;72:1169-73.

[14] Schildberger A, Rossmann E, Eichhorn T, Strassl K, Weber V. Monocytes, peripheral blood mononuclear cells, and THP-1 cells exhibit different cytokine expression patterns following stimulation with lipopolysaccharide. *Mediators of Inflammation* 2013;2013:697972.

[15] Park EK, Jung HS, Yang HI, Yoo MC, Kim C, Kim KS. Optimized THP-1 differentiation is required for the detection of responses to weak stimuli. *Inflammation Research* 2007;56:45-50.

[16] Chamberlain LM, Godek ML, Gonzalez-Juarrero M, Grainger DW. Phenotypic non-equivalence of murine (monocyte-) macrophage cells in biomaterial and inflammatory models. *J Biomed Mater Res A* 2009;88A:858-71.

[17] Schutte RJ, Parisi-Amon A, Reichert WM. Cytokine profiling using monocytes/macrophages cultured on common biomaterials with a range of surface chemistries. *J Biomed Mater Res A* 2009;88A:128-39.

[18] Pan H, Jiang HL, Kantharia S, Chen WL. A fibroblast/macrophage co-culture model to evaluate the biocompatibility of an electrospun Dextran/PLGA scaffold and its potential to induce inflammatory responses. *Biomedical Materials* 2011;6.

[19] Parks AC, Sung K, Wu BM. A three-dimensional in vitro model to quantify inflammatory response to biomaterials. *Acta Biomaterialia* 2014;10:4742-9.

[20] Zeng Q, Chen W. The functional behavior of a macrophage/fibroblast co-culture model derived from normal and diabetic mice with a marine gelatin oxidized alginate hydrogel. *Biomaterials* 2010;31:5772-81.

[21] Swartzlander MD, Lynn AD, Blakney AK, Kyriakides TR, Bryant SJ. Understanding the host response to cell-laden poly(ethylene glycol)-based hydrogels. *Biomaterials* 2013;34:952-64.

[22] Mensink A, Mul FPJ, van der Wijk T, Brouwer A, Koeman JH. Macrophages influence gap junctional intercellular communication between smooth muscle cells in a co-culture model. *Environmental Toxicology and Pharmacology* 1998;5:197-203.

[23] Llopis-Hernandez V, Rico P, Ballester-Beltran J, Moratal D, Salmeron-Sanchez M. Role of surface chemistry in protein remodeling at the cell-material interface. *Plos One* 2011;6.

[24] Bota PCS, et al. Biomaterial topography alters healing in vivo and monocyte/macrophage activation in vitro. *J Biomed Mater Res Part A* 2010;95A:649-57.

[25] Groth T, Altankov G, Klosz K. Adhesion of human peripheral-blood lymphocytes is dependent on surface wettability and protein preadsorption. *Biomaterials* 1994;15:423-8.

[26] Lourenco BN, et al. Wettability influences cell behavior on superhydrophobic surfaces with different topographies. *Biointerphases* 2012;7.

[27] Fedel M, Motta A, Maniglio D, Migliaresi C. Surface properties and blood compatibility of commercially available diamond-like carbon coatings for cardiovascular devices. *J Biomed Mater Res Part B* 2009;90B:338-49.

[28] Brodbeck WG, Nakayama Y, Matsuda T, Colton E, Ziats NP, Anderson JM. Biomaterial surface chemistry dictates adherent monocyte/macrophage cytokine expression in vitro. *Cytokine* 2002;18:311-9.

[29] Chang DT, et al. Lymphocyte/macrophage interactions: Biomaterial surface-dependent cytokine, chemokine, and matrix protein production. *J Biomed Mater Res A* 2008;87A:676-87.

[30] Maciel J, Oliveira MI, Goncalves RM, Barbosa MA. The effect of adsorbed fibronectin and osteopontin on macrophage adhesion and morphology on hydrophilic and hydrophobic model surfaces. *Acta Biomaterialia* 2012;8:3669-77.

[31] Battiston KG, Labow RS, Santerre JP. Protein binding mediation of biomaterial-dependent monocyte activation on a degradable polar hydrophobic ionic polyurethane. *Biomaterials* 2012;33:8316-28.

[32] Brodbeck WG, Shive MS, Colton E, Nakayama Y, Matsuda T, Anderson JM. Influence of biomaterial surface chemistry on the apoptosis of adherent cells. *J Biomed Mater Res* 2001;55:661-8.

[33] Ostuni E, Chapman RG, Holmlin RE, Takayama S, Whitesides GM. A survey of structure-property relationships of surfaces that resist the adsorption of protein. *Langmuir* 2001;17:5605-20.

[34] Ulman A. Formation and structure of self-assembled monolayers. *Chem Rev* 1996;96:1533-54.

[35] Schreiber F. Structure and growth of self-assembling monolayers. *Prog Surf Sci* 2000;65:151-256.

[36] Faucheux N, Schweiss R, Lutzow K, Werner C, Groth T. Self-assembled monolayers with different terminating groups as model substrates for cell adhesion studies. *Biomaterials* 2004;25:2721-30.

[37] Goncalves IC, Martins MCL, Barbosa JN, Oliveira P, Barbosa MA, Ratner BD. Platelet and leukocyte adhesion to albumin binding self-assembled monolayers. *J Mater Sci-Mater Med* 2011;22:2053-63.

[38] Arima Y, Iwata H. Effect of wettability and surface functional groups on protein adsorption and cell adhesion using well-defined mixed self-assembled monolayers. *Biomaterials* 2007;28:3074-82.

[39] Toworfe GK, Composto RJ, Shapiro IM, Ducheyne P. Nucleation and growth of calcium phosphate on amine-, carboxyl- and hydroxyl-silane self-assembled monolayers. *Biomaterials* 2006;27:631-42.

[40] Fischer EG, Stingl A, Kirkpatrick CJ. Migration assay for endothelial-cells in multiwells - application to studies on the effect of opioids. *J Immunol Methods* 1990;128:235-9.

[41] McNally AK, MacEwan SR, Anderson JM. Alpha subunit partners to  $\beta 1$  and  $\beta 2$  integrins during IL-4-induced foreign body giant cell formation. *J Biomed Mater Res A* 2007;82A:568-74.

[42] McNally AK, Anderson JM. Beta 1 and beta 2 integrins mediate adhesion during macrophage fusion and multinucleated foreign body giant cell formation. *Am J Pathol* 2002;160:621-30.

[43] Katzur V, et al. Surface-immobilized pamam-dendrimers modified with cationic or anionic terminal functions: Physicochemical surface properties and conformational changes after application of liquid interface stress. *J Colloid Interface Sci* 2012;366:179-90.

[44] Luzinov I, Julthongpiput D, Liebmann-Vinson A, Cregger T, Foster MD, Tsukruk VV. Epoxy-terminated self-assembled monolayers: Molecular glues for polymer layers. *Langmuir* 2000;16:504-16.

[45] Faucheux N, Tzoneva R, Nagel MD, Groth T. The dependence of fibrillar adhesions in human fibroblasts on substratum chemistry. *Biomaterials* 2006;27:234-45.

[46] Schutte RJ, Xie LL, Klitzman B, Reichert WM. In vivo cytokine-associated responses to biomaterials. *Biomaterials* 2009;30:160-8.

[47] Altankov G, Grinnell F, Groth T. Studies on the biocompatibility of materials: Fibroblast reorganization of substratum-bound fibronectin on surfaces varying in wettability. *J Biomed Mater Res* 1996;30:385-91.

[48] Lee MH, Brass DA, Morris R, Composto RJ, Ducheyne P. The effect of non-specific interactions on cellular adhesion using model surfaces. *Biomaterials* 2005;26:1721-30.

[49] Shyue JJ, De Guire MR. Acid-base properties and zeta potentials of self-assembled monolayers obtained via in situ transformations. *Langmuir* 2004;20:8693-8.

[50] Werner C, Jacobasch HJ, Reichelt G. Surface characterization of hemodialysis membranes based on streaming potential measurements. *J Biomat Sci-Polym E* 1995;7:61-76.

[51] Werner C, Korber H, Zimmermann R, Dukhin S, Jacobasch HJ. Extended electrokinetic characterization of flat solid surfaces. *J Colloid Interface Sci* 1998;208:329-46.

[52] Cheng SS, Scherson DA, Sukenik CN. In-situ attenuated total reflectance fourier-transform infrared-spectroscopy of carboxylate-bearing, siloxane-anchored, self-assembled monolayers - a study of carboxylate reactivity and acid-base properties. *Langmuir* 1995;11:1190-5.

[53] Keselowsky BG, Collard DM, Garcia AJ. Surface chemistry modulates focal adhesion composition and signaling through changes in integrin binding. *Biomaterials* 2004;25:5947-54.

[54] Grinnell F, Feld MK. Fibronectin adsorption on hydrophilic and hydrophobic surfaces detected by antibody-binding and analyzed during cell-adhesion in serum-containing medium. *J Biol Chem* 1982;257:4888-93.

[55] Tidwell CD, Ertel SI, Ratner BD, Tarasevich BJ, Atre S, Allara DL. Endothelial cell growth and protein adsorption on terminally functionalized, self-assembled monolayers of alkanethiolates on gold. *Langmuir* 1997;13:3404-13.

[56] Liu L, Elwing H. Complement activation on solid-surfaces as determined by C3 deposition and hemolytic consumption. *J Biomed Mater Res* 1994;28:767-73.

[57] Falkenhagen D, et al. Behavior of white blood-cells and the complement-system. *Nephrol Dial Transplant* 1993;8:8-14.

[58] Barbosa JN, Barbosa MA, Aguas AP. Inflammatory responses and cell adhesion to self-assembled monolayers of alkanethiolates on gold. *Biomaterials* 2004;25:2557-63.

[59] Anderson JM. Biological responses to materials. *Ann Rev Mater Res* 2001;31:81-110.

[60] Anderson JM, Miller KM. Biomaterial biocompatibility and the macrophage. *Biomaterials* 1984;5:5-10.

[61] Zickus C, et al. Differential regulation of C-C chemokines during fibroblast-monocyte interactions: Adhesion vs. Inflammatory cytokine pathways. *Mediators of Inflammation* 1998;7:269-74.

[62] Kyriakides TR, et al. The CC chemokine ligand, CCL2/MCP1, participates in macrophage fusion and foreign body giant cell formation. *Am J Pathol* 2004;165:2157-66.

[63] Loppnow H, Brade H, Rietschel ET, Flad HD. Induction of cytokines in mononuclear and vascular cells by endotoxin and other bacterial products. *Methods Enzymol* 1994;236:3-10.

[64] Loppnow H, et al. IL-1 induction-capacity of defined lipopolysaccharide partial structures. *J Immunol* 1989;142:3229-38.

[65] Chen L, et al. Interaction of vascular smooth muscle cells and monocytes by soluble factors synergistically enhances IL-6 and MCP-1 production. *American Journal of Physiology-Heart and Circulatory Physiology* 2009;296:H987-H96.

[66] Fu H, et al. Interleukin-1 potently contributes to 25-hydroxycholesterol-induced synergistic cytokine production in smooth muscle cell-monocyte interactions. *Atherosclerosis* 2014;237:443-52.

[67] Loppnow H, et al. Statins potently reduce the cytokine-mediated IL-6 release in SMC/MNC cocultures. *Journal of Cellular and Molecular Medicine* 2011;15:994-1004.

[68] Vancheri C, et al. Human lung fibroblasts inhibit tumor necrosis factor-alpha production by LPS-activated monocytes. *Am J Resp Cell Mol* 1996;15:460-6.

[69] Jones JA, et al. Proteomic analysis and quantification of cytokines and chemokines from biomaterial surface-adherent macrophages and foreign body giant cells. *J Biomed Mater Res Part A* 2007;83A:585-96.

[70] Jenney CR, DeFife KM, Colton E, Anderson JM. Human monocyte/macrophage adhesion, macrophage motility, and IL-4-induced foreign body giant cell formation on silane-modified surfaces in vitro. *J Biomed Mater Res* 1998;41:171-84.

[71] Nair A, Zou L, Bhattacharyya D, Timmons RB, Tang L. Species and density of implant surface chemistry affect the extent of foreign body reactions. *Langmuir* 2008;24:2015-24.



[72] Kamath S, Bhattacharyya D, Padukudru C, Timmons RB, Tang L. Surface chemistry influences implant-mediated host tissue responses. *J Biomed Mater Res Part A* 2008;86A:617-26.

[73] Lukacs NW, et al. Production of monocyte chemoattractant protein-1 and macrophage inflammatory protein-1-alpha by inflammatory granuloma fibroblasts. *Am J Pathol* 1994;144:711-8.

[74] Deshmane SL, Kremlev S, Amini S, Sawaya BE. Monocyte chemoattractant protein-1 (MCP-1): An overview. *J Interferon Cytokine Res* 2009;29:313-26.

[75] de Giglio E, et al. Biocompatibility of poly(acrylic acid) thin coatings electro-synthesized onto titanium-based implants. *J Bioact Compat Polym* 2010;25:374-91.

[76] Bridges AW, et al. Chronic inflammatory responses to microgel-based implant coatings. *J Biomed Mater Res Part A* 2010;94A:252-8.

[77] Lu Y, et al. Poly(vinyl alcohol)/poly(acrylic acid) hydrogel coatings for improving electrode-neural tissue interface. *Biomaterials* 2009;30:4143-51.

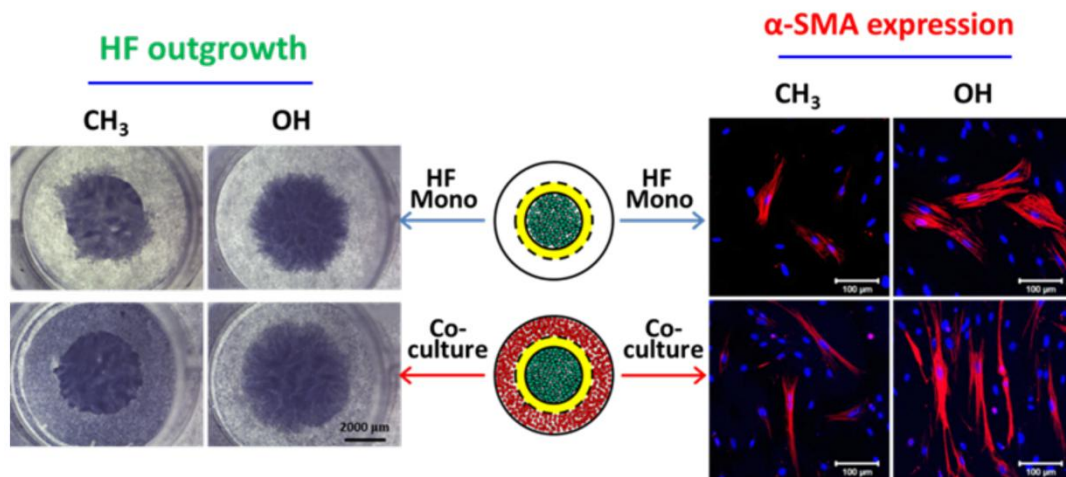
[78] Bridges AW, Singh N, Burns KL, Babensee JE, Lyon LA, Garcia AJ. Reduced acute inflammatory responses to microgel conformal coatings. *Biomaterials* 2008;29:4605-15.

[79] Gong S, Tu H, Zheng H, Xu H, Yin Y. Chitosan-g-PAA hydrogels for colon-specific drug delivery: Preparation, swelling behavior and in vitro degradability. *Journal of Wuhan University of Technology-Materials Science Edition* 2010;25:248-51.

[80] Nho Y-C, Park J-S, Lim Y-M. Preparation of poly(acrylic acid) hydrogel by radiation crosslinking and its application for mucoadhesives. *Polymers* 2014;6:890-8.

### 3 A fibroblast/macrophage co-culture system to study host responses of model biomaterials

Guoying Zhou, Thomas Groth



#### 3.1 Abstract

Surface properties are believed to play important roles in initial inflammatory and subsequent fibrotic responses after implantation of biomaterials. To investigate the surface property effect in mediating these host responses, we used an *in vitro* fibroblast/macrophage co-culture model established with a cell migration chamber, and a series of self-assembling monolayers (SAMs) bearing different terminal groups as model surfaces to study the effect of surface properties on fibroblast attachment, spreading morphology, proliferation, outgrowth, as well as pro- (Interleukin-6) and anti- (Interleukin-10) inflammatory cytokine production, expression of ED-A fibronectin (FN) and alpha-smooth muscle actin ( $\alpha$ -SMA). The obtained results show that the hydrophobic CH<sub>3</sub> surfaces caused high levels of inflammatory but low levels of fibrotic responses, while the hydrophilic/anionic COOH surface resulted in both low levels of inflammatory and fibrotic responses. Interestingly, the hydrophilic OH surface was found to possess low potential of inducing inflammatory response but high potential of inducing fibrotic responses. These results reveal that the extent of inflammation and fibrosis

might not be always related *in vitro*. However, more important is the observation of macrophage contributions in facilitating the fibrotic responses by up-regulation of fibroblast outgrowth, cytokine production as well as ED-A FN and  $\alpha$ -SMA expression. Overall, by linking the surface properties to cell activities, we could provide useful clues for designing of more biocompatible biomaterials for biomedical and tissue engineering applications.

**Keywords:** inflammation, fibrosis, macrophage, fibroblast, myofibroblast, cytokines

## 3.2 Introduction

The implantation of biomaterials often triggers a series of host responses, among which the chronic inflammation and fibrotic encapsulation at the end stage are main important concerns for the design of biocompatible materials [1]. Macrophages and fibroblasts are two dominating effector cells involved in the cascade of host reactions [2]. Although macrophages are more dominant during the inflammatory responses while fibroblasts are more crucial during wound healing and fibrosis, the regulation of the whole host responses needs the orchestration of both cell types by soluble signals such as cytokines, chemokines, and growth factors, but also fixed cues through direct cell-cell contacts [3]. Additionally, we and many others have shown that macrophages, in the presence of foreign materials, can produce significant amounts of pro-inflammatory and pro-fibrotic cytokines, such as interleukin-1 $\beta$  (IL-1 $\beta$ ), interleukin-6 (IL-6), tumour necrosis factor- $\alpha$  (TNF- $\alpha$ ), and transforming growth factor- $\beta$  (TGF- $\beta$ ), which are believed to affect the ensuing fibrotic reactions [4, 5]. Acting on these signals, fibroblasts can be activated in terms of up-regulation of fibroblast proliferation, migration, expansion, synthesis of extracellular matrix (ECM) such as collagens, and finally leading to implant encapsulation [6]. Thereupon, fibroblasts can differentiate into myofibroblasts, characterized by expression of ED-A splice variant of fibronectin (ED-A FN) and  $\alpha$ -smooth muscle actin ( $\alpha$ -SMA), which are incorporated into stress fibres and thereby produce contractile forces to promote wound healing, but also scar formation [7]. However, the prolonged presence of myofibroblasts can lead to excessive collagen production and tissue contraction, which turns to fibrosis ultimately [8]. Since fibrosis is one of the key factors leading to failure of medical implants, it has become an ubiquitous problem and global burden.

In order to know more about fibrosis and improve the implant function and longevity, intensive research work has been done to study host responses by using different *in vitro* and *in vivo* models [9, 10]. Due to the key effects of macrophages and fibroblasts in regulation of inflammation and fibrotic reactions, different *in vitro* macrophages/fibroblasts co-culture models have been used to study inflammation and fibrosis [11, 12]. However, most of the studies focused only on the pro-inflammatory responses while studies of the fibrotic reactions are largely missing [13]. On the other hand, self-assembling monolayers (SAMs) or micron-sized particles with different functional groups, were implanted in subcutaneous air pouches of a mice model to investigate the surface chemistry effect on fibrous capsule formation [14]. But a systematic study to correlate the surface properties with a wide scale of inflammatory reactions and fibrotic processes is still lacking. Furthermore, macrophages and fibroblasts were used to correlate the effect of surface properties on cellular behaviour, conditioned medium from one cell type was used to challenge the other one, and thus lack of in-situ signal exchanges, but also missed a more accurate way to mimic the complexity of the *in vivo* situations [15].

To overcome limitations of the previous models, we present here an *in vitro* fibroblast/macrophage co-culture system with the use of migration fence chambers, which possess an internal and an external compartment, to allow seeding of fibroblast and macrophages separately on model biomaterials. After 24h incubation, the fence chambers were removed to allow the exchange of soluble signals, and at the same time for fibroblast outgrowth, macrophage migration and interaction of the two cell types. THP-1 cells were applied and differentiated into macrophage-like cells by treatment with phorbol-12-myristate-13-acetate (PMA) [16] due to their uniform genetic background with the advantage of no donor variation [17]. Besides, previous evidences have supported that the THP-1-derived macrophages upon PMA treatment were with M2 wound healing functional profiles [18], which seems to be suitable for the fibrotic response studies done here. On the other hand, SAMs possess a well-defined chemistry to tailor the material surfaces to obtain specific surface properties and are suitable to study interactions with proteins and cells [19]. Therefore, SAMs with methyl (CH<sub>3</sub>), amine (NH<sub>2</sub>), hydroxyl (OH) and carboxyl (COOH) terminated groups having different wettability and surface potentials were used here as model surfaces to compare the surface chemistry effect on the host responses by fibroblasts and macrophages. The host reactions on different SAM surfaces were studied with respect to fibroblast attachment, spreading morphology, fibroblast proliferation, outgrowth, as well as

pro- (IL-6) and anti- (IL-10) inflammatory cytokine production and expression of two markers for myofibroblasts, namely ED-A FN and  $\alpha$ -SMA. Results are reported herein.

### **3.3 Materials and Methods**

#### **3.3.1 Preparation of self-assembling monolayers (SAMs)**

Round glass cover slides ( $\varnothing$ 15 mm, Menzel, Germany) were cleaned with 0.5 M NaOH in 96% ethanol (Roth, Germany) for 2 h. Subsequently, the slides were extensively rinsed with double-distilled water (10 $\times$ 5 min) and dried under nitrogen flow.

SAMs with different terminated groups were obtained by immersing the cleaned glass slides in different silane solutions. Chlorodimethyloctadecylsilane (ODS), 3-aminopropyltriethoxysilane (APTES), glycidoxypropyl trimethoxysilane (GPTMS) and triethoxysilylpropyl succinic anhydride (TESPSA) were all obtained from ABCR (Karlsruhe, Germany). The formation of SAMs was performed according to previously described report [20] with slight modifications, and also reported in our previous work [12]. Briefly, CH<sub>3</sub>-terminated SAMs were generated by immersion of clean glass in a 5% (v/v) solution of ODS in n-hexane for 1 h at room temperature. Then the surfaces were washed with n-hexane (2 $\times$ 5 min), ethanol (2 $\times$ 5 min), double-distilled water (6 $\times$ 5 min) and dried under nitrogen flow. NH<sub>2</sub>-, epoxy- and COOH-terminated surfaces were obtained by immersion of clean glass in 1% (v/v) solution of APTES, GPTMS and TESPSA, respectively, in ethanol for 16 h at room temperature. After immersion, the surfaces were rinsed extensively with ethanol, washed with double-distilled water (10 $\times$ 5 min) and dried with nitrogen. The OH-terminated surfaces were obtained by further treatment of epoxy-terminated surfaces in 100 mM HCl at 80 °C for 1 h [20].

#### **3.3.2 Characterization of surface properties of SAMs**

##### **3.3.2.1 Water contact angle measurements**

Static water contact angle (WCA) measurements were carried out using sessile drop method at room temperature with OCA 15+ device from Dataphysics (Filderstadt, Germany). Five droplets of 2  $\mu$ L ultrapure water were dropped onto each surface and the obtained values were used to calculate means and standard deviations. The experiments were run in triplicate and means and standard deviations of two independent experiments were calculated.

### 3.3.2.2 Zeta Potential measurements

Zeta potentials of different SAMs were measured with a SurPASS device (Anton Paar, Graz, Austria). Two SAM-coated glass slides were fixed and placed oppositely into the adjustable gap cell. The width of the flow cell was adjusted to a distance where a flow rate of 100 to 150 mL min<sup>-1</sup> was achieved at a maximum pressure of 300 mbar. A flow check was performed to achieve a constant flow in both directions. 1 mM potassium chloride (KCl) was used as model electrolyte and 100 mM hydrochloric acid (HCl) was used for pH titration. The pH value of the KCl was adjusted to pH 10.5 using 1 M sodium hydroxide (NaOH) before starting the measurement. Finally, the measurements were performed by an automated titration program using titration steps of 0.03 µL from pH 10.5 to 5.0 and 0.25 µL from pH 5.0 to 3.0.

### 3.3.3 Cell experiments

#### 3.3.3.1 Cell culture

Primary human dermal fibroblasts (HF, PromoCell, Heidelberg, Germany,) were grown in Dulbecco's modified Eagle's medium (DMEM, Biochrom AG, Berlin, Germany) supplemented with 10% fetal bovine serum (FBS, Biochrom AG), 1% antibiotic-antimycotic solution (AAS, Sigma-Aldrich, Germany) at 37 °C in a humidified 5% CO<sub>2</sub>/95% air atmosphere using a NUAIRE® DH Autoflow incubator (NuAire Corp., Plymouth, Minnesota, USA). Cells were harvested after confluence by treatment with 0.25% trypsin/0.02% EDTA (Biochrom AG) for 5 min at 37 °C. The fibroblasts were used before passage 10 in the present study.

Cells of the human monocytic cell line THP-1 (DSMZ, Braunschweig, Germany) were cultured in RPMI-1640 medium (Biochrom AG, Germany) supplemented with 10% (v/v) FBS (Biochrom AG) and 1% (v/v) AAS (Sigma-Aldrich, Germany) at 37 °C in a humidified 5% CO<sub>2</sub>/95% air atmosphere. Suspended cells were split by centrifugation. The old medium was removed and the cell pellet was resuspended in fresh medium every second day in order to maintain a cell density of 0.5-1.0 x 10<sup>6</sup> cells mL<sup>-1</sup>. The THP-1-derived macrophages were obtained by incubation of THP-1 cells with 200 nM phorbol-12-myristate-13-acetate (PMA, Sigma-Aldrich, Germany) for 48 h in T75 cell culture flasks (Greiner Bio-One, Frickenhausen, Germany). Afterwards, the PMA-differentiated adherent macrophages were detached by 0.25% trypsin/0.02% EDTA (Biochrom AG) and used for seeding in the co-culture systems.

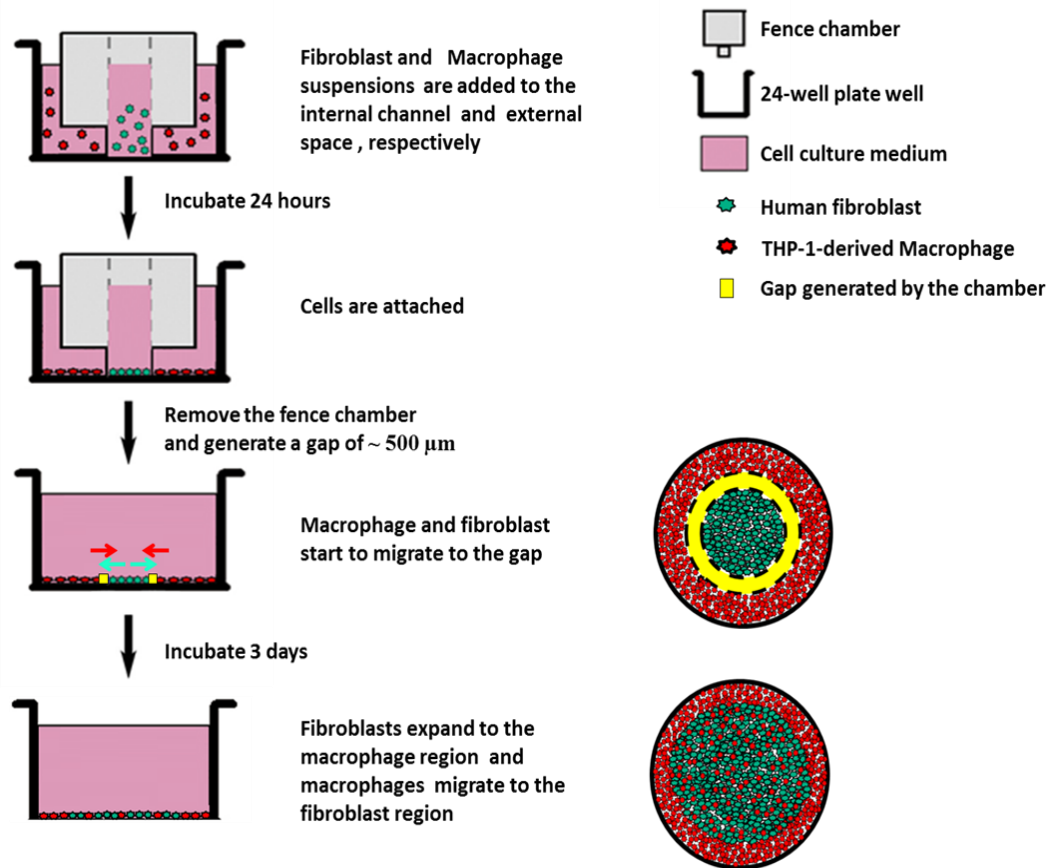


Figure 3.1. Schematic description for establishment of the fibroblast/macrophage co-culture model using the cell migration fence chamber.

### 3.3.3.2 Establishment of the co-culture model

Cell migration fence chambers (Aix Scientifics, Aachen, Germany) [21], which possess internal and external compartments were used to separate fibroblasts and macrophages at the beginning. Figure 3.1 shows the scheme for establishment of the fibroblast/macrophage co-culture model with cell migration fence chambers in a 24-well plate. 0.15 mL of a HF cell suspension with a cell density of  $2.5 \times 10^4$  cells  $\text{mL}^{-1}$  was seeded into the internal channel of the fence chamber, while 0.65 mL of a macrophage cell suspension with a cell density of  $5.0 \times 10^5$  cells  $\text{mL}^{-1}$  was seeded into the external compartment of the chamber for each well. The HF mono-culture contained the same condition of HFs but with only 0.65 mL RPMI in the external compartment. After incubation for 24 h, the fence chambers were removed, resulting in a gap of approximately 500  $\mu\text{m}$  between the two cell types, allowing for the exchange of soluble signals and interactions between the two cell types.

### 3.3.3.3 HF adhesion studies

HF cells were seeded on SAM surfaces at a cell density of  $2.5 \times 10^4$  cells mL<sup>-1</sup> in serum-containing DMEM medium. Cultures were incubated at 37 °C in a humidified 5% CO<sub>2</sub>/95% air atmosphere for 4 h. Afterwards, the surfaces were gently washed with PBS once to remove the unbound HF cells. The attached cells were fixed and stained by 0.5% (w/v) crystal violet (Carl Roth, Karlsruhe, Germany) in methanol. The images of adherent HF cells were taken with a light microscope (Axiovert 100, Carl Zeiss MicroImaging GmbH, Germany) equipped with a CCD camera (Sony, MC-3254, AVT-Horn, Aalen, Germany). Cell number and area on different surfaces were evaluated by ImageJ (version 1.46r).

### 3.3.3.4 Immunofluorescence staining of HF cells

The HF cells were treated and incubated the same as described above. After 24 h incubation, the attached HF cells on different surfaces were fixed with 4% (w/v) paraformaldehyde (PFA, Sigma-Aldrich, Germany) in PBS for 15 min. Then the cells were permeabilized with 0.1% (v/v) Triton X-100 (Sigma, Germany) for 10 min. After two times rinsing with PBS, the non-specific binding sites were blocked by incubation with 1% (w/v) bovine serum albumin (BSA, Merk, Germany) for 1 h. Antibodies were diluted in 1% (w/v) BSA in PBS. The cells were firstly incubated with a mouse monoclonal antibody against vinculin (1:100, Sigma, Germany) for 30 min at room temperature. Subsequently, after washing with PBS twice, the secondary goat-anti-mouse antibody conjugated with CY2 (1:100, Dianova, Germany) were incubated with the cells for another 30 min. Actin and nuclei were stained by Bodipy® Phalloidin (1:50, Invitrogen, Germany) and TO-PRO3 (1:500, Invitrogen, Germany) by 30 min incubation each. The samples were then washed, mounted with Mowiol (Calbiochem, Darmstadt, Germany) and examined with confocal laser scanning microscopy (CLSM, LSM 710, Carl Zeiss, Oberkochen, Germany) using a 63x oil immersion objective. Images were processed with the ZEN2011 software (Carl Zeiss, Oberkochen, Germany).

### 3.3.3.5 HF proliferation studies

Different SAM-coated glass surfaces were placed into 24-well tissue culture plates (Greiner Bio-One GmbH, Frickenhausen, Germany), sterilized with 70% ethanol for 10min



and rinsed with sterile PBS twice. 1 mL of HF cell suspension was added to each surface at  $2.0 \times 10^4$  cells mL<sup>-1</sup> in serum-containing DMEM medium. Cultures were incubated for 1 and 3 days respectively at 37 °C in a humidified 5% CO<sub>2</sub>/95% air atmosphere. After the desired incubation time, a QBlue<sup>®</sup> cell viability assay kit (Biochain, Hayward, USA) was applied to quantify the amount of metabolic active cells. Briefly, the cells were firstly washed once with sterile PBS to remove the old medium. Then, 500 µL of pre-warmed colourless DMEM with QBlue<sup>®</sup> assay reagent (10:1) were added to each well and incubated at 37 °C for 2 h. Thereafter, 100 µL of supernatant from each well was transferred to a black 96-well plate, and the fluorescence intensities were measured at an excitation wavelength of 544 nm and emission wavelength of 590 nm with a plate reader (FLUOstar, BMG LabTech, Offenburg, Germany).

#### 3.3.3.6 HF outgrowth studies

To measure the HF outgrowth on different SAM surfaces, 0.15 mL of a HF cell suspension with a cell density of  $2.0 \times 10^5$  cells mL<sup>-1</sup> was seeded into the internal channel, while 0.65 mL of a macrophage cell suspension with a cell density of  $5.0 \times 10^5$  cells mL<sup>-1</sup> was seeded into the external compartment of the chamber for each well in 24-well tissue plate. The HF mono-culture was performed under the same condition but with only 0.65 mL RPMI in the external compartment. After 24 h incubation, the fence chambers were removed and the surfaces were washed once with PBS. 1 mL of fresh serum-containing DMEM was added to each well. The fibroblasts were then left to outgrow for 3 days in both HF mono- and co-cultures. Afterwards, the cells were fixed and stained by 0.5% (w/v) crystal violet in methanol. HF outgrowth areas were photographed by a stereo microscope (SMZ-168, Motic, Wetzlar, Germany) equipped with an attachable C-mount camera (Moticam 1000, Motic, Germany) to evaluate the outgrowth distances on different SAM surfaces. The macrophage regions were viewed by an inverted contrasting microscope (Leica DMIL, Leica Mikrosysteme Vertrieb GmbH, Wetzlar, Germany) equipped with a high speed digital camera (Leica EC3, Leica Mikrosysteme Vertrieb GmbH, Germany) to evaluate the foreign body giant cell (FBGC) formation on different SAM surfaces.

#### 3.3.3.7 Cytokine production assays

0.15 mL of HF cell suspension with a density of  $2.0 \times 10^4$  cells mL<sup>-1</sup> in serum-free DMEM and 0.65 mL of macrophage cell suspension with a density of  $5.0 \times 10^5$  cells mL<sup>-1</sup> in 10%

FBS-containing RPMI were added into the internal channel and external compartment of the chamber, respectively. The HF mono-cultures were performed under the same condition but with only 0.65 mL RPMI in the external compartment. After 24 h incubation, the fence chambers were removed and the surfaces were washed once with PBS. 1mL of 10 ng mL<sup>-1</sup> TGF- $\beta$ 1 (PeproTech, Hamburg, Germany) in serum-free DMEM was then added to each well and incubated with the cells for 3 days at 37 °C. After that, supernatants in both HF mono- and HF/macrophage co-cultures were collected for analysing the pro-inflammatory cytokine IL-6 and anti-inflammatory cytokine IL-10 production. The cytokine production on different SAM surfaces was detected using enzyme-linked immunosorbent assay (ELISA) according to the manufacturers' instructions for IL-6 Elisa kit (BD Biosciences Pharmingen, Heidelberg, Germany) and IL-10 Elisa kit (Promokine, Heidelberg, Germany).

#### 3.3.3.8 Expression of ED-A FN and $\alpha$ -SMA

The cells were treated and incubated the same as described in 2.3.7. After incubation with 10 ng mL<sup>-1</sup> TGF- $\beta$ 1 for 3 days, the cells were washed, fixed by 4% PFA, permeabilized with 0.1% Triton X-100, and blocked with 1% BSA. Then, the cells were incubated against the primary antibody ED-A FN (1:100, Santa Cruz Biotechnology, Germany), secondary antibody CY2 (1:100, Dianova, Germany), CY3-conjugated anti- $\alpha$ -SMA (1:200, Sigma-Aldrich, Germany) and TO-PRO3 (1:500, Invitrogen, Germany) one after another, by 30 min incubation each. The samples were then washed, mounted with Mowiol and examined with CLSM (Carl Zeiss, Oberkochen, Germany) using a 20x objective. Images were processed with the ZEN2011 software (Carl Zeiss, Germany).

#### 3.3.4 Statistics

All data are represented as mean values  $\pm$  standard deviations (SD). Statistical examination was performed using one-way analysis of variance (ANOVA) followed by post-hoc Tukey testing. The significance level was set as  $p < 0.05$  and indicated by an asterisk. The number of samples has been indicated in the respective figure caption.

## 3.4 Results and discussion

### 3.4.1 Surface properties of SAMs

The wettability of the SAM surfaces was evaluated by static water contact angle (WCA) measurements (Figure 3.2A). As expected,  $-\text{CH}_3$  terminated SAMs provided an extremely hydrophobic substrate with WCA  $\sim 101^\circ$ , while the  $-\text{NH}_2$  [22] and  $-\text{epoxy}$  [23] terminated SAMs formed moderately wettable substrates with WCA  $\sim 53^\circ$  and  $51^\circ$ , respectively. By contrast, SAMs terminated with  $-\text{COOH}$  groups exhibited highly wettable surfaces with WCA  $\sim 27^\circ$ , which is in good agreement with published values [24]. Furthermore, the WCA of epoxy-terminated surfaces decreased from  $51^\circ$  to  $31^\circ$  after modification with HCl, indicating the successful conversion of epoxy to OH groups according to previous protocols [20]. In general, the WCA values of the  $-\text{CH}_3$ ,  $-\text{NH}_2$ ,  $-\text{epoxy}$ ,  $-\text{OH}$  and  $-\text{COOH}$  terminated SAMs corresponded well with previous studies [19, 25].

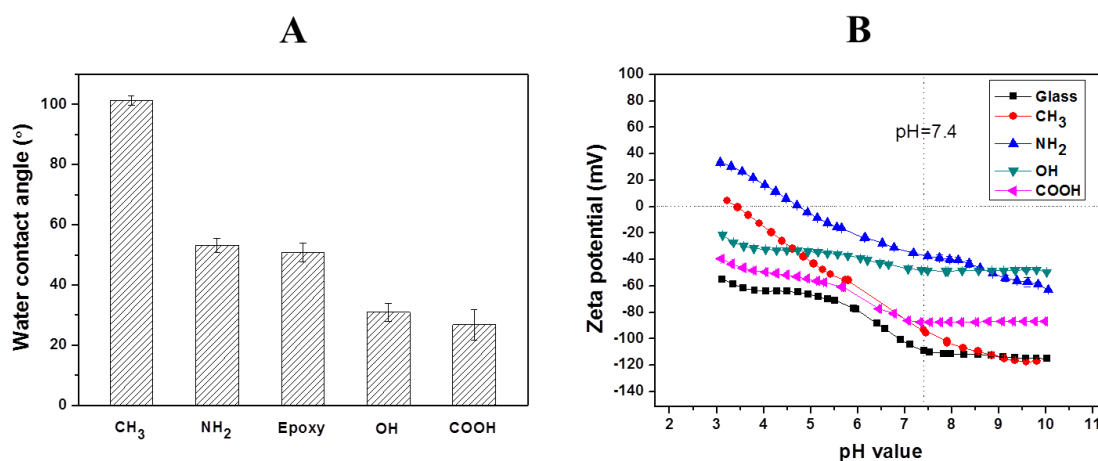


Figure 3.2. Physical characterization of the SAM surfaces. (A) Static water contact angle (WCA) measurement of  $\text{CH}_3$ ,  $\text{NH}_2$ , epoxy, OH and COOH SAMs. Results are the means  $\pm$  SD of two independent experiments, each performed in triplicate. (B) Zeta potential measurements of the SAMs with different terminating groups compared with bare glass. Zeta potentials were measured in the pH range 3–10.

Figure 3.2B shows the zeta potentials versus pH value of a standard electrolyte solution (1mM KCl) for bare glass and different SAM surfaces. The bare glass, OH, and COOH SAMs exhibited negative surface potentials throughout the whole measured pH range. By contrast,  $\text{CH}_3$  and  $\text{NH}_2$  SAMs were found to have a point of zero charge (PZC) at pH 3.4 and 4.8,

respectively. The highest potential at pH 7.4 was found on the  $-\text{NH}_2$  terminated SAM surface, which is attributed to the partial protonation of amino groups in the low pH region [26]. The neutral  $-\text{OH}$  and  $-\text{CH}_3$  terminated surfaces displayed negative zeta potentials at pH 7.4 because of a preferential anion adsorption on the non-charged surfaces [27]. The curve for  $-\text{COOH}$  terminated surface possessed a negative surface potential from pH 3–10 and a plateau at the basic pH region arising from the presence of dissociable acidic groups on this surface [26]. Additionally, the zeta potential values of all SAMs-modified surfaces were higher compared to bare glass at pH 7.4, which indicates the successful immobilization of the organosilanes and formation of SAMs on the bare glass substrate.

The physical characterization studies confirmed the functionalized SAMs with different wetting and surface charge properties, and thus were served as model surfaces to study the surface property effect in mediating the fibroblast reactions in the following sections.

### **3.4.2 HF adhesion, spreading and proliferation**

As fibroblasts are one of the key effector cells during wound healing and host responses to injuries after biomaterial implantation, the initial adhesion, spreading as well as the following proliferation and outgrowth of fibroblasts are crucial for the potential fibrotic development. We therefore studied the surface property effects on such cellular activation by use of the different SAM surfaces.

We firstly evaluated the HF morphology in the initial cell spreading on different SAMs by analysis of the focal adhesion complexes using vinculin (green) and actin (red) staining as shown in Figure 3.3A. After 4 h incubation in the presence of serum, HFs adhering to  $\text{NH}_2$  and  $\text{COOH}$  SAMs were well spread and contained short focal adhesion plaques at the cell periphery. Strong actin stress fibres were also formed. Additionally, a colocalization of actin and vinculin was observed, illustrated by the yellow colour. By contrast, adhesion and spreading of HFs on  $\text{CH}_3$  and  $\text{OH}$  SAMs were largely suppressed. No focal adhesions or actin stress fibres were observed on these surfaces. Considering the serum used in the medium, it can be anticipated that  $\text{NH}_2$  and  $\text{COOH}$  SAMs are favourable to bind adhesion-promoting proteins such as fibronectin and vitronectin from serum [28, 29], which promoted fibroblast adhesion and spreading. By contrast,  $\text{OH}$  surface was reported to inhibit protein adsorption, and thus impaired cell adhesion [24]. On the other hand, despite  $\text{CH}_3$  surfaces can bind large quantities of proteins, the conformation of the adsorbed proteins can easily change due to the

hydrophobic interactions between the surfaces and hydrophobic domains of proteins [30, 31]. As a result, cell adhesion was also reduced on this surface.

Apart from the HF morphology studies, a quantitative estimation of cell adhesion (cell count) and spreading (cell area) were conducted on different SAM surfaces after 4 h incubation in the presence of serum (Figure 3.3B and Figure 3.3C). The results show that there were significantly more cells adhering on NH<sub>2</sub> and COOH than on OH and CH<sub>3</sub> SAMs. The analysis of cell spreading data also revealed significantly higher spreading area of HFs on NH<sub>2</sub> and COOH surfaces in comparison to OH and CH<sub>3</sub> surfaces. These findings are well in line with previous observations showing that cells prefer to adhere and spread more on moderate hydrophilic and hydrophilic/anionic surfaces compared to hydrophobic and non-ionic hydrophilic surfaces [19, 24, 32].

The proliferation of HFs on different SAM surfaces was studied after incubation periods of 24 and 72 h. Figure 3.3D shows the metabolic activity of HFs measured from QBlue assay that represents an indication of the quantity of metabolic active cells on the different SAMs. The obtained data illustrate that cell growth was higher on NH<sub>2</sub> and COOH surfaces compared to OH and CH<sub>3</sub> surfaces after both 24 and 72 h, which is in line with the observed HF adhesion and spreading results. In general, surface properties dictate the protein adsorption from serum-containing medium, which affects the ligand binding to adhesion receptors of cells like integrins [28, 33]. Such ligand-receptor binding mediates cell adhesion, signal transduction followed by cytoskeleton reorganization, protein synthesis and cell proliferation [34].

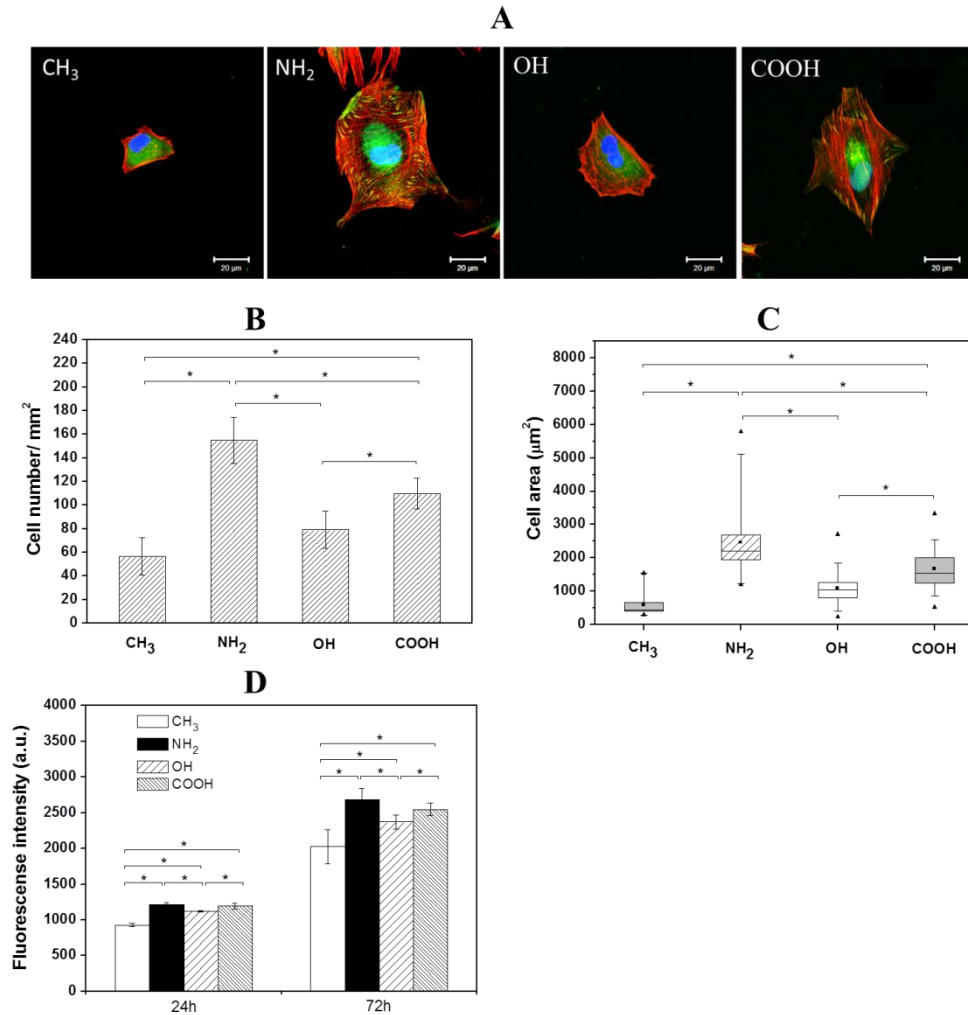


Figure 3.3. Adhesion, spreading and proliferation of human fibroblasts (HF) on CH<sub>3</sub>, NH<sub>2</sub>, OH and COOH SAMs. Representative CLSM images (A) of HF after 4 h incubation with immune fluorescence staining of vinculin (green), actin (red) and nuclei (blue). Bar = 20 µm. Quantitative cell adhesion number (B) and spreading area (C) of HF adhesion on different SAMs after 4 h incubation in serum-containing medium. Data represent mean ± SD, n = 4, \*p < 0.05. (D) HF proliferation after 24 h and 72 h culture on CH<sub>3</sub>, NH<sub>2</sub>, OH and COOH SAMs in serum-containing medium. Data represent mean ± SD, n = 4, \*p < 0.05.

### 3.4.3 HF outgrowth studies

HF migration and growth are very important during the processes associated with wound healing and fibrosis and strongly affected by cytokine release from macrophages [35]. Therefore, we further evaluated the surface property effect on HF growth by a specific outgrow study. Figure 3.4A shows the crystal violet staining images of HF outgrowth after 3

days in the presence (co-culture) or absence (HF mono) of macrophages. During these experiments, the macrophages were seeded at the same time like HFs, but in the external compartment of the chamber, which separated them by a 500  $\mu\text{m}$  gap after lifting up the chamber. Figure 3.4B depicts the quantitative outgrowth distances on different SAMs after subtracting the original diameter of the HF region. It was observed that  $\text{CH}_3$  SAM induced the minimum outgrowth distance in both HF mono- and co-culture. This can be explained by the impaired HF adhesion and proliferation due to the high hydrophobicity of this surface, leading to conformational changes of adsorbed adhesive proteins and impaired cell responses [24, 36]. Contradictory, the  $\text{NH}_2$  SAM with most cell adhesion and proliferation in single cell cultures shown before, generated only an intermediate outgrowth, less than OH and COOH SAMs. This might be due to the strong interactions between HFs and the  $\text{NH}_2$  SAM, illustrated by the multiple, extended focal adhesion complexes (see Figure 3.4A ), which caused an impaired ability of cell migration [37], although with higher cell proliferation. The migration of HFs on  $\text{NH}_2$  and COOH surfaces has been reported by Faucheux et al. previously, also revealing that HFs on FN-coated COOH surface migrated faster than on  $\text{NH}_2$  surface [24]. Additionally, it is notable that OH SAM caused a comparable outgrowth distance like COOH SAM. This might be probably due to the weak adhesion of HFs on OH SAM, resulting in higher migration ability [28, 38]. Besides, OH SAM provoked a moderate proliferation of HFs as observed in the proliferation studies shown here and by others [39]. However, the most important finding of these experiments was that the outgrowth distance was significantly increased in co-cultures compared to fibroblast monocultures on all SAMs. During these experiments it was also observed that the effect of surface chemistry on HF outgrow was the same as observed in the HF monoculture experiments. The increased outgrow distance is obviously attributed to the presence of the surrounding macrophages. It was reported previously that cytokines such as IL-1 $\beta$  and IL-6 secreted by macrophages promote HF migration and proliferation [40, 41], which supports the findings made here.

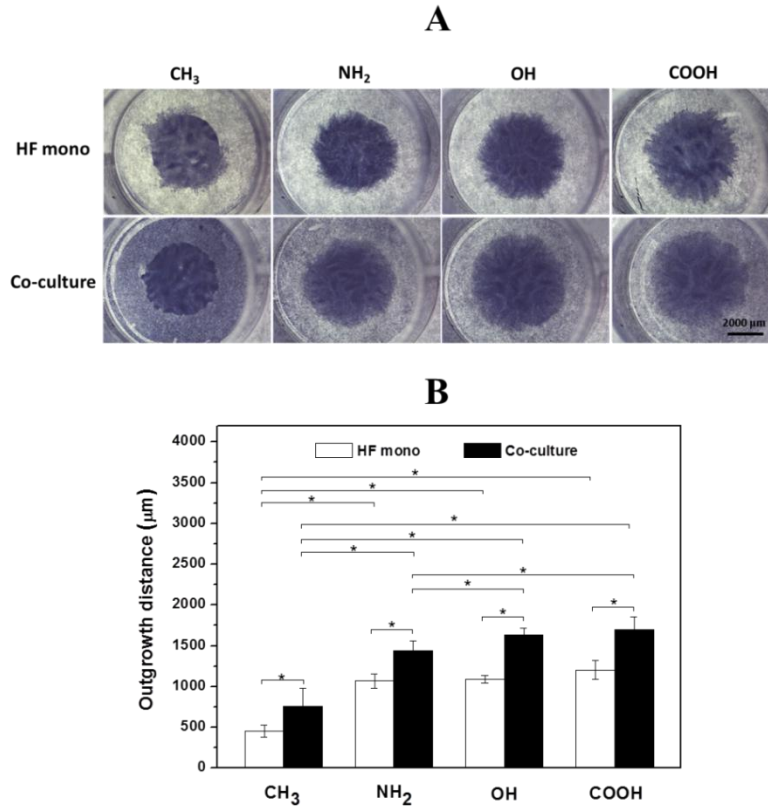


Figure 3.4. Representative crystal violet staining images (A) and quantitative outgrowth distances (B) of HF outgrowth in HF monocultures (HF mono, white bars) and fibroblast/macrophage co-cultures (Co-culture, black bars) on CH<sub>3</sub>, NH<sub>2</sub>, OH and COOH SAMs. The cells were seeded and cultured for 24 h before removal of the fence chambers. The fibroblasts were then left to grow for 3 days in both mono- and co-cultures. Afterwards, the cells were fixed and stained by 0.5% (w/v) crystal violet in methanol. Bar = 2000 μm. Data represent mean ± SD, n = 6, \*p < 0.05.

#### 3.4.4 Macrophage fusion studies

In addition to the analysis of HF outgrowth distance, the macrophage fusion on different SAM surfaces was also evaluated in the macrophage regions of the co-culture system (Figure 3.5). It can be seen that large quantities of foreign body giant cells (FBGCs) were formed on CH<sub>3</sub> SAM, illustrated by large size of cells shown by crystal violet staining (red arrows). By contrast, fewer FBGCs with lower size were found on NH<sub>2</sub>, OH and COOH SAMs. Macrophages fuse to form FBGCs in order to increase their phagocytosis ability when facing foreign materials larger sized than themselves [42]. It was also found that the fusion extent



represents a measure of biocompatibility of a given material [43]. Hence, the difference in FBGC formation classifies the CH<sub>3</sub> SAM as more pro-inflammatory than the other SAMs.

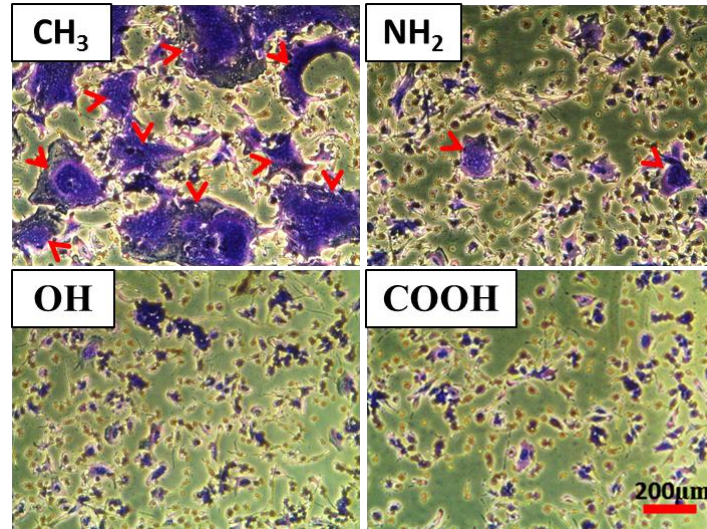


Figure 3.5. Foreign body giant cells (FBGCs) formation on CH<sub>3</sub>, NH<sub>2</sub>, OH and COOH SAMs in the macrophage region of co-cultures after 3 days of HF outgrowth. Afterwards, the cells were fixed and stained by 0.5% (w/v) crystal violet in methanol. The red arrows show the FBGCs. Bar = 200 μm.

### 3.4.5 Pro- and anti-inflammatory cytokine production

The soluble signals including pro- and anti-inflammatory cytokines are important mediators in inflammation and wound healing. Macrophages have high degree of functional plasticity, which can act as both M1 inflammatory and M2 wound healing phenotype in response to different stimuli [44]. M1 macrophages display more pro-inflammatory function by secretion of cytokines such as IL-1 $\beta$ , IL-6 and TNF- $\alpha$ , while M2 macrophages have anti-inflammatory function and promote wound healing by secretion of cytokines like IL-10 and TGF- $\beta$ 1 [45]. Besides, fibroblasts can modulate the cytokine production by macrophages but also are able to generate both pro- and anti-inflammatory cytokines including IL-1 $\beta$ , IL-6, TGF- $\beta$  and IL-10 [46, 47]. The balance between the pro- and anti-inflammatory mediators is critical for orchestrating the outcome of the inflammation and whole wound healing responses. Therefore, we tested here the pro-inflammatory cytokine IL-6 and anti-inflammatory cytokine IL-10 production on different SAMs after 3 day incubation in the presence of TGF- $\beta$ 1.

Figure 3.6A shows that there was no significant difference of IL-6 release among the various SAMs in HF monocultures. This might be related to the limited HF population due to the low seeding density in the internal channel of the chambers (0.15 mL of HFs at  $2.5 \times 10^4$  cells mL<sup>-1</sup>) and limited proliferation of HFs in the absence of serum. By contrast, the IL-6 released from cells adherent to different SAMs in co-cultures showed a surface-dependent behavior. It was found that cells adhering on CH<sub>3</sub> SAM produced significantly higher levels of IL-6 in comparison to the other SAMs. This result indicates that the IL-6 production is provoked by the hydrophobic nature of CH<sub>3</sub> SAM, which is in consistent with previous findings that hydrophobic surfaces induced highest levels of pro-inflammatory cytokine such as IL-1 $\beta$ , IL-6 and TNF- $\alpha$  [12, 15, 48]. On the other hand, IL-10 production showed an opposite surface-dependent effect compared to IL-6 in co-cultures (Figure 3.6B). The results show that the COOH SAM produced significantly higher amounts of IL-10 than CH<sub>3</sub>, NH<sub>2</sub> and OH SAMs. This is also in line with other reports documenting that the hydrophilic/anionic surfaces reduce pro-inflammatory responses and promote the wound healing processes [4]. Additionally, the production of both IL-6 and IL-10 increased significantly in fibroblast/macrophage co-cultures compared to HF monocultures on all SAMs. This indicates that macrophages contribute largely to both pro- and anti-inflammatory signal production. Moreover, a much higher amount of IL-10 compared to IL-6 was observed for the same samples. This might imply a reduced inflammatory response and an increased wound healing response under the measuring conditions due to the presence of TGF- $\beta$  1, but also corresponding to the previous observations that PMA-treated THP-1 cells are differentiated into macrophages with predominant M2 functional profile [18].

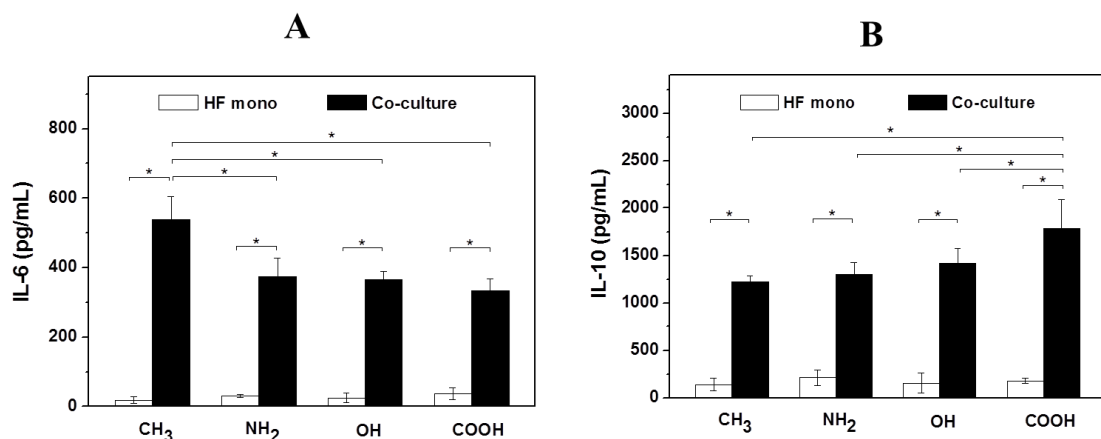


Figure 3.6. IL-6 (A) and IL-10 (B) release in human fibroblast monocultures (HF mono, white bars) and fibroblast/macrophage co-cultures (Co-culture, black bars) on CH<sub>3</sub>, NH<sub>2</sub>, OH and

COOH SAMs after 3 days of incubation with  $10 \text{ ng mL}^{-1}$  TGF- $\beta$ 1. Data represent mean  $\pm$  SD,  $n = 6$ ,  $*p < 0.05$ .

### 3.4.6 ED-A FN and $\alpha$ -SMA expression

Myofibroblast phenotype transformation is an essential step during wound healing and fibrotic processes, which is normally accompanied by abundant ED-A FN and  $\alpha$ -SMA expression [7]. TGF- $\beta$ 1 can stimulate fibroblasts differentiation into myofibroblasts and is known as important contributor to fibrosis both *in vitro* and *in vivo* [49]. Hence, the levels of ED-A FN and  $\alpha$ -SMA expression on different SAMs were studied in the presence of TGF- $\beta$ 1 as done also in other studies [50, 51] to mimic to some extent the *in vivo* situation.

Figure 3.7A presents the ED-A FN expression on different SAM surfaces in both HF mono- and co-cultures. A comparison of the staining revealed obvious surface chemistry-dependent differences with  $\text{NH}_2$  SAM expressing the highest level of ED-A FN in both mono- and co-cultures. By contrast, on  $\text{CH}_3$  surface considerably lower levels of ED-A FN were detected, while COOH and OH surfaces exhibited intermediated expression compared to  $\text{NH}_2$  and  $\text{CH}_3$  SAMs. Overall, the ED-A FN expression results corresponded well to the HF adhesion, proliferation and outgrowth experiments and showed an order of  $\text{NH}_2 > \text{COOH} \sim \text{OH} > \text{CH}_3$ . Besides, the markedly increased expression levels of ED-A FN in all co-cultures revealed that macrophages amplified the ED-A FN matrix synthesis by HFs. Indeed, a large body of researches have confirmed that macrophage contribute to wound healing and fibrosis by promoting fibroblast activation, proliferation and differentiation into myofibroblasts [40, 41].

Furthermore, the expression of  $\alpha$ -SMA, a key feature of fibrotic reactions, was also analysed on different SAMs (Figure 3.7B). Notably more  $\alpha$ -SMA positively stained HFs ( $\alpha$ -SMA-positive HFs) were observed on  $\text{NH}_2$ , OH and COOH surfaces in comparison to  $\text{CH}_3$  surface. Moreover, the  $\alpha$ -SMA-positive HFs on all co-culture surfaces were much more elongated than in the corresponding mono-cultures. Figure 3.8A depicts the quantitative evaluation of cell aspect ratio of the  $\alpha$ -SMA-positive HFs on the different SAMs. First, no significant difference of aspect ratio was observed among  $\text{NH}_2$ , OH and COOH SAMs in both HF mono- and co-cultures. By contrast, the cells on  $\text{CH}_3$  SAM exhibited significant lower aspect ratio than  $\text{NH}_2$ , OH and COOH SAMs in co-cultures. The elongation extent of the cells represents their contractile capability, which plays important roles in wound healing and fibrotic processes. Therefore, the *in vitro* data obtained here may suggest that the

hydrophobic CH<sub>3</sub> SAM had lower potential of promoting wound healing and fibrosis. Furthermore, the aspect ratio of the  $\alpha$ -SMA-positive HFs in all co-cultures significantly increased compared to the corresponding mono-cultures. This can be attributed to the promoting effects in wound healing and fibrosis of the M2 phenotypic macrophages in co-cultures [44].

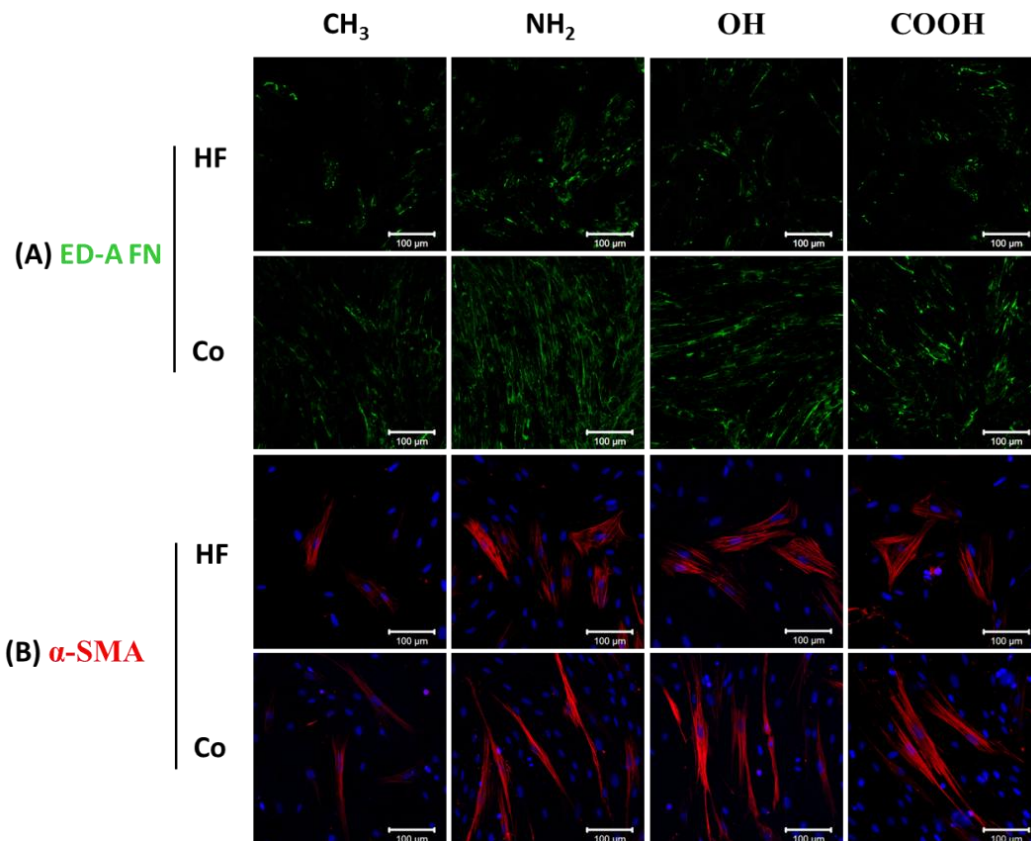


Figure 3.7. Immunofluorescence staining of (A) ED-A FN (green), (B)  $\alpha$ -SMA (red) and nuclei (blue) after 3 day incubation with 10ng mL<sup>-1</sup> TGF- $\beta$  in HF mono-cultures (HF mono) and fibroblast/macrophage co-cultures (Co-culture) on CH<sub>3</sub>, NH<sub>2</sub>, OH and COOH SAMs. Bar = 100  $\mu$ m.

The determination of percentage of  $\alpha$ -SMA-positive cells in Figure 3.8B reveals that OH surface caused the highest percentage ratio of  $\alpha$ -SMA-positive cells, while COOH surface induced the minimum percentage, followed with the order OH > NH<sub>2</sub> ~ CH<sub>3</sub> > COOH. Here, the higher adhesion and outgrowth of fibroblasts on the hydrophilic/anionic COOH SAM resulted in the lowest percentage of  $\alpha$ -SMA-positive cells, indicating a lower potential of inducing wound healing and fibrosis. This might be also related to the highest IL-10 cytokine

production on this surface, which was reported to have both anti-inflammatory and anti-fibrotic effects [52]. By contrast, the hydrophilic OH surface which evoked a lower extent of pro-inflammatory responses as observed in FBGC formation and pro-inflammatory cytokine IL-6 production indicates here the highest potential of inducing wound healing and fibrosis. These findings are generally consistent with previous work using polypropylene microspheres with different functional groups as also used here to study the extent of fibrotic tissue reactions elicited by the different functionalities, and their data show that OH surface triggers the strongest capsule formation while COOH surface promotes the least capsule formation [53]. It was suggested that the complement activation can affect the recruitment of inflammatory cells and the following fibrotic tissue reactions [54]. OH groups are reported to bind with C3b component and activate the alternatively pathway of complement to a much greater extent than COOH groups [55], which may explain partly the findings here.

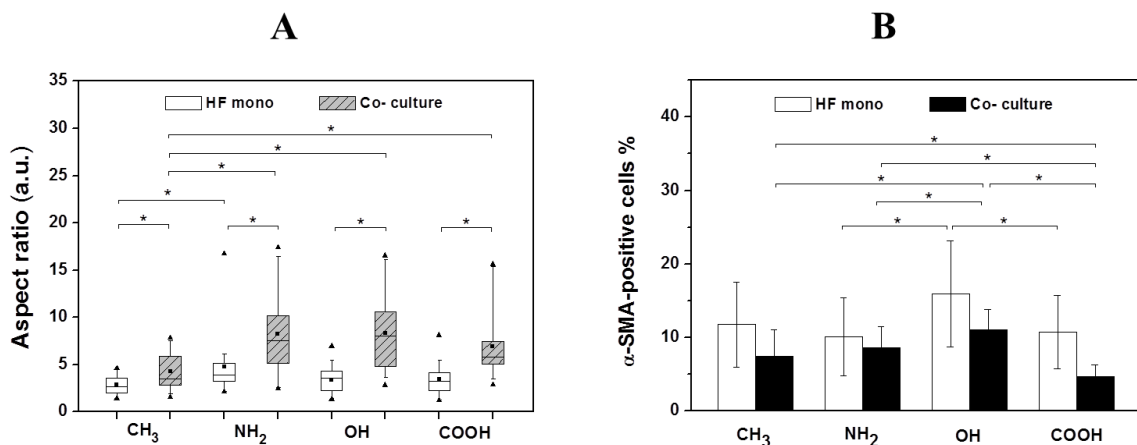


Figure 3.8. Surface chemistry-dependent differences in  $\alpha$ -SMA expression after 3 day incubation in the presence of  $10 \text{ ng mL}^{-1}$  TGF- $\beta$ . Aspect ratio (A) and percentage (B) of  $\alpha$ -SMA positively stained cells on CH<sub>3</sub>, NH<sub>2</sub>, OH and COOH SAMs in both HF mono-cultures (HF mono) and fibroblast/macrophage co-cultures (Co-culture). Data represent mean  $\pm$  SD,  $n \geq 20$ , \* $p < 0.05$ .

A summary of the measured parameters involved in inflammatory and fibrotic responses on CH<sub>3</sub>, NH<sub>2</sub>, OH and COOH SAMs is shown in Table 3.1. First, the results reveal that the inflammatory and fibrotic responses on SAMs seems to be not always consistent. For example, the hydrophobic CH<sub>3</sub> SAM, which was observed with the highest potential of inducing inflammatory responses, illustrated by the highest level of FBGC formation and IL-6 production, revealed a low potential of inducing fibrotic responses through the observation of

fibroblast activations. On the other hand, the hydrophilic OH SAM triggered a low level of inflammatory responses but indicated a high potential of inducing fibrotic reactions. Here, the inconsistency of the inflammatory/fibrotic responses could be attributed to the different cellular responses of macrophages and fibroblasts to the same surface, which was also observed by other *in vitro* studies previously [56]. Furthermore, the *in vivo* inflammatory/fibrotic investigations by Baker et al. documented that fibroblasts, rather than macrophages are the key contributor to the *in vivo* outcome of the implant-induced fibrotic responses [56]. Therefore, although the inflammatory responses have certain influence in the subsequent fibrotic responses; the relation between inflammatory and fibrotic responses might not be always linked [57]. In other words, the inflammatory response alone cannot predict the following implant-mediated fibrotic reactions. Further in-depth inflammation-fibrosis link studies will help to design of biomaterials with appropriate fibrotic tissue responses.

Table 3.1 Surface chemistry differentially affects parameters of the inflammatory (dark grey color) and fibrotic responses (light grey color) on CH<sub>3</sub>, NH<sub>2</sub>, OH and COOH SAMs (+ weak, ++ strong, +++ very strong).

Parameters	Surfaces	CH <sub>3</sub>	NH <sub>2</sub>	OH	COOH
IL-6 production		+++	+	+	+
Macrophage fusion		+++	+	+	+
HF adhesion/ spreading		+	+++	++	+++
HF proliferation		+	+++	++	+++
HF outgrowth		+	++	+++	+++
IL-10 production		+	+	+	+++
ED-A FN expression		+	+++	++	++
$\alpha$ -SMA expression		+	+++	+++	+++
% $\alpha$ -SMA positive cells		++	++	+++	+

In addition, we observed that the hydrophilic/anionic COOH SAM caused lower inflammatory reactions in comparison to CH<sub>3</sub> SAM. Further, although highest fibroblast adhesion, proliferation, outgrowth, as well as strong expression of ED-A FN and  $\alpha$ -SMA were found on COOH SAM, the percentage of the  $\alpha$ -SMA positive cells was the lowest, indicating a lower extent of inducing fibrosis. Therefore, it can be concluded that the hydrophilic/anionic COOH SAM has both anti-inflammatory and anti-fibrotic potential. These results are consistent with *in vivo* inflammatory/fibrotic studies by Kamath et al. showing that *in vivo*

subcutaneous implantation of microspheres bearing COOH groups triggered the least capsule formation and inflammatory cell infiltration [53]. By contrast, the low pro-fibrotic effects of the hydrophobic CH<sub>3</sub> SAM seems to be contradictory to *in vivo* findings that hydrophobic surfaces induced thicker fibrous capsules [58]. It was suggested there that the high level of recruited and/or adherent inflammatory cells such as Mac-1<sup>+</sup> cell may account for the thick fibrous capsule formation around the implanted CH<sub>3</sub> surface [58]. However, many recent researches suggest that fibroblast-like cells play vital roles in wound healing and fibrotic reactions [56]. Moreover, by comparison of the *in vitro* and *in vivo* results, it was found a poor relationship between *in vitro* macrophage proliferation and *in vivo* fibrotic capsule formation, but a good linear relationship between fibroblast proliferation and the *in vivo* fibrotic tissue responses [56]. Therefore, the impaired fibroblast adhesion, spreading, proliferation and outgrowth on the hydrophobic CH<sub>3</sub> surface might be responsible for the reduced potential of inducing fibrotic reactions observed here.

### 3.5 Conclusion

We have provided here a systematic characterization of inflammatory and fibrotic responses on SAMs with different terminating groups, representing different surface chemistry effects. It was found that the hydrophobic CH<sub>3</sub> surfaces possessed the highest potential of inducing inflammatory responses reflected by the highest levels of FBGC formation and IL-6 production, however induced a low level of fibrotic responses. By contrast, the hydrophilic OH SAM which evoked a lower extent of pro-inflammatory responses, but revealed a higher potential of inducing fibrosis. These results suggest that the relation between inflammatory and fibrotic responses might not be always linked and the inflammatory response alone is insufficient to predict the degree of implant-mediated fibrotic reactions. Overall, these observations can provide useful clues for the design of biomaterials with triggering appropriate host responses for different biomedical and clinical applications. Furthermore, the established *in vitro* fibroblast/macrophage co-culture systems have certain predictive values for estimating the inflammatory/fibrotic potential provoked by new biomaterials before implantation. Last but importantly, one can study here the *in vitro* effects of additional factors like cytokines and other bioactive molecules on the interplay between two cell types using our presented *in vitro* system.

### 3.6 Disclosure

No conflicts of interests are declared.

### 3.7 Acknowledgement

G. Zhou thanks the China Scholarship Council for offering the scholarship to work in Germany. Mrs M. Porobin is gratefully acknowledged for the assistance of zeta potential measurement.

### 3.8 References

[1] Anderson JM, Rodriguez A, Chang DT. Foreign body reaction to biomaterials. *Semin Immunol* 2008;20:86-100.

[2] Glaros T, Larsen M, Li LW. Macrophages and fibroblasts during inflammation, tissue damage and organ injury. *Front Biosci* 2009;14:3988-93.

[3] Franz S, Rammelt S, Scharnweber D, Simon JC. Immune responses to implants - A review of the implications for the design of immunomodulatory biomaterials. *Biomaterials* 2011;32:6692-709.

[4] Brodbeck WG, Nakayama Y, Matsuda T, Colton E, Ziats NP, Anderson JM. Biomaterial surface chemistry dictates adherent monocyte/macrophage cytokine expression in vitro. *Cytokine* 2002;18:311-9.

[5] Zhou G, Niepel MS, Saretia S, Groth T. Reducing the inflammatory responses of biomaterials by surface modification with glycosaminoglycan multilayers. *J Biomed Mater Res Part A* 2016;104:493-502.

[6] Wynn TA. Cellular and molecular mechanisms of fibrosis. *Journal of Pathology* 2008;214:199-210.

[7] Serini G, Bochaton-Piallat ML, Ropraz P, Geinoz A, Borsi L, Zardi L, et al. The fibronectin domain ED-A is crucial for myofibroblastic phenotype induction by transforming growth factor-beta 1. *J Cell Biol* 1998;142:873-81.

[8] Mutsaers SE, Bishop JE, McGrouther G, Laurent GJ. Mechanisms of tissue repair: From wound healing to fibrosis. *Int J Biochem Cell Biol* 1997;29:5-17.



[9] Hu WJ, Eaton JW, Tang LP. Molecular basis of biomaterial-mediated foreign body reactions. *Blood* 2001;98:1231-8.

[10] Marques AP, Reis RL, Hunt JA. An in vivo study of the host response to starch-based polymers and composites subcutaneously implanted in rats. *Macromol Biosci* 2005;5:775-85.

[11] Battiston KG, Labow RS, Santerre JP. Protein binding mediation of biomaterial-dependent monocyte activation on a degradable polar hydrophobic ionic polyurethane. *Biomaterials* 2012;33:8316-28.

[12] Zhou G, Loppnow H, Groth T. A macrophage/fibroblast co-culture system using a cell migration chamber to study inflammatory effects of biomaterials. *Acta Biomaterialia* 2015;26:54-63.

[13] MacEwan MR, Brodbeck WG, Matsuda T, Anderson JM. Monocyte/lymphocyte interactions and the foreign body response: in vitro effects of biomaterial surface chemistry. *J Biomed Mater Res Part A* 2005;74A:285-93.

[14] Barbosa JN, Madureira P, Barbosa MA, Aguas AP. The influence of functional groups of self-assembled monolayers on fibrous capsule formation and cell recruitment. *J Biomed Mater Res Part A* 2006;76A:737-43.

[15] Damanik FFR, Rothuizen TC, van Blitterswijk C, Rotmans JI, Moroni L. Towards an in vitro model mimicking the foreign body response: tailoring the surface properties of biomaterials to modulate extracellular matrix. *Scientific Reports* 2014;4.

[16] Park EK, Jung HS, Yang HI, Yoo MC, Kim C, Kim KS. Optimized THP-1 differentiation is required for the detection of responses to weak stimuli. *Inflammation Research* 2007;56:45-50.

[17] Schildberger A, Rossmannith E, Eichhorn T, Strassl K, Weber V. Monocytes, peripheral blood mononuclear cells, and THP-1 cells exhibit different cytokine expression patterns following stimulation with lipopolysaccharide. *Mediators of Inflammation* 2013;2013:697972.

[18] Tjiu J-W, Chen J-S, Shun C-T, Lin S-J, Liao Y-H, Chu C-Y, et al. Tumor-Associated Macrophage-Induced Invasion and Angiogenesis of Human Basal Cell Carcinoma Cells by Cyclooxygenase-2 Induction. *J Invest Dermatol* 2009;129:1016-25.

[19] Altankov G, Grinnell F, Groth T. Studies on the biocompatibility of materials: Fibroblast reorganization of substratum-bound fibronectin on surfaces varying in wettability. *J Biomed Mater Res* 1996;30:385-91.

[20] Toworfe GK, Composto RJ, Shapiro IM, Ducheyne P. Nucleation and growth of calcium phosphate on amine-, carboxyl- and hydroxyl-silane self-assembled monolayers. *Biomaterials* 2006;27:631-42.

[21] Fischer EG, Stingl A, Kirkpatrick CJ. Migration assay for endothelial-Cells in multiwells - Application to studies on the effect of opioids. *J Immunol Methods* 1990;128:235-9.

[22] Katzur V, Eichler M, Deigele E, Stage C, Karageorgiev P, Geis-Gerstoffer J, et al. Surface-immobilized PAMAM-dendrimers modified with cationic or anionic terminal functions: Physicochemical surface properties and conformational changes after application of liquid interface stress. *J Colloid Interface Sci* 2012;366:179-90.

[23] Luzinov I, Julthongpiput D, Liebmann-Vinson A, Cregger T, Foster MD, Tsukruk VV. Epoxy-terminated self-assembled monolayers: Molecular glues for polymer layers. *Langmuir* 2000;16:504-16.

[24] Faucheux N, Schweiss R, Lutzow K, Werner C, Groth T. Self-assembled monolayers with different terminating groups as model substrates for cell adhesion studies. *Biomaterials* 2004;25:2721-30.

[25] Faucheux N, Tzoneva R, Nagel MD, Groth T. The dependence of fibrillar adhesions in human fibroblasts on substratum chemistry. *Biomaterials* 2006;27:234-45.

[26] Shyue JJ, De Guire MR. Acid-base properties and zeta potentials of self-assembled monolayers obtained via in situ transformations. *Langmuir* 2004;20:8693-8.

[27] Werner C, Korber H, Zimmermann R, Dukhin S, Jacobasch HJ. Extended electrokinetic characterization of flat solid surfaces. *J Colloid Interface Sci* 1998;208:329-46.

[28] Keselowsky BG, Collard DM, Garcia AJ. Surface chemistry modulates focal adhesion composition and signaling through changes in integrin binding. *Biomaterials* 2004;25:5947-54.

[29] Grinnell F, Feld MK. Fibronectin adsorption on hydrophilic and hydrophobic surfaces detected by antibody-binding and analyzed during cell-adhesion in serum-containing medium. *J Biol Chem* 1982;257:4888-93.

[30] Keselowsky BG, Collard DM, Garcia AJ. Surface chemistry modulates fibronectin conformation and directs integrin binding and specificity to control cell adhesion. *J Biomed Mater Res Part A* 2003;66A:247-59.

[31] Wertz CF, Santore MM. Effect of surface hydrophobicity on adsorption and relaxation kinetics of albumin and fibrinogen: Single-species and competitive behavior. *Langmuir* 2001;17:3006-16.

[32] Arima Y, Iwata H. Effect of wettability and surface functional groups on protein adsorption and cell adhesion using well-defined mixed self-assembled monolayers. *Biomaterials* 2007;28:3074-82.

[33] Llopis-Hernandez V, Rico P, Ballester-Beltran J, Moratal D, Salmeron-Sanchez M. Role of surface chemistry in protein remodeling at the cell-material interface. *Plos One* 2011;6.

[34] Miyamoto S, Teramoto H, Coso OA, Gutkind JS, Burbelo PD, Akiyama SK, et al. Integrin function - molecular hierarchies of cytoskeletal and signaling molecules. *J Cell Biol* 1995;131:791-805.

[35] Zhao JJ, Hu L, Gong NY, Tang QM, Du LY, Chen LL. The effects of macrophage-stimulating protein on the migration, proliferation, and collagen synthesis of skin fibroblasts in vitro and in vivo. *Tissue Eng Part A* 2015;21:982-91.

[36] Hummer G, Garde S, Garcia AE, Pohorille A, Pratt LR. An information theory model of hydrophobic interactions. *Proceedings of the National Academy of Sciences of the United States of America* 1996;93:8951-5.

[37] Huttenlocher A, Horwitz AR. Integrins in Cell Migration. *Cold Spring Harbor Perspect Biol* 2011;3.

[38] Huttenlocher A, Ginsberg MH, Horwitz AF. Modulation of cell migration by integrin-mediated cytoskeletal linkages and ligand-binding affinity. *J Cell Biol* 1996;134:1551-62.

[39] Altankov G, Richau K, Groth T. The role of surface zeta potential and substratum chemistry for regulation of dermal fibroblasts interaction. *Materialwiss Werkstofftech* 2003;34:1120-8.

[40] Chow FY, Nikolic-Paterson DJ, Atkins RC, Tesch GH. Macrophages in streptozotocin-induced diabetic nephropathy: potential role in renal fibrosis. *Nephrol Dial Transplant* 2004;19:2987-96.

[41] Van Linthout S, Miteva K, Tschöpe C. Crosstalk between fibroblasts and inflammatory cells. *Cardiovasc Res* 2014;102:258-69.

[42] MacLauchlan S, Skokos EA, Mezrarich N, Zhu DH, Raof S, Shipley JM, et al. Macrophage fusion, giant cell formation, and the foreign body response require matrix metalloproteinase 9. *Journal of Leukocyte Biology* 2009;85:617-26.

[43] Anderson JM, Miller KM. Biomaterial biocompatibility and the macrophage. *Biomaterials* 1984;5:5-10.

[44] Murray PJ, Wynn TA. Protective and pathogenic functions of macrophage subsets. *Nat Rev Immunol* 2011;11:723-37.

[45] Mantovani A, Sozzani S, Locati M, Allavena P, Sica A. Macrophage polarization: tumor-associated macrophages as a paradigm for polarized M2 mononuclear phagocytes. *Trends in Immunology* 2002;23:549-55.

[46] Pan H, Jiang HL, Kantharia S, Chen WL. A fibroblast/macrophage co-culture model to evaluate the biocompatibility of an electrospun Dextran/PLGA scaffold and its potential to induce inflammatory responses. *Biomedical Materials* 2011;6.

[47] Sundararaj KP, Samuvel DJ, Li Y, Sanders JJ, Lopes-Virella MF, Huang Y. Interleukin-6 released from fibroblasts is essential for up-regulation of matrix metalloproteinase-1 expression by U937 macrophages in coculture cross-talking between fibroblasts and U937 macrophages exposed to high glucose. *J Biol Chem* 2009;284:13714-24.

[48] Hamlet S, Alfarsi M, George R, Ivanovski S. The effect of hydrophilic titanium surface modification on macrophage inflammatory cytokine gene expression. *Clinical Oral Implants Research* 2012;23:584-90.

[49] Vaughan MB, Howard EW, Tomasek JJ. Transforming growth factor-beta 1 promotes the morphological and functional differentiation of the myofibroblast. *Exp Cell Res* 2000;257:180-9.

[50] Watarai A, Schirmer L, Thoenes S, Freudenberg U, Werner C, Simon JC, et al. TGF beta functionalized starPEG-heparin hydrogels modulate human dermal fibroblast growth and differentiation. *Acta Biomaterialia* 2015;25:65-75.

[51] van der Smissen A, Samsonov S, Hintze V, Scharnweber D, Moeller S, Schnabelrauch M, et al. Artificial extracellular matrix composed of collagen I and highly

sulfated hyaluronan interferes with TGF $\beta$  1 signaling and prevents TGF $\beta$  1-induced myofibroblast differentiation. *Acta Biomaterialia* 2013;9:7775-86.

[52] Shi J-H, Guan H, Shi S, Cai W-X, Bai X-Z, Hu X-L, et al. Protection against TGF-beta 1-induced fibrosis effects of IL-10 on dermal fibroblasts and its potential therapeutics for the reduction of skin scarring. *Arch Dermatol Res* 2013;305:341-52.

[53] Nair A, Zou L, Bhattacharyya D, Timmons RB, Tang L. Species and density of implant surface chemistry affect the extent of foreign body reactions. *Langmuir* 2008;24:2015-24.

[54] Liu L, Elwing H. Complement activation on solid-surfaces as determined by c3 deposition and hemolytic consumption. *J Biomed Mater Res* 1994;28:767-73.

[55] Barbosa JN, Barbosa MA, Aguas AP. Inflammatory responses and cell adhesion to self-assembled monolayers of alkanethiolates on gold. *Biomaterials* 2004;25:2557-63.

[56] Baker DW, Liu X, Weng H, Luo C, Tang L. Fibroblast/Fibrocyte: Surface Interaction Dictates Tissue Reactions to Micropillar Implants. *Biomacromolecules* 2011;12:997-1005.

[57] Tang LP, Wu YL, Timmons RB. Fibrinogen adsorption and host tissue responses to plasma functionalized surfaces. *J Biomed Mater Res* 1998;42:156-63.

[58] Barbosa JN, Madureira P, Barbosa MA, Águas AP. The influence of functional groups of self-assembled monolayers on fibrous capsule formation and cell recruitment. *J Biomed Mater Res Part A* 2006;76A:737-43.

## 4 Reducing the inflammatory responses of biomaterials by surface modification with glycosaminoglycan multilayers

Guoying Zhou, Marcus S. Niepel, Shivam Saretia, Thomas Groth

### 4.1 Abstract

Chronic inflammatory responses after implantation of biomaterials can lead to fibrotic encapsulation and failure of implants. The present study was designed to reduce the inflammatory responses to biomaterials by assembling polyelectrolyte multilayers (PEMs) composed of glycosaminoglycans (GAGs) and chitosan (Chi) on glass as model surfaces through layer-by-layer (LBL) technique. Surface plasmon resonance (SPR) and water contact angle (WCA) investigations confirmed the multilayer build-up with alternating deposition of GAGs and Chi layers, while zeta potential measurements showed significant negative charges after multilayer deposition, which further proved the PEM formation. Macrophage adhesion, macrophage spreading morphology, foreign body giant cell (FBGC) formation, as well as  $\beta 1$  integrin expression and interleukin-1 $\beta$  (IL-1 $\beta$ ) production were all significantly decreased by GAG-Chi multilayer deposition in comparison to the primary poly (ethylene imine) (PEI) layer. Thereby, the type of GAGs played a pivotal role in inhibiting the inflammatory responses to various extents. Especially heparin (Hep)-Chi multilayers hindered all inflammatory responses to a significantly higher extent in comparison to hyaluronic acid (HA)-Chi and chondroitin sulfate (CS)-Chi multilayer systems. Overall, the present study suggests a great potential of GAG-Chi multilayer coating on implants, particularly the Hep-Chi based systems, to reduce the inflammatory responses.

**Keywords:** inflammation, glycosaminoglycans, layer-by-layer technique, macrophages, cytokines

## 4.2 Introduction

Inflammatory responses triggered by implantation of biomaterials can lead to chronic inflammation resulting in fibrotic encapsulation and failure of implants [1]. Monocytes/macrophages are key effector cells associated with these responses, of which their activation upon contact with the implant reflects the proinflammatory potential of a given material [2]. Monocytes/macrophages are triggered rapidly to the wound site caused by the injuries required for implantation, aiming to phagocytose and destroy bacteria or any other foreign objects [3]. In addition, macrophages fuse to form foreign body giant cells (FBGCs) to increase the phagocytosis capability when facing a foreign object larger sized than themselves [4]. Furthermore, once activated, macrophages secrete soluble signals such as cytokines, chemokines, and growth factors to further drive the inflammatory responses and foreign body reaction (FBR) [5]. Proinflammatory cytokines such as interleukin-1 $\beta$  (IL-1 $\beta$ ), IL-6 and tumor necrosis factor- $\alpha$  (TNF- $\alpha$ ) are up-regulated immediately after implantation of biomaterials as a response to the injury [3]. Such up-regulation represents a useful response to prevent infection of the wounded area as well as onset of chronic inflammatory state of macrophages, serving to amplify, and later resolve the biomaterial-induced inflammation [6]. However, the persistence of chronic inflammation can be contributed to attraction and activation of fibroblasts, which can differentiate into myofibroblasts upon activation and produce extracellular matrix (ECM), specifically collagens leading to implant encapsulation and failure [7]. To overcome these undesirable effects, plenty of efforts have been devoted to reduce the inflammatory responses by incorporation of anti-inflammatory agents to generate more biocompatible materials [8].

Among various anti-inflammatory compounds, glycosaminoglycans (GAGs) such as hyaluronic acid (HA), chondroitin sulfate (CS), and heparin (Hep), which are important components of the ECM, have shown great anti-inflammatory potentials [9]. In general, GAGs can interact and bind with a wide range of proteins including ECM adhesive proteins (e.g. collagen, fibronectin, laminin), as well as chemokines, cytokines, growth factors and enzymes to modulate biological processes such as cell migration, homing, growth, differentiation and thus can modulate events associated with inflammation [10]. On the other hand, chitosan (Chi), a natural polycation obtained by deacetylation of chitin, has been proved to possess biocompatibility, non-toxicity, antibacterial and antitumor activities, and therefore might be another suitable candidate for surface modification [11]. Layer-by-layer (LbL) technique, which is based on the alternate adsorption of oppositely charged molecules onto charged surfaces, has been frequently used to modify material surfaces with a multilayer deposition

[12]. The LbL approach is quite flexible and cost effective, which can be applied to virtually any material of any shape and can also utilize many natural or synthetic molecules [13]. The application of molecules with anti-inflammatory properties for incorporation into polyelectrolyte multilayers (PEMs) as biomaterial coatings could enable for better control of the biological response after implantation [8]. Based on this clue, many GAGs- and/or Chi-based PEMs have been developed for surface modification and functionalization of biomedical devices [14]. It was found recently that deposition of multilayers composed of collagen (COL) and HA reduced significantly macrophage activation *in vitro* and capsule formation *in vivo*. Hence, the LbL technique is a promising tool to modulate the inflammatory responses of biomaterials.

Due to the key effects of monocytes/macrophages in regulation of inflammation, different *in vitro* monocytes/macrophages-based cell models have been used to study inflammation and FBR [15, 16]. Among which, the THP-1 cell lines were often applied as model monocyte systems owing to their uniform genetic background with no absent donor variation [17] as well as their effective differentiation into macrophage-like cells by treatment with phorbol-12-myristate-13-acetate (PMA) [18]. Hence, by using the THP-1-derived macrophages, the current study aims to evaluate the anti-inflammatory effects of multilayers composed of different GAGs as polyanions and Chi as polycation in a simple *in vitro* setting. The multilayer formation and their surface properties were monitored by surface plasmon resonance (SPR), static water contact angle (WCA) and zeta potential measurements. We could clearly show that GAG-Chi multilayer deposition has a strong effect in reducing the inflammatory reactions in terms of macrophage adhesion, spreading, FBGC formation,  $\beta 1$  integrin expression as well as proinflammatory cytokine production. In addition, the inflammatory responses were largely dependent on the type of GAGs, with Hep-Chi multilayers showing the best potential in reducing inflammatory responses.

## **4.3 Materials and Methods**

### **4.3.1 Preparation of polyelectrolyte multilayers (PEMs)**

#### **4.3.1.1 Substrate preparation**

Glass cover slips ( $\varnothing$  12 mm, Menzel GmbH, Germany) were cleaned with 0.5 M NaOH in 96% ethanol (Roth, Germany) for 2 h followed by extensive rinsing with double-distilled water (10x5 min). New SPR sensors were rinsed with ethanol (p.a., Roth) and double-distilled water. After drying with nitrogen, the cleaned sensors were incubated in 2 mM



mercaptoundecanoic acid (MUDA, 95%, Sigma, Germany) in ethanol (p.a.) overnight to generate a negatively charged surface due to terminal carboxyl groups [19].

#### 4.3.1.2 Glycosaminoglycans (GAGs) and chitosan (Chi) solution preparation

Polyelectrolyte (PEL) solutions ( $2 \text{ mg mL}^{-1}$ ), hyaluronic acid (HA,  $M_w \sim 1.3 \text{ MDa}$ , Innovent e.V., Jena, Germany), chondroitin sulfate A (CS,  $M_w \sim 25 \text{ kDa}$ , Sigma, Germany), heparin (Hep,  $M_w \sim 15 \text{ kDa}$ , SERVA, Germany) and chitosan (Chi,  $M_w \sim 500 \text{ kDa}$ , 85/500/A1, Hepe Medical Chitosans, Halle, Germany) with a deacetylation degree of 85% were prepared by dissolution in  $150 \text{ mM NaCl}$  at pH 4.0. Poly (ethylene imine) (PEI,  $M_w \sim 750 \text{ kDa}$ , Sigma) was dissolved in  $150 \text{ mM NaCl}$  pH 7.4 at a concentration of  $5 \text{ mg mL}^{-1}$ . All solutions were sterile filtered with poly (ether sulfone) filters of  $0.2 \mu\text{m}$  pore size.

#### 4.3.1.3 Preparation of polyelectrolyte multilayers (PEMs)

PEI was used as anchoring base layer to obtain a positive surface net charge on glass coverslips or MUDA-modified gold sensors. It was adsorbed for 15 min and rinsed with  $150 \text{ mM NaCl}$  pH 7.4 three times for 5 min. Subsequently, multilayers of GAGs (HA, CS, Hep) as polyanions and Chi as polycation were formed on top of PEI. Again, each polyelectrolyte was adsorbed for 15 min, but rinsed with  $150 \text{ mM NaCl}$  pH 4.0 three times for 5 min. Overall, 10 single layers of each GAG in combination with Chi were formed and abbreviated as  $(\text{HA-Chi})_4\text{HA}$ ,  $(\text{CS-Chi})_4\text{CS}$ ,  $(\text{Hep-Chi})_4\text{Hep}$ , respectively (PEI plus 4 bilayers of GAGs and Chi plus a terminal GAG layer).

### 4.3.2 Characterization of multilayer formation and surface properties

#### 4.3.2.1 Multilayer growth

Surface plasmon resonance (SPR) was used here to determine the so-called 'optical' mass of the multilayers by using the iSPR (IBIS Technologies B.V., Enschede, Netherlands). The principal of SPR uses the changes in refractive index (RI) upon adsorption of molecules to calculate the corresponding mass. A shift in the angle of incident light is recorded ( $m^\circ$ ), which is proportional to the mass ( $\Gamma_{\text{SPR}}$ ) adsorbed on the gold sensor surface. According to the manufacturer, a change of  $122 m^\circ$  corresponds to a change  $1 \text{ ng/mm}^2$  in adsorbed mass [20]. A new gold sensor was modified with MUDA and mounted to the iSPR equipped with a

flow cell. The setup of the experiment was performed similar to the one described above for glass surfaces. Briefly, PEI was introduced and allowed to adsorb for 15 min at a flow rate of  $3 \mu\text{L min}^{-1}$  at  $25^\circ\text{C}$ . After rinsing with 150 mM NaCl pH 7.4 three times for 5 min, GAGs and Chi were adsorbed alternately for 15 min each and rinsed again three times with 150 mM NaCl pH 4.0. Multilayer formation was stopped and examined after adsorption of maximum 10 single layers.

#### 4.3.2.2 Surface wettability studies

Static water contact angle (WCA) measurements were conducted using the OCA 15+ device from Dataphysics (Filderstadt, Germany). Here, five droplets of 2  $\mu\text{L}$  fresh ultrapure water were placed onto each surface at room temperature and the sessile drop method was applied. The experiments were run in triplicate and mean and standard deviations of two independent experiments were calculated.

#### 4.3.2.3 Surface potential measurements

Zeta potentials of PEM-modified surfaces were determined with a SurPASS device (Anton Paar, Graz, Austria). Glass cover slips with specific dimensions were used for sample preparation and zeta potential measurements. Two identically modified cover slips were fixed and placed oppositely into the adjustable gap cell. The gap was adjusted to a distance where a flow rate of 100 to 150  $\text{mL min}^{-1}$  was achieved at a maximum overpressure of 300 mbar. 1 mM potassium chloride (KCl) was used as model electrolyte and 100 mM sodium hydroxide (NaOH) was used for pH titration. The pH value of KCl was adjusted to pH 2.0 using 1 M hydrochloric acid (HCl) and the measurements were performed by an automated titration program from pH 2.0 to pH 10.0 using volume increments of 20  $\mu\text{L}$  for adjustment of pH values in 0.25 pH steps.

### 4.3.3 Cell experiments

#### 4.3.3.1 Cell culture

Cells of the human monocytic cell line THP-1 (DSMZ, Germany) were cultured in RPMI-1640 medium (Biochrom AG, Germany) supplemented with 10% (v/v) fetal bovine serum (FBS, Biochrom AG), 1% (v/v) antibiotic–antimycotic solution (AAS, Promocell,

Germany) at 37 °C in a humidified 5% CO<sub>2</sub>/ 95% air atmosphere using a NUAIRE<sup>®</sup> DH Autoflow incubator (NuAire Corp., Plymouth, Minnesota, USA). Suspended cells were split by centrifugation. The old medium was removed and the cell pellet was resuspended in fresh medium every second day in order to maintain a cell density of 0.5-1.0 x 10<sup>6</sup> cells mL<sup>-1</sup>. THP-1-derived macrophages were obtained by incubation with 200 nM phorbol-12-myristate-13-acetate (PMA, Sigma) in T75 cell culture flasks (Greiner Bio-One, Germany) for 48 h. Afterwards, the differentiated macrophages were detached by incubation with 0.25% trypsin/ 0.02% EDTA (Biochrom AG) and used for seeding on PEM-modified surfaces.

#### 4.3.3.2 Cell adhesion studies

The multilayer-modified samples were sterilized in an ultraviolet light (UV) chamber (Bio-Link BLX, LTF Labortechnik GmbH & Co. KG, Wasserburg, Germany) at 254 nm (50 J cm<sup>-2</sup>) for 30 min and placed into 24-well tissue culture plates (Greiner Bio-One). THP-1-derived macrophages were detached by incubation with 0.25% trypsin/ 0.02% EDTA (Biochrom AG) and seeded on the multilayer surfaces at a cell density of 2.5 x 10<sup>4</sup> cells mL<sup>-1</sup> in serum-free RPMI-1640 medium. Cultures were incubated at 37 °C in a humidified 5% CO<sub>2</sub>/ 95% air atmosphere for 24 h. Thereafter, the surfaces were gently washed with PBS once to remove non-adherent cells. Attached cells were fixed with methanol and stained with 10% (v/v) Giemsa (Merck KGaA, Germany) in ultrapure water. Cells were imaged with a transmitted light microscope (Axiovert 100, Carl Zeiss MicroImaging GmbH, Germany) equipped with a CCD camera (Sony, MC-3254, AVT-Horn, Aalen, Germany) and the cell count on different multilayers was calculated using ImageJ software (version 1.46r).

#### 4.3.3.3 Immunofluorescence staining of macrophages

Macrophages were treated and incubated as described above. After 24 h incubation, attached cells were fixed with 4% paraformaldehyde solution (Roti<sup>®</sup> Histofix, Roth) for 15 min. Then the cells were permeabilized with 0.1% (v/v) Triton X-100 (Sigma) for 10 min and rinsed with PBS twice. Non-specific binding sites were blocked by incubation with 1% (w/v) bovine serum albumin (BSA, Merck) in PBS for 1 h, while all antibodies were diluted in the very solution. At first, the cells were incubated with a mouse monoclonal antibody raised against vinculin (1:100, Sigma) for 30 min. After washing with PBS twice, a secondary goat anti-mouse antibody conjugated with CY2 (1:100, Dianova, Germany) was applied for another

30 min. Actin fibers and cell nuclei were stained by BODIPY<sup>®</sup>-Phalloidin (1:50, Invitrogen, Germany) and TO-PRO3 (1:500, Invitrogen), respectively, by additional 30 min each. All fixation, washing, and staining steps were performed at room temperature. Finally, all samples were washed with PBS, dipped into ultrapure water, and mounted with Mowiol (Calbiochem, Germany) to object holders. All surfaces were examined by confocal laser scanning microscopy (CLSM, Carl Zeiss Microimaging, Jena, Germany) using a 63-fold oil immersion objective and images were processed with the ZEN2011 software (Carl Zeiss, Germany).

#### 4.3.3.4 Foreign body giant cell (FBGC) characterization

The FBGC formation on different surfaces was evaluated after 10 days incubation in presence or absence of  $1 \mu\text{g mL}^{-1}$  lipopolysaccharide (LPS, Sigma) in serum-containing RPMI-1640 medium. The surfaces were gently washed with PBS once and attached cells were fixed with cold methanol and stained with 10% (v/v) Giemsa (Merck) in ultrapure water. Cells were photographed using a transmitted light microscope equipped with a CCD camera and the area percentage of FBGC on different PEM surfaces was calculated by ImageJ software.

#### 4.3.3.5 $\beta$ 1 integrin expression

The cells were treated as described above in FBGC characterization. The  $\beta$ 1 integrin expression on different PEM surfaces was then evaluated by immunofluorescence staining [21]. Cells were fixed with 4% paraformaldehyde solution (Roth), permeabilized with 0.1% (v/v) Triton X-100 (Sigma) for 10 min at room temperature and rinsed with PBS twice. Again, non-specific binding sites were blocked with 1% (w/v) BSA in PBS for 1 h. Thereafter, cells were incubated with a mouse monoclonal antibody raised against  $\beta$ 1 integrin (1:50, Santa Cruz Biotechnology, Germany) for 30 min. After washing with PBS twice, a secondary goat anti-mouse antibody conjugated with CY2 (1:100, Dianova) was applied for another 30 min. The nuclei were stained with TO-PRO3 (1:500, Invitrogen) for 30 min. Finally, all samples were mounted with Mowiol (Calbiochem) and examined with a CLSM (Carl Zeiss) using a 40-fold oil immersion objective. Images were processed with the ZEN2011 software (Carl Zeiss).

#### 4.3.3.6 Pro-inflammatory cytokine production

The medium supernatants of untreated and LPS-challenged samples were collected after 24 h of incubation and stored at -20°C until needed for investigation of IL-1 $\beta$  production. An enzyme-linked immunosorbent assay (ELISA) was used here according to the manufacturer's instructions (Thermo Scientific, Germany). The cell viability was determined by a QBlue<sup>®</sup> cell viability assay (BioChain, USA) to normalize the cytokine production to the quantity of metabolic active cells on the different PEM surfaces. Briefly, after collecting the supernatant, cells were washed carefully with sterile PBS once and 500  $\mu$ L of pre-warmed, colorless Dulbecco's modified Eagle's medium (DMEM) supplemented with the QBlue<sup>®</sup> reagent (10:1) were added to each well. After incubation at 37°C for 2 h, 100  $\mu$ L supernatant from each well were transferred to a black 96-well plate and the relative fluorescence units (RFU) were measured at 544 nm excitation and 590 nm emission with plate reader (FLUOstar, BMG LabTech, Offenburg, Germany). Finally, the cytokine production values were normalized to the RFU values.

#### 4.3.4 Statistics

All data are represented as mean values  $\pm$  standard deviations (SD). Statistical examination was performed using one-way analysis of variance (ANOVA) followed by post-hoc Tukey testing. The significance level was set as  $p \leq 0.05$  and indicated by an asterisk. The number of samples has been indicated in the respective figures caption.

## 4.4 Results

### 4.4.1 Characterization of multilayer formation and surface properties

Multilayer growth was determined using SPR. As an optical method, minute variations in changes of the refractive index (RI) due to the adsorption of molecules on the surface are related to a certain mass increase. However, only the dry mass without absorbed water is determined here due to the experimental setup, where all solutions are water-based with the RI of water used as reference [22]. Figure 4.1 shows the calculated increase in adsorbed mass for all multilayer combinations. It can be seen that all PEM systems grew exponentially, but to a different extent. The lowest growth was found in systems containing Hep as polyanion. Here, the increase in adsorbed mass for each succeeding layer was similar to that of the preceding layer, leading to only slight exponential growth regimes. In contrast, the growth

regimes of HA and CS paired with Chi had a slight staircase character, i.e. adsorption was always higher for the GAGs in comparison to Chi. Here, even though the molecular weight of HA was much higher than that of CS, lower mass increases were observed, which is probably due to the lower charge density of HA lacking sulfate groups. By contrast, CS as much smaller molecule with a higher charge density compared to HA led to highest multilayer masses.

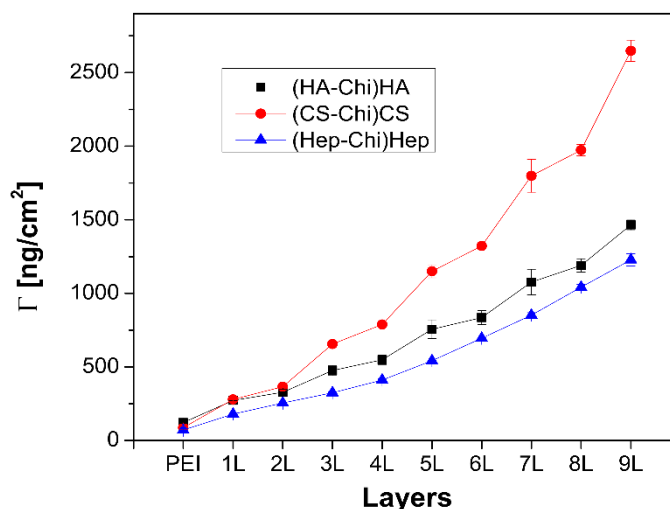
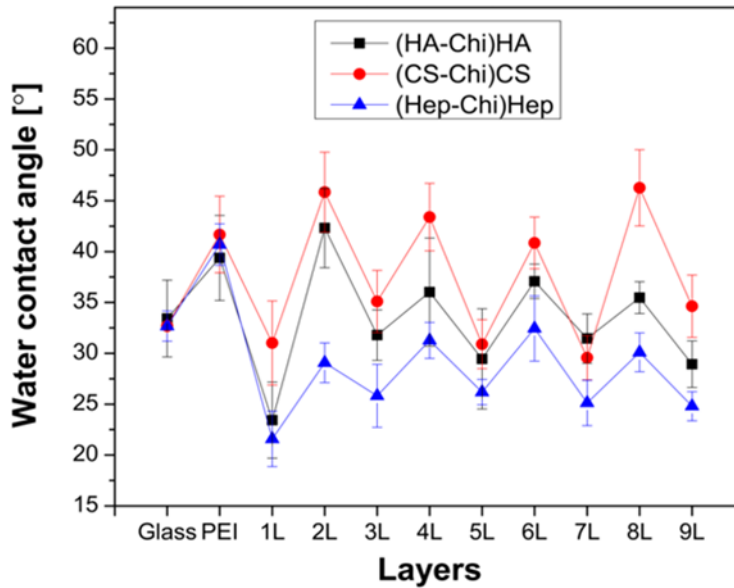


Figure 4.1. Multilayer mass calculated from angle shifts obtained with surface plasmon resonance (SPR). Up to nine layers were adsorbed on the primary PEI layer and abbreviated as follows: (HA-Chi)HA (■), (CS-Chi)CS (●), and (Hep-Chi)Hep (▲). Odd layers: GAGs - hyaluronic acid (HA), chondroitin sulfate (CS), and heparin (Hep). Even layers: chitosan (Chi). Results are means  $\pm$  SD of two independent experiments.

Static WCA measurements are a common and simple technique to determine the changes in surface composition upon adsorption of molecules and have been used to characterize multilayer formation processes with LbL technique [23]. Here, the incorporation of different GAGs within PEMs resulted in varying wettability as depicted by Figure 4.2. First, the adsorption of PEI resulted in moderately wettable surfaces while the adsorption of GAGs led to hydrophilic surfaces. Further, the alternating adsorption of GAGs and Chi led to an oscillation in WCA with higher values for Chi and lower values for GAGs, no matter for which layer number. Among the GAGs, Hep had the highest wettability followed by HA and CS. Moreover, the wettability of Chi was different in various GAG-Chi systems with the following

order Hep-Chi > HA-Chi > CS-Chi. Finally, the WCA shift between GAGs and Chi appeared



more sharply in the CS-Chi system than in HA-Chi and Hep-Chi systems.

Figure 4.2. Static water contact angles (WCA) for up to nine layers on top of PEI abbreviated as (HA-Chi)HA (■), (CS-Chi)CS (●), and (Hep-Chi)Hep (▲). Odd layers: GAGs - hyaluronic acid (HA), chondroitin sulfate (CS), and heparin (Hep). Even layers: chitosan (Chi). Results are means  $\pm$  SD of two independent experiments and triplicate samples for each condition.

The multilayer composition had a strong effect on the overall charge of the terminal layer, indicated by different surface zeta potentials as shown in Figure 4.3. However, zeta potential measurements do not only determine the potential of the very last layer, but also represent the potential of swollen, permeable layers beneath, which is contradictory to WCA measurements, where only the terminal layer composition influences the wettability [24]. In general, polyanions dominate the surface potential at basic pH, while polycations dominate it at acidic pH due to protonation. It can be seen that the formation of the primary PEI layer resulted in a positive potential below pH 8.3, which is its reported  $pK_a$  value [25]. By contrast, significant increase of negative charges was observed for GAGs-terminated multilayers, especially with a negative surface potential at physiological pH. Furthermore, clear differences were found in zeta potentials of the terminal GAG layers, especially at acidic pH values. Hep as the strongest polyanion had the lowest potentials throughout the whole measured pH range, followed by HA and CS.

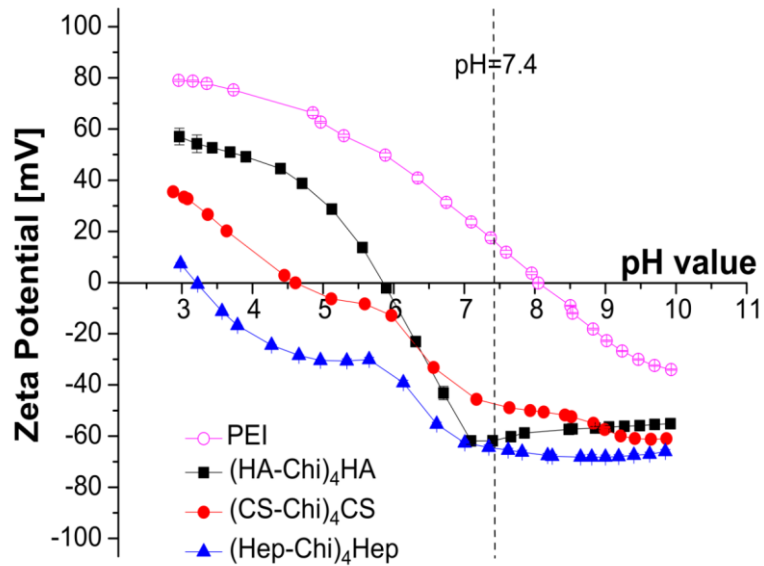


Figure 4.3. Zeta potential measurements of the initial PEI layer (○) and multilayers abbreviated as (HA-Chi)<sub>4</sub>HA (■), (CS-Chi)<sub>4</sub>CS (●), and (Hep-Chi)<sub>4</sub>Hep (▲).

#### 4.4.2 Adhesion and fusion of macrophages

The aim of the study was to investigate the anti-inflammatory potential of different GAG-Chi multilayer systems. For this reason, THP-1 cells were used as model system and differentiated into macrophages by PMA treatment. At first, adhesion of these differentiated macrophages to the different terminal GAG layers in comparison to the primary PEI layer was investigated using histochemical (Figure 4.4) as well as immunocytochemical (Figure 4.5) techniques.



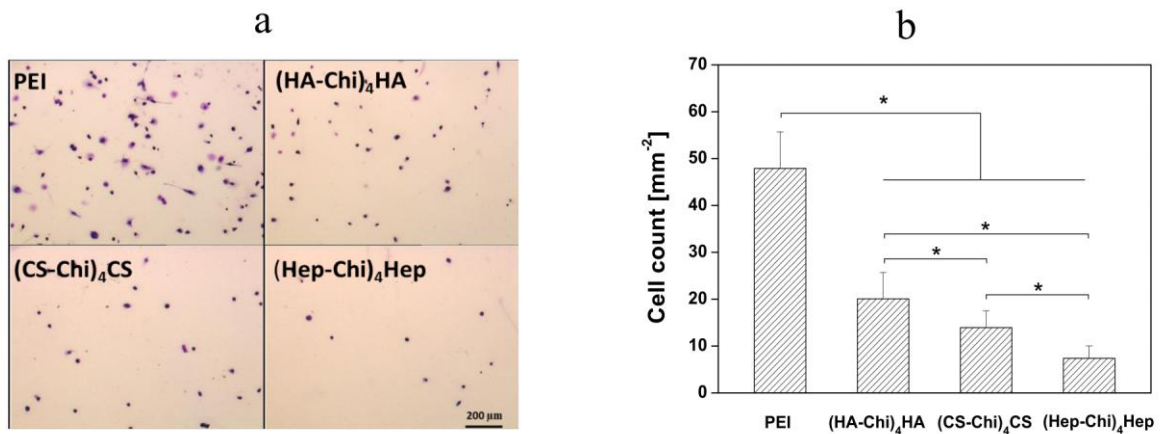


Figure 4.4. (a) Transmitted light microscopic images of macrophage adhesion on the primary PEI layer and terminal layer of (HA-Chi)<sub>4</sub>HA, (CS-Chi)<sub>4</sub>CS, and (Hep-Chi)<sub>4</sub>Hep. THP-1 cells were differentiated by incubation with 200 nM PMA for 48 h. The resulting macrophage cells were collected and cultured for additional 24 h in serum-free RPMI medium as well as stained with 10% (v/v) Giemsa solution [Scale bar: 200 μm]. (b) Quantified macrophages per area adherent on PEI and different terminal GAG layers after 24 h. Data represent mean ± SD, n = 4, \*p ≤ 0.05.

Figure 4.4 shows that macrophages adhered differently to the various surfaces. The significantly highest cell count was found on the primary PEI layer (Figure 4.4b). In contrast, the cell adhesion on GAGs-terminated multilayer surfaces were much reduced. Moreover, macrophages on PEI surfaces adhered stronger and spread more with a larger cell area than on multilayer surfaces (Figure 4.4a and Figure 4.5). However, the formation of actin stress fibers was not observed even on PEI surfaces. Instead, plenty of filopodia were formed at the periphery of cells (Figure 4.5). Further, focal adhesion plaques were lacking resulting in a rather clustered distribution of vinculin in the cells. As expected, cell spreading on GAGs-terminated multilayers were largely suppressed compared with PEI surface, illustrated by the smaller cell area and reduced actin and vinculin expression. The highest extent in inhibiting cell spreading was found on Hep surfaces. There, cells kept a round shape with no actin cytoskeleton polymerization nor vinculin expression, indicated by the ring-like cytoplasmic staining of actin. On CS surfaces, macrophages started to spread with slight filopodia formation, but not to a high extent within 24 h of culture. By contrast, adhesion and spreading were significantly improved ( $p \leq 0.05$ ) on HA surface in comparison to CS and Hep surfaces, but still much weaker than on PEI surfaces. Overall, GAG-Chi multilayers

significantly reduced macrophage adhesion and spreading. Meanwhile, multilayer architecture especially of the outermost layers is important for these adhesion and spreading behavior, and thus will be investigated in the succeeding events.

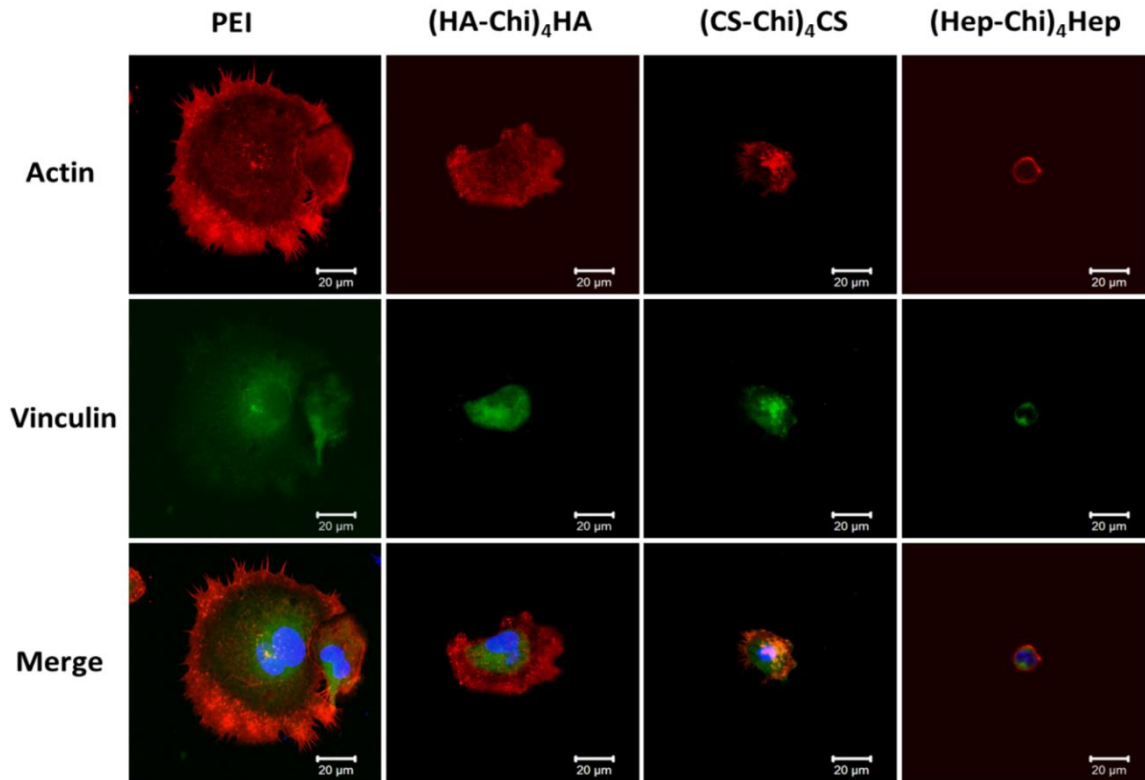


Figure 4.5. Representative confocal laser scanning microscopy (CLSM) images of macrophages after 24 h incubation in serum-free RPMI medium on the initial PEI layer and terminal layers of (HA-Chi)<sub>4</sub>HA, (CS-Chi)<sub>4</sub>CS, and (Hep-Chi)<sub>4</sub>Hep. The cells were stained for vinculin (green), actin (red), and nucleus (blue). [63-fold oil immersion objective, scale: 20 μm].

As well known, macrophage fusion with other macrophages to form FBGCs is a hallmark of chronic inflammation and FBR [26]. Besides, it is generally believed that the extent of FBGC formation could reflect the biocompatibility of biomaterials [2, 27]. Although LPS is known as a strong stimulant for macrophage activation such as up-regulation of proinflammatory cytokine production [28], yet no reports have documented its effect on FBGC formation and  $\beta$ 1 integrin expression. Here, formation of FBGCs and expression of  $\beta$ 1 integrin on different surfaces after 10 days incubation in presence or absence of LPS were investigated to collect clues for studying FBR.

Figure 4.6 shows that macrophage fusion on different surfaces followed a similar trend as observed in macrophage adhesion either with or without LPS treatment. There, the fusion extent and the differences of FBGC formation between different surfaces were enlarged upon LPS treatment. Marked macrophage fusion on PEI surface was observed in terms of more ( $n \geq 2$ ) nuclei accumulation randomly within an extensively spread cell body, especially after LPS treatment. In contrast, less nuclei and reduced size of FBGCs were found on GAGs-terminated multilayers. Again, the Hep-terminated multilayers resulted in lowest degree of fusion, illustrated by fewer nuclei in one cell body and much suppressed spreading of FBGCs. Figure 4.7 depicts the area percentages of formed FBGCs on different surfaces with the order of PEI > (HA-Chi)<sub>4</sub>HA ~ (CS-Chi)<sub>4</sub>CS > (Hep-Chi)<sub>4</sub>Hep. Moreover, the area percentage of FBGCs increased upon LPS treatment on all surfaces except Hep-terminated multilayers.

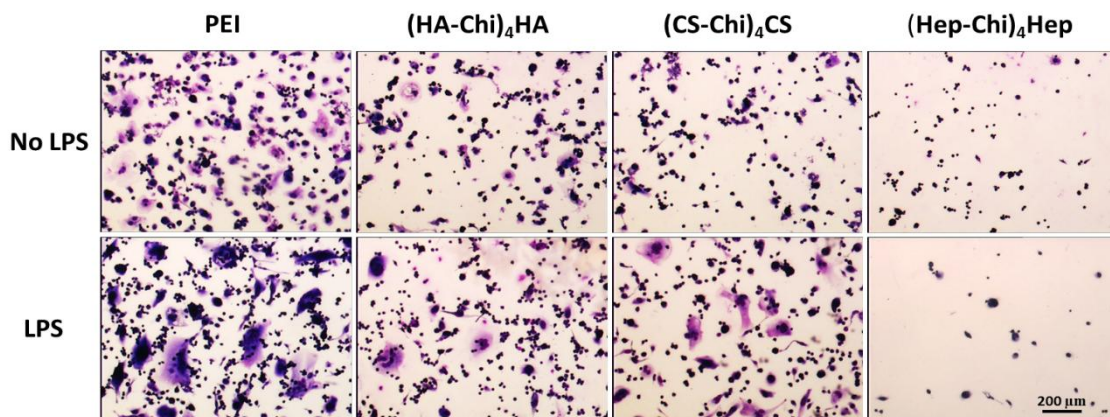


Figure 4.6. Transmitted light microscopic images of Giemsa-stained foreign body giant cells (FBGCs) after 10 days incubation in absence (upper row) and presence (lower row) of lipopolysaccharide (LPS) on the initial PEI layer and terminal layers of (HA-Chi)<sub>4</sub>HA, (CS-Chi)<sub>4</sub>CS, and (Hep-Chi)<sub>4</sub>Hep [Scale: 200 μm].

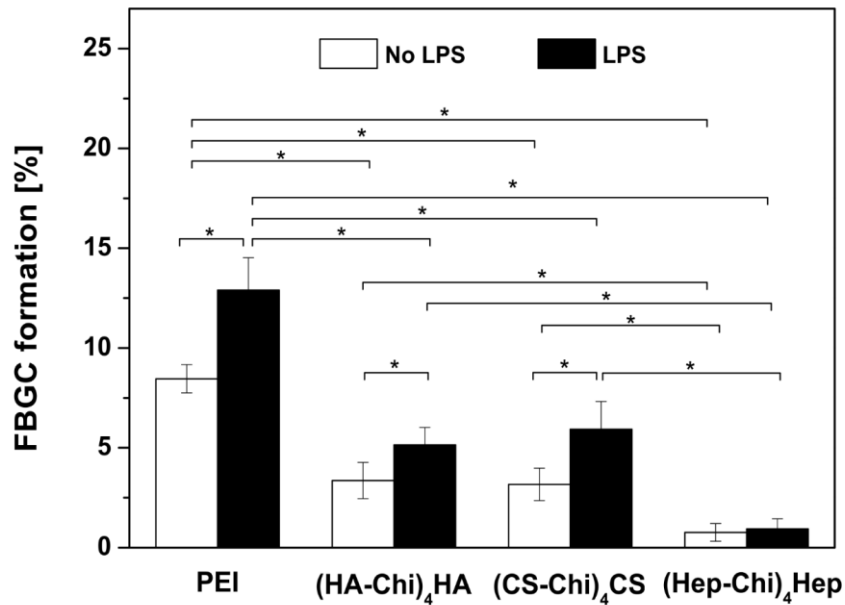


Figure 4.7. The area percentage of FBGCs adherent on the initial PEI layer as well as terminal GAG layers of (HA-Chi)<sub>4</sub>HA, (CS-Chi)<sub>4</sub>CS, and (Hep-Chi)<sub>4</sub>Hep was determined after 10 days incubation in absence (white bars) and presence (black bars) of lipopolysaccharide (LPS) by quantitative evaluation of micrographs. Data represent mean  $\pm$  SD,  $n = 10$ ,  $*p \leq 0.05$ .

$\beta 1$  integrin was reported to play crucial roles during macrophage fusion and FBGC formation [21], and thus was studied and served here as another parameter to characterize the anti-inflammatory effects induced by GAG-Chi multilayers. Figure 4.8 shows significant reduction of  $\beta 1$  integrin expression (green staining) and cell spreading on multilayers terminated with GAGs in comparison to PEI. Additionally, cells on PEI surfaces possessed more nuclei per cell body or larger sized nuclei (in presence of LPS) than on multilayer surfaces. Furthermore, LPS treatment enhanced the expression of  $\beta 1$  integrin on all surfaces. Last but importantly, the  $\beta 1$  integrin expression among the GAGs followed a similar trend as observed in macrophage fusion showing an order of (HA-Chi)<sub>4</sub>HA  $\sim$  (CS-Chi)<sub>4</sub>CS > (Hep-Chi)<sub>4</sub>Hep.

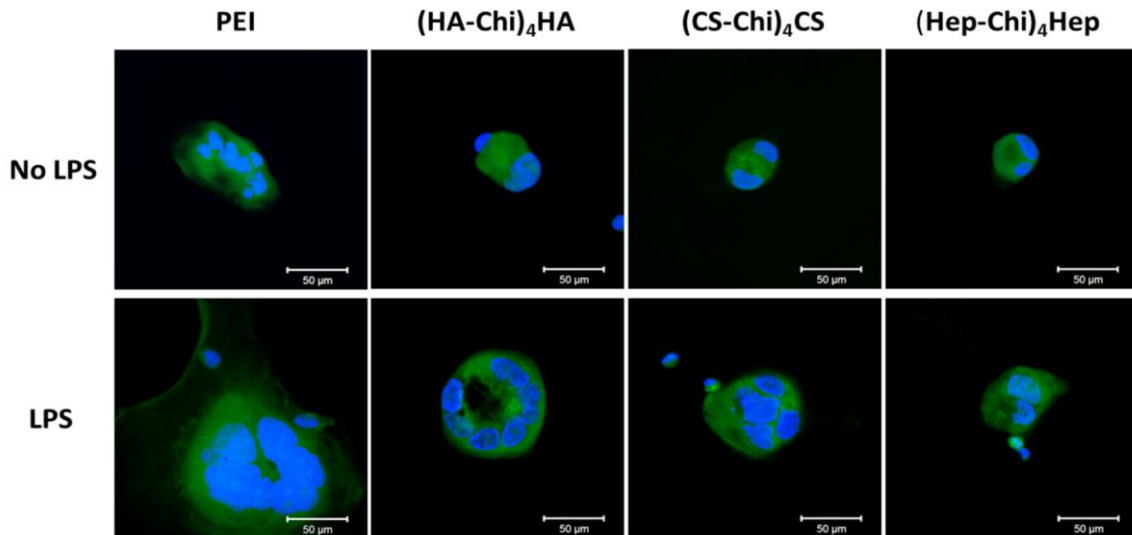


Figure 4.8. Expression of  $\beta 1$  integrin was determined on fusing macrophages/FBGCs after 10 days incubation in absence (upper row) and presence (lower row) of lipopolysaccharide (LPS) on the initial PEI layer and the terminal GAG layer of (HA-Chi)<sub>4</sub>HA, (CS-Chi)<sub>4</sub>CS, and (Hep-Chi)<sub>4</sub>Hep. Cells were fixed with 4% paraformaldehyde and stained for  $\beta 1$  integrin (green) and nuclei (blue) [Scale: 50  $\mu$ m].

#### 4.4.3 IL-1 $\beta$ cytokine production

Upon activation, macrophages can secrete a variety of molecules including cytokines and chemokines to drive the inflammatory responses further [4]. Thus, the production of the typical proinflammatory IL-1 $\beta$  [29] was studied here to investigate the anti-inflammatory potential of the GAG-Chi multilayers. Figure 4.9 shows the IL-1 $\beta$  production after 24 h of incubation on different surfaces in absence (white bars) and presence (black bars) of LPS stimuli. As expected, macrophages adherent to PEI and Hep-terminated multilayer surfaces produced the highest and lowest amounts of IL-1 $\beta$ , respectively, while HA and CS terminated multilayers caused intermediate IL-1 $\beta$  production. In addition, IL-1 $\beta$  production was up-regulated on all surfaces after LPS treatment.

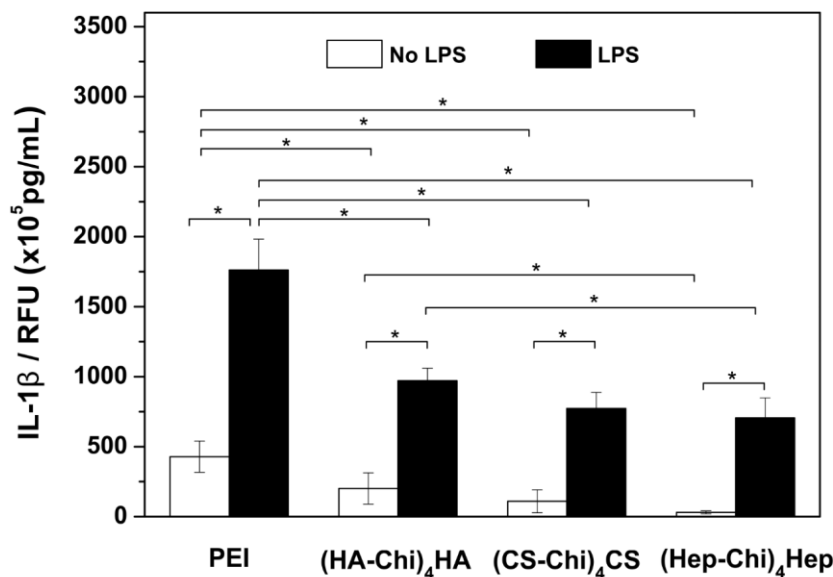


Figure 4.9. IL-1 $\beta$  production of macrophages after 24 h incubation in absence (white bars) and presence (black bars) of lipopolysaccharide (LPS) on the initial PEI layer and the terminal layer of (HA-Chi)<sub>4</sub>HA, (CS-Chi)<sub>4</sub>CS, and (Hep-Chi)<sub>4</sub>Hep. Data represent mean  $\pm$  SD, n = 6, \*p  $\leq$  0.05.

## 4.5 Discussion

It was shown here that inflammatory responses of macrophages could be greatly hindered by GAG-Chi multilayers deposition on a model biomaterial surface. Additionally, the types of terminal GAGs played pivotal roles in tailoring the multilayer surface properties and subsequent cellular behavior and inflammatory responses.

Physicochemical studies were performed to follow formation of multilayers in dependence on type of GAGs and resulting surface properties. Exponential growth regimes observed by SPR measurements were also shown by others for polysaccharide-based multilayers, especially for Hep and Chi as polyelectrolytes having a diffusible component in the system [22]. The SPR data, indicated also that ion pairing dominates with complete charge reversal after each adsorption step [30]. The staircase character in HA and CS-based multilayers could be attributed to the molecular weight difference between HA/CS and Chi [22]. The resulting WCA oscillation is an indicator for different terminal layer composition, showing that one molecule is dominating the surface properties with more separated and less intermingled single layers [22]. The high wettability of Hep originates from its high content of sulfate monoesters and sulfamido groups [31]. Even though CS possesses sulfate groups, its

wettability was lower than that of HA, which possesses less charged carboxylic acid groups. The ability of HA to absorb high amounts of water could enhance its wettability [32] and the strong WCA oscillation in CS-Chi systems might be a result of high CS amounts observed with SPR measurement. However, it should be noted here that all terminal GAG layers were highly wettable with moderate differences between the different GAGs. The point of zero charge (PZC) observed during zeta potential measurement is a further indicator of a different multilayer composition. The PZC of PEI close to its reported  $pK_a$  value indicated a complete charge reversal of negatively charged glass after PEI adsorption with a positive potential at pH 7.4. The data after multilayer deposition showed that the strong polyelectrolyte Hep is the dominating molecule in Hep-Chi multilayers with a PZC at pH 3.2 close to the  $pK_a$  value of carboxylic acid groups. CS with the second highest charge density formed multilayers slightly less negative than the Hep-based system. Further, the PZC at pH~6.0 of the terminal HA layer indicates the dominance of Chi, since it is close to its  $pK_a$ . Altogether, the results of physicochemical studies reveal modest differences in surface wettability and charge properties between the three GAG-based multilayer systems.

Macrophage adhesion and spreading showed significant reduction on GAGs-terminated multilayers in comparison to the primary PEI layer. The highest adhesion on PEI surface is due to the high amount of amino groups with resulting moderate wettability and positive surface potential at pH 7.4 as observed with WCA and zeta potential measurements. By contrast, the cell adhesion and spreading were largely decreased on GAGs-terminated surfaces owing to the more hydrophilic and negatively charged properties. These results are consistent with previous findings showing that proteins and cells prefer to adsorb and attach on moderate hydrophilic and positively charged surfaces than on hydrophilic and negatively charged surfaces [33]. Subsequently, the macrophage spreading morphology observed by immunofluorescence staining (Figure 1.5) further confirmed the observations in histochemical staining (Figure 1.4a). It was shown a largely suppressed spreading morphology on GAG-Chi multilayers compared to PEI. During various GAGs-terminated surfaces, Hep-based multilayer was found the most efficiency in inhibiting macrophage adhesion and spreading. The highest wettability and negative charge at pH 7.4 of this surface might account partly for this. Furthermore, many researches have indicated the anti-inflammatory potential of Hep [34]. By contrast, the slightly reduced wettability and negative charge of CS resulted in a slightly enhanced spreading behavior on CS in comparison to Hep surface. Moreover, a significantly improved adhesion and spreading was found on HA surface in comparison to CS and Hep surfaces. The reason might be that macrophages possess specific receptors (e.g. CD44) for

HA, which enhanced the specific ligand-receptor interaction and resulted in the improved adhesion of macrophages [35].

FBGC formation and  $\beta 1$  integrin expression on various surfaces followed a similar trend as observed in macrophage adhesion in both presence and absence of LPS treatment. These data consistently showed an order of PEI > (HA-Chi)<sub>4</sub>HA ~ (CS-Chi)<sub>4</sub>CS > (Hep-Chi)<sub>4</sub>Hep. Here, the observed similar tendency between FBGC formation,  $\beta 1$  integrin expression and macrophage adhesion is reasonable, since a certain cell adhesion density and spreading of the cells are needed for one macrophage to fuse with other macrophages on this surface. Further, a higher fusion extent might account for a more striking  $\beta 1$  integrin expression. Therefore, the variance of FBGC formation and  $\beta 1$  integrin expression on different surfaces stems from the difference in the initial macrophage adhesion. In general, the material surface properties could dedicate the protein adsorption from the serum-containing medium, and thus affect the ligand binding to adhesion receptors (e.g. integrins and CD44), which further mediated the macrophage adhesion and fusion behavior [36].

Finally, the reduction of proinflammatory cytokine IL-1 $\beta$  production by GAG-Chi multilayers revealed their great potential in inhibiting the proinflammatory responses. Here, the physiochemical properties of the GAG-Chi multilayers, together with the physiologic roles of various GAGs in regulation of inflammatory responses, might account for the different anti-inflammatory activities of varying multilayer systems. In fact, the anti-inflammatory effects of GAGs have been reported by others previously. For example, high molecule weight HA (HMW-HA) was reported to impair macrophage adhesion and macrophage multi-nucleation [37] as well as to reduce the proinflammatory cytokine production by multiple cell types [38]. The mechanism of the anti-inflammatory effects of HMW-HA is attributed to the crosslink interactions with the cell receptor CD44, which could translate clues from HA into signals to down-regulate proinflammatory responses and promote wound healing [39]. Consistently, CS, commonly used as therapeutic agent in osteoarthritis due to its strong anti-inflammatory effects in synovitis, was also proven to inhibit LPS-induced inflammatory effects such as suppressing of proinflammatory cytokine production [40]. It was found that the inflammatory inhibiting effects of CS are based on reduction of NF- $\kappa$ B nuclear translocation, which down-regulates the subsequent proinflammatory mediators [41]. Last but most importantly, the highest inhibition of proinflammatory responses on Hep-terminated surfaces was attributed to the highest wettability and most negative zeta potential. Additionally, since the assembling of the multilayers was based on physical adsorption of GAGs and Chi, it might allow here the uptake of Hep molecules by the cells, which could lead also to a reduction of



NF- $\kappa$ B nuclear translocation and thus lowered expression of cytokines [42]. On the other hand, Chi was also reported with improved anti-inflammatory capacity [43]. Therefore, the deposition of GAG-Chi multilayers, based on the combination of anti-inflammatory effects from both GAGs and Chi, exerted here the great influence in reducing the inflammatory responses in comparison to the primary PEI layer.

## 4.6 Conclusions

In the present work, GAG-Chi multilayers were assembled on glass substrates as model surfaces using the LbL method to investigate their effects in regulating inflammatory reactions. The inflammatory responses were found greatly reduced on all GAG-Chi multilayers compared to the primary PEI layer in terms of macrophage adhesion, spreading, FBGC formation,  $\beta$ 1 integrin expression as well as proinflammatory cytokine IL-1 $\beta$  production, which goes along the hydrophilic character and negative surface charge of all multilayers terminated by GAG. However, more important is the observation of the pivotal roles of different types of GAGs in tuning the multilayer surface properties, which further modulated the cellular behavior and inflammatory responses. It was found that the Hep-terminated multilayers caused the lowest extent of proinflammatory responses, indicating the highest biocompatibility of these surfaces. Overall, our results suggest that the GAG-Chi multilayer coating, especially the Hep-Chi multilayer systems, may have a great potential in reducing the inflammatory potential of materials used in various biomedical and tissue engineering applications.

## 4.7 Disclosure

No conflicts of interests are declared.

## 4.8 Acknowledgements

G. Zhou thanks the China Scholarship Council for offering the scholarship to work in Germany. The assistance of Mrs. M. Porobin in zeta potential measurement is gratefully acknowledged.

## 4.9 References

- [1] Tang LP, Eaton JW. Inflammatory responses to biomaterials. *Am J Clin Pathol* 1995;103:466-71.
- [2] Anderson JM, Miller KM. Biomaterial biocompatibility and the macrophage. *Biomaterials* 1984;5:5-10.
- [3] Xia Z, Triffitt JT. A review on macrophage responses to biomaterials. *Biomedical Materials* 2006;1:R1-R9.
- [4] Anderson JM, Rodriguez A, Chang DT. Foreign body reaction to biomaterials. *Semin Immunol* 2008;20:86-100.
- [5] Schutte RJ, Parisi-Amon A, Reichert WM. Cytokine profiling using monocytes/macrophages cultured on common biomaterials with a range of surface chemistries. *J Biomed Mater Res Part A* 2009;88A:128-39.
- [6] Luttikhuisen DT, Harmsen MC, Van Luyn MJA. Cellular and molecular dynamics in the foreign body reaction. *Tissue Engineering* 2006;12:1955-70.
- [7] Westergren-Thorsson G, Larsen K, Nihlberg K, Andersson-Sjoland A, Hallgren O, Marko-Varga G, Bjermer L. Pathological airway remodelling in inflammation. *Clin Respir J* 2010;4:1-8.
- [8] Franz S, Rammelt S, Scharnweber D, Simon JC. Immune responses to implants - a review of the implications for the design of immunomodulatory biomaterials. *Biomaterials* 2011;32:6692-709.
- [9] Severin IC, Soares A, Hantson J, Teixeira M, Sachs D, Valognes D, Scheer A, Schwarz MK, Wells TNC, Proudfoot AEI, Shaw J. Glycosaminoglycan analogs as a novel anti-inflammatory strategy. *Frontiers in immunology* 2012;3:293.
- [10] Taylor KR, Gallo RL. Glycosaminoglycans and their proteoglycans: Host-associated molecular patterns for initiation and modulation of inflammation. *Faseb J* 2006;20:9-22.
- [11] Dash M, Chiellini F, Ottenbrite RM, Chiellini E. Chitosan-a versatile semi-synthetic polymer in biomedical applications. *Progress in Polymer Science* 2011;36:981-1014.
- [12] Richardson JJ, Bjornmalm M, Caruso F. Multilayer assembly. Technology-driven layer-by-layer assembly of nanofilms. *Science* 2015;348:aaa2491.

[13] Borges J, Mano JF. Molecular interactions driving the layer-by-layer assembly of multilayers. *Chemical Reviews* 2014;114:8883-942.

[14] Silva JM, Georgi N, Costa R, Sher P, Reis RL, Van Blitterswijk CA, Karperien M, Mano JF. Nanostructured 3D constructs based on chitosan and chondroitin sulphate multilayers for cartilage tissue engineering. *Plos One* 2013;8:e55451.

[15] Battiston KG, Labow RS, Santerre JP. Protein binding mediation of biomaterial-dependent monocyte activation on a degradable polar hydrophobic ionic polyurethane. *Biomaterials* 2012;33:8316-28.

[16] Zhou G, Loppnow H, Groth T. A macrophage/fibroblast co-culture system using a cell migration chamber to study inflammatory effects of biomaterials. *Acta Biomaterialia* 2015;26:54-63.

[17] Theus SA, Cave MD, Eisenach KD. Activated THP-1 cells: An attractive model for the assessment of intracellular growth rates of mycobacterium tuberculosis isolates. *Infect Immun* 2004;72:1169-73.

[18] Park EK, Jung HS, Yang HI, Yoo MC, Kim C, Kim KS. Optimized THP-1 differentiation is required for the detection of responses to weak stimuli. *Inflammation Research* 2007;56:45-50.

[19] Patel N, Davies MC, Hartshorne M, Heaton RJ, Roberts CJ, Tendler SJB, Williams PM. Immobilization of protein molecules onto homogeneous and mixed carboxylate-terminated self-assembled monolayers. *Langmuir* 1997;13:6485-90.

[20] Schasfoort RBM, Tudos AJ. Handbook of surface plasmon resonance. 1st ed. Cambridge: Rsc publishing; 2008. p 128.

[21] McNally AK, Anderson JM. Beta 1 and beta 2 integrins mediate adhesion during macrophage fusion and multinucleated foreign body giant cell formation. *Am J Pathol* 2002;160:621-30.

[22] Aggarwal N, Groth T. Multilayer films by blending heparin with semisynthetic cellulose sulfates: Physico-chemical characterization and cell responses. *J Biomed Mater Res Part A* 2014;102:4224-33.

[23] Aggarwal N, Altgärde N, Svedhem S, Michanetzis G, Missirlis Y, Groth T. Tuning cell adhesion and growth on biomimetic polyelectrolyte multilayers by variation of pH during layer-by-layer assembly. *Macromol Biosci* 2013;13:1327-38.

[24] Duval JF, Kuttner D, Werner C, Zimmermann R. Electrohydrodynamics of soft polyelectrolyte multilayers: Point of zero-streaming current. *Langmuir* 2011;27:10739-52.

[25] Choosakoonkriang S, Lobo BA, Koe GS, Koe JG, Middaugh CR. Biophysical characterization of PEI/DNA complexes. *Journal of Pharmaceutical Sciences* 2003;92:1710-22.

[26] Kou PM, Babensee JE. Macrophage and dendritic cell phenotypic diversity in the context of biomaterials. *J Biomed Mater Res A* 2011;96A:239-60.

[27] Anderson JM. Biological responses to materials. *Ann Rev Mater Res* 2001;31:81-110.

[28] Loppnow H, Brade H, Rietschel ET, Flad HD. Induction of cytokines in mononuclear and vascular cells by endotoxin and other bacterial products. *Methods Enzymol* 1994;236:3-10.

[29] Dinarello CA. Immunological and inflammatory functions of the interleukin-1 family. *Annu rev immunol* 2009;27:519-50.

[30] Boddohi S, Killingsworth CE, Kipper MJ. Polyelectrolyte multilayer assembly as a function of pH and ionic strength using the polysaccharides chitosan and heparin. *Biomacromolecules* 2008;9:2021-8.

[31] Wang HM, Loganathan D, Linhardt RJ. Determination of the pKa of glucuronic acid and the carboxy groups of heparin by <sup>13</sup>C-nuclear-magnetic-resonance spectroscopy. *Biochemical Journal* 1991;278:689-95.

[32] Yamanlar S, Sant S, Boudou T, Picart C, Khademhosseini A. Surface functionalization of hyaluronic acid hydrogels by polyelectrolyte multilayer films. *Biomaterials* 2011;32:5590-9.

[33] Bacakova L, Filova E, Parizek M, Ruml T, Svorcik V. Modulation of cell adhesion, proliferation and differentiation on materials designed for body implants. *Biotechnology Advances* 2011;29:739-67.

[34] Young E. The anti-inflammatory effects of heparin and related compounds. *Thrombosis Research* 2008;122:743-52.

[35] Sladek Z, Rysanek D. Expression of macrophage CD44 receptor in the course of experimental inflammatory response of bovine mammary gland induced by lipopolysaccharide and muramyl dipeptide. *Research in Veterinary Science* 2009;86:235-40.

[36] Keselowsky BG, Collard DM, Garcia AJ. Surface chemistry modulates focal adhesion composition and signaling through changes in integrin binding. *Biomaterials* 2004;25:5947-54.

[37] Hsieh CYC, Hu F-W, Chen W-S, Tsai W-B. Reducing the foreign body reaction by surface modification with collagen/hyaluronic acid multilayered films. *ISRN Biomaterials* 2014;2014:718432.

[38] Neuman MG, Nanau RM, Oruna L, Coto G. In vitro anti-inflammatory effects of hyaluronic acid in ethanol-induced damage in skin cells. *Journal of Pharmacy and Pharmaceutical Sciences* 2011;14:425-37.

[39] Ruppert SM, Hawn TR, Arrigoni A, Wight TN, Bollyky PL. Tissue integrity signals communicated by high-molecular weight hyaluronan and the resolution of inflammation. *Immunologic Research* 2014;58:186-92.

[40] Iovu M, Dumais G, du Souich P. Anti-inflammatory activity of chondroitin sulfate. *Osteoarthritis and cartilage / OARS, Osteoarthritis Research Society* 2008;16 Suppl 3:S14-8.

[41] Iovu M, Dumais G, du Souich P. Anti-inflammatory activity of chondroitin sulfate. *Osteoarthritis Cartilage* 2008;16:S14-S8.

[42] Brito AS, Arimateia DS, Souza LR, Lima MA, Santos VO, Medeiros VP, Ferreira PA, Silva RA, Ferreira CV, Justo GZ, Leite EL, Andrade GPV, Oliveira FW, Nader HB, Chavante SF. Anti-inflammatory properties of a heparin-like glycosaminoglycan with reduced anti-coagulant activity isolated from a marine shrimp. *Bioorganic & Medicinal Chemistry* 2008;16:9588-95.

[43] Yoon HJ, Moon ME, Park HS, Im SY, Kim YH. Chitosan oligosaccharide (COS) inhibits LPS-induced inflammatory effects in raw 264.7 macrophage cells. *Biochemical and Biophysical Research Communications* 2007;358:954-9.

## 5 Covalent immobilization of glycosaminoglycans to reduce the inflammatory effects of biomaterials

Guoying Zhou, Hala Al-Khoury, Thomas Groth

### 5.1 Abstract

**Background:** The inflammatory responses evoked by artificial organs and implantation of devices like biosensors and guide wires can lead to acute and chronic inflammation, largely limiting the functionality and longevity of the devices with negative effects on patients.

**Aims:** The present study aimed to reduce the inflammatory responses to biomaterials by covalent immobilization of glycosaminoglycans (GAGs) on amino-terminated surfaces used as model biomaterials here.

**Methods and results:** Water contact angle (WCA) and zeta potential measurements showed a significant increase in wettability and negative charges on the GAG-modified surfaces, respectively, confirming the successful immobilization of GAGs on the amino-terminated surfaces. THP-1-derived macrophages were used as a model cell type to investigate the efficacy of GAG-modified surfaces in modulating inflammatory responses. It was found that macrophage adhesion, macrophage spreading morphology, foreign body giant cell (FBGC) formation, as well as  $\beta 1$  integrin expression and interleukin- $1\beta$  (IL- $1\beta$ ) production were all significantly decreased on GAG-modified surfaces compared to the initial amino-terminated surface.

**Conclusions:** This study demonstrates the potential of covalent GAG immobilization to reduce the inflammatory potential of biomaterials in different clinical settings.

**Keywords:** Cytokines, Foreign body giant cells, Glycosaminoglycans, Inflammation, Macrophages

## 5.2 Introduction

Biomaterial implants and medical devices are widely used nowadays and their performance is crucial for the safety and quality of life of patients (1). Nevertheless, the implantation of any foreign material or device will trigger a cascade of inflammatory responses, which can lead to chronic inflammation and fibrotic encapsulation, resulting in failure of implants and devices (2). In addition, the periprosthetic inflammatory responses to wear particles released from implanted prosthetics can cause osteolysis, leading to aseptic loosening of joint prosthetics, which is one of the most frequent reasons for the failure of total joint replacement surgeries (3). Monocytes/macrophages play central roles in these inflammatory responses, acting as a first line of defense in order to phagocytose the bacterial and foreign materials (4). Further, when facing materials that are much larger sized than themselves, several macrophages fuse to form foreign body giant cells (FBGCs) in order to increase their phagocytosis ability (5). Moreover, they are involved in these processes by secreting a variety of inflammatory mediators such as cytokines, chemokines and growth factors to attract other cell types such as fibroblasts (6). In response to these signals, fibroblasts are activated and differentiate into myofibroblasts to produce extracellular matrix (ECM) proteins such as collagen, leading to implant encapsulation and potential failure of the device (7). It has been confirmed that surface properties of biomaterials such as surface chemistry, wettability, surface potential and topography dictate the plasma protein adsorption onto the material surface immediately after implantation, and thereby affecting the subsequent cellular inflammatory responses to implants (8, 9). Therefore, an appropriate design and/or modification of the biomaterial surface properties has been considered as useful strategy for reducing the inflammatory responses and improving the implant performance (10).

Recently, many studies on prevention of the inflammatory responses have focused on incorporation of various anti-inflammatory agents like dexamethasone (DEX), alpha melanocyte-stimulating hormone ( $\alpha$ -MSH) and glycosaminoglycans (GAGs) to generate more biocompatible materials (10, 11). Among which, GAGs, linear unbranched polysaccharides such as hyaluronic acid (HA), chondroitin sulfate (CS), and heparin (Hep) are important components of ECM with various biological activities that include also some anti-inflammatory potential (12). GAGs participate in cell-matrix interactions and bind cytokines, growth factors, chemokines and enzymes affecting biological processes like cell migration, homing, growth, differentiation, which is also related to inflammation (13). In addition, both CS and Hep can bind to L- and P-selectin, which impairs leukocyte adhesion,

activation and transmigration activities (14). Furthermore, they can mediate anti-inflammatory effects by inhibition of nuclear factor- $\kappa$ B (NF- $\kappa$ B) translocation, which is a crucial transcription factor of many proinflammatory mediators, leading to suppression of proinflammatory cytokine production (15). By contrast, high molecular weight HA (HMW-HA) prevents inflammatory responses through interactions with CD44, which translates the signals from HA to down-regulate leukocyte activation, growth, and differentiation (16). Hence, the use of GAGs to modify the biomaterial surfaces seems to be a promising tool to reduce or prevent the inflammatory potential of biomaterials. Moreover, our recent work showed the deposition of GAG-chitosan multilayers on glass surfaces significantly reduced macrophage adhesion, fusion and down-regulated proinflammatory cytokine production (17).

The current study aims to evaluate the effect of covalent immobilization of GAGs on material surface for reduction of the inflammatory responses of macrophages to biomaterials. For this purpose, GAGs were covalently immobilized onto amino-terminated self-assembling monolayer (SAM) surface by 1-ethyl-3-(3-dimethylaminopropyl) carbodiimide (EDC)/N-hydroxysuccinimide (NHS) crosslinking chemistry (18). THP-1 cells were applied as a model monocyte system and differentiated into macrophage-like cells by treatment with phorbol-12-myristate-13-acetate (PMA) (19). By using the THP-1-derived macrophages, an anti-inflammatory effect of GAGs was observed in an *in vitro* setting. Results are reported herein.

## 5.3 Materials and Methods

### 5.3.1 Materials

Hyaluronic acid (HA, Mw~1.3 MDa) was provided by INNOVENT e.V. (Jena, Germany). Chondroitin sulfate sodium salt (CS, Mw~25 kDa) was purchased from Sigma-Aldrich (Taufkirchen, Germany). Heparin sodium salt (Hep, Mw~15 kDa) was provided by SERVA (Heidelberg, Germany). N-hydroxysuccinimide (NHS) and Triton X-100 were obtained from Sigma-Aldrich (Schnelldorf, Germany). Other used compounds were: 3-aminopropyltriethoxysilane (APTES) (ABCR GmbH & Co., KG, Karlsruhe, Germany), 2-(N-morpholino)ethanesulfonic acid monohydrate (MES) (VWR International, Poole, England), ethylenediamine (Sigma-Aldrich, Taufkirchen, Germany) and 1-ethyl-3-(3-dimethylaminopropyl) carbodiimide (EDC) (Alfa Aesar, Karlsruhe, Germany).



### **5.3.2 Preparation of GAGs-modified surfaces**

#### 5.3.2.1 Preparation of amino-terminated SAM

Round glass cover slips ( $\varnothing$ 15 mm, Menzel GmbH, Germany) were cleaned with 0.5 M NaOH in 96% ethanol (Roth, Germany) for 2 h. Subsequently, the slides were extensively rinsed with double-distilled water (10 $\times$ 5 min) and dried under nitrogen flow.

The amino-terminated SAMs were obtained by immersing the cleaned glass slides in 2% (v/v) solution of APTES in 99.8% acetone (Roth, Germany) for 1 h at room temperature (RT). After that, the surfaces were rinsed extensively with acetone, ethanol and washed with double-distilled water (8 $\times$ 5 min). Then the surfaces were dried with streaming nitrogen and baked for 1 h at 100 °C.

#### 5.3.2.2 Immobilization of GAGs onto amino-terminated SAM

GAG solutions of HA, CS and Hep at 4 mg mL<sup>-1</sup> were firstly prepared by dissolution in freshly prepared MES-buffered solution (50 mM, pH 4.7). Subsequently, 5 mg mL<sup>-1</sup> of EDC and 3 mg mL<sup>-1</sup> of NHS were added respectively to the GAG solutions for 30 min each at RT. Thereafter, the amino-terminated glass surfaces were immersed in the EDC/NHS-activated GAG solutions for 24 h. After that, 1M ethylenediamine solution was added to inactivate the remaining reactive carboxyl species of the EDC linker (18). The surfaces were then rinsed with ethanol, washed with double-distilled water (8 $\times$ 5 min), and dried under nitrogen flow.

### **5.3.3 Characterization of GAGs-modified surfaces**

#### 5.3.3.1 Surface wettability studies

Static water contact angle (WCA) measurements were conducted using the OCA 15+ device from Dataphysics (Filderstadt, Germany). Here, five droplets of 2  $\mu$ L fresh ultrapure water were placed onto each surface at RT and the sessile drop method was applied. The experiments were run in triplicate and mean and standard deviations of two independent experiments were calculated.

### 5.3.3.2 Surface potential measurements

Zeta potentials of amino-terminated SAM and GAGs-modified surfaces were determined with a SurPASS device (Anton Paar, Graz, Austria). Glass cover slips with specific dimensions were used for sample preparation and zeta potential measurements. Two identically modified cover slips were fixed and placed oppositely into the adjustable gap cell. The gap was adjusted to a distance where a flow rate of 100 to 150 mL min<sup>-1</sup> was achieved at a maximum overpressure of 300 mbar. 1 mM potassium chloride (KCl) was used as model electrolyte and 0.1 M hydrochloric acid (HCl) was used for pH titration. The pH value of KCl was adjusted to pH 10.5 using 1 M sodium hydroxide (NaOH) before starting the measurement. Then the measurements were performed by an automated titration program using titration steps of 0.03 µL from pH 10.5 to 5.0 and 0.25 µL from pH 5.0 to 3.0.

## 5.3.4 Cell experiments

### 5.3.4.1 Cell culture

Cells of the human monocytic cell line THP-1 (DSMZ, Germany) were cultured in RPMI-1640 medium (Biochrom AG, Germany) supplemented with 10% (v/v) fetal bovine serum (FBS, Biochrom AG), 1% (v/v) antibiotic–antimycotic solution (AAS, Promocell, Germany) at 37 °C in a humidified 5% CO<sub>2</sub>/ 95% air atmosphere using a NUAIRE® DH Autoflow incubator (NuAire Corp., Plymouth, Minnesota, USA). Suspended cells were passaged by centrifugation. The old medium was removed and the cell pellet was resuspended in fresh medium every second day in order to maintain a cell density of 0.5-1.0 x 10<sup>6</sup> cells mL<sup>-1</sup>. THP-1-derived macrophages were obtained by incubation of THP-1 cells with 200 nM phorbol-12-myristate-13-acetate (PMA, Sigma) in T75 cell culture flasks (Greiner Bio-One, Germany) for 48 h. Afterwards, the differentiated macrophages were detached by incubation with 0.25% trypsin/ 0.02% EDTA (Biochrom AG) and used for seeding on the different surfaces.

### 5.3.4.2 Cell adhesion studies

THP-1-derived macrophages were seeded on amino-terminated SAM and GAGs-modified surfaces at a cell density of 2.5 x 10<sup>4</sup> cells mL<sup>-1</sup> in serum-free RPMI-1640 medium. Cultures were incubated at 37 °C in a humidified 5% CO<sub>2</sub>/ 95% air atmosphere for 24 h. Thereafter, the surfaces were gently washed with PBS once to remove non-adherent

cells. Attached cells were fixed by methanol and stained with 10% (v/v) Giemsa (Merck KGaA, Germany) in ultrapure water. Cells were visualized with a transmitted light microscope (Axiovert 100, Carl Zeiss MicroImaging GmbH, Germany) equipped with a CCD camera (Sony, MC-3254, AVT-Horn, Aalen, Germany). The cell count on different surfaces was calculated using ImageJ software (version 1.46r).

#### 5.3.4.3 Immunofluorescence staining of macrophages

Cells were treated and incubated as described above. After 24 h incubation, attached cells were fixed with 4% paraformaldehyde solution (Roti<sup>®</sup> Histofix, Roth) for 15 min. Then the cells were permeabilized with 0.1% (v/v) Triton X-100 for 10 min and rinsed with PBS twice. Non-specific binding sites were blocked by incubation with 1% (w/v) bovine serum albumin (BSA, Merck) in PBS for 1 h, while all antibodies were diluted in the very solution. At first, the cells were incubated with a mouse monoclonal antibody raised against vinculin (1:100, Sigma) for 30 min. After washing with PBS twice, a secondary goat anti-mouse antibody conjugated with CY2 (1:100, Dianova, Germany) was applied for another 30 min. Actin fibers and cell nuclei were stained by BODIPY<sup>®</sup>-Phalloidin (1:50, Invitrogen, Germany) and TO-PRO3 (1:500, Invitrogen), respectively, by additional 30 min each. All fixation, washing, and staining steps were performed at RT. Finally, all samples were washed with PBS, dipped into ultrapure water, and mounted with Mowiol (Calbiochem, Germany) to object holders. All surfaces were examined by confocal laser scanning microscopy (CLSM, Carl Zeiss Microimaging, Jena, Germany) using a 63-fold oil immersion objective and images were processed with the ZEN2011 software (Carl Zeiss, Germany).

#### 5.3.4.4 Foreign body giant cell (FBGC) characterization

The FBGC formation on different surfaces was evaluated after 10 days incubation in serum-containing RPMI-1640 medium. The surfaces were gently washed with PBS once and the attached cells were fixed with cold methanol and stained with 10% (v/v) Giemsa (Merck) in ultrapure water. Cells were photographed using a transmitted light microscope equipped with a CCD camera and the area percentage of FBGC on different surfaces was calculated by ImageJ software.

#### 5.3.4.5 $\beta$ 1 integrin expression

The cells were treated as described above in FBGC characterization. The  $\beta$ 1 integrin expression on different surfaces was then evaluated by immunofluorescence staining (20). Cells were fixed with 4% paraformaldehyde solution (Roth), permeabilized with 0.1% (v/v) Triton X-100 (Sigma) for 10 min at RT and rinsed with PBS twice. Again, non-specific binding sites were blocked with 1% (w/v) BSA in PBS for 1 h. Thereafter, cells were incubated with a mouse monoclonal antibody raised against  $\beta$ 1 integrin (1:50, Santa Cruz Biotechnology, Germany) for 30 min. After washing with PBS twice, a secondary goat anti-mouse antibody conjugated with CY2 (1:100, Dianova) was applied for another 30 min. The nuclei were stained with TO-PRO3 (1:500, Invitrogen) for 30 min. Finally, all samples were mounted with Mowiol (Calbiochem) and examined with a CLSM (Carl Zeiss) using a 40-fold oil immersion objective. Images were processed with the ZEN2011 software (Carl Zeiss).

#### 5.3.4.6 Pro-inflammatory cytokine production

Thp-1-derived macrophages were seeded on amino-terminated SAM and GAGs-modified surfaces at a cell density of  $5.0 \times 10^5$  cells mL<sup>-1</sup> and incubated for 24 h in presence or absence of 1  $\mu$ g mL<sup>-1</sup> lipopolysaccharide (LPS, Sigma) in serum-containing RPMI-1640 medium. After that, the medium supernatants of the untreated and LPS-challenged samples were collected and stored at -20°C until needed for investigation. The IL-1 $\beta$  production on different surfaces was detected using enzyme-linked immunosorbent assay (ELISA) according to the manufacturers' instructions (Thermo Scientific, Bonn, Germany).

### 5.3.5 Statistics

All data are represented as mean values  $\pm$  standard deviations (SD). Statistical examination was performed using one-way analysis of variance (ANOVA) followed by post-hoc Tukey testing. The significance level was set as  $p \leq 0.05$  and indicated by an asterisk. The number of samples has been indicated in the respective figures caption.

## 5.4 Results and Discussion

### 5.4.1 Characterization of GAGs-modified surfaces

The wettability of substrata after immobilization of different GAGs was evaluated by static water contact angle (WCA) measurements. Here, the covalent immobilization of different GAGs onto amino-terminated surfaces resulted in varying wettability as depicted by Figure 5.1. First, the amino-terminated SAM ( $\text{NH}_2$ ) resulted in moderately wettable surfaces with WCA  $\sim 53^\circ$ , which is in line with previous reports (21). Further, the WCA significantly decreased after the immobilization of GAGs onto  $\text{NH}_2$  surface. This is due to the presence of hydrophilic sulfate and carboxylic acid groups of immobilized GAGs (22). Among the GAGs, Hep-modified surface had the highest wettability indicated by the smallest WCA followed by CS and HA. The highest wettability of Hep is due to its high content of sulfate monoesters and sulfamido groups (23). By contrast, CS possesses less sulfate groups than Hep while HA possesses only carboxylic acid groups but not sulfate groups that resulted in lower wettability of both compared to Hep.

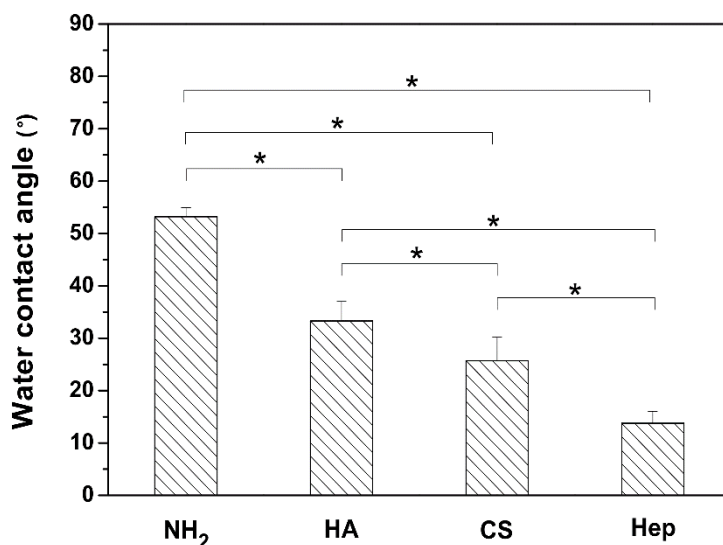


Figure 5.1. Static water contact angle (WCA) measurements for amino-terminated SAM ( $\text{NH}_2$ ) and surfaces after immobilization of hyaluronic acid (HA), chondroitin sulfate (CS) and heparin (Hep) onto  $\text{NH}_2$  SAM. Results are means  $\pm$  SD of two independent experiments and triplicate samples for each condition, \* $p \leq 0.05$ .

The immobilization of GAGs onto  $\text{NH}_2$  surface had also a strong effect on the surface charge, indicated by different zeta potentials as shown in Figure 5.2. It can be seen that  $\text{NH}_2$  surface resulted in a positive zeta potential below pH 4.7, which is due to protonation of amino groups in the low pH region (24). By contrast, significant decrease of zeta potentials was observed for all GAGs-modified surfaces. This is attributed to the deprotonation of sulfate and carboxylic groups, especially at basic pH region. Furthermore, clear differences were found in zeta potentials among the GAGs-modified surfaces. Hep had the lowest zeta potentials due to the highest content of sulfate groups, followed by CS and HA, which is consistent with the wettability shown by WCA measurements.

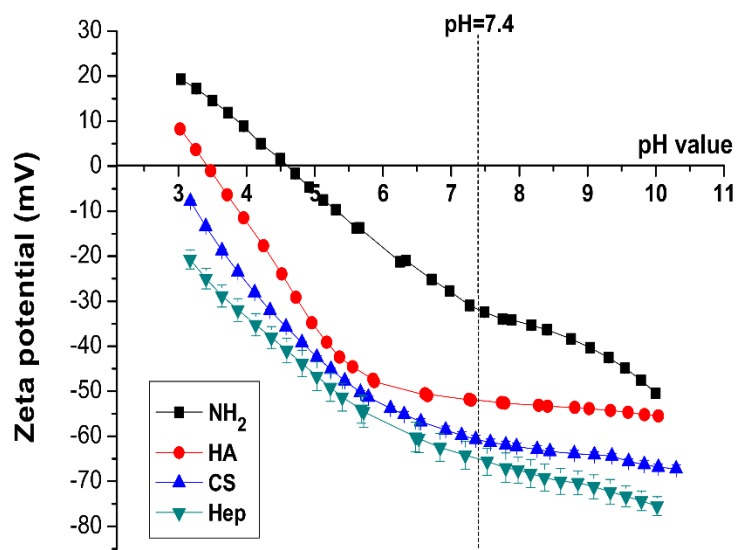


Figure 5.2. Zeta potential measurements of amino-terminated SAM ( $\text{NH}_2$ , ■) and surfaces after immobilization of hyaluronic acid (HA, ●), chondroitin sulfate (CS, ▲) and heparin (Hep, ▼) onto  $\text{NH}_2$  SAM.

#### 5.4.2 Adhesion and fusion of macrophages

THP-1 cells were used as a model monocyte system and differentiated into macrophages by PMA treatment. The adhesion and spreading of the THP-1-derived macrophages were investigated on different GAGs-modified surfaces in comparison to  $\text{NH}_2$  surface using histochemical (Figure 5.3) as well as immuno histochemical (Figure 5.4) techniques.

Figure 5.3 shows that macrophages adhered differently to the various surfaces. Here, the significantly highest cell count was found on  $\text{NH}_2$  surface (Figure 5.3b), which is due to the

high amount of amino groups with resulting moderate wettability and the least negative surface potential at pH 7.4 as observed with WCA and zeta potential measurements. The finding of high cell adhesion is also well in line with many previous studies (25). By contrast, the cell adhesion on all GAGs-modified surfaces was significantly reduced, which is obviously also related to the higher wettability and more negative potential of these surfaces. However, a first observation here was that despite certain differences in surface properties among the GAGs-immobilized surfaces, no significant difference in adhesion of macrophages was observed here.

Figure 5.4a shows the morphology of spreading macrophage on different surfaces by immunofluorescence staining of actin (red) and vinculin (green). It can be seen that macrophages on  $\text{NH}_2$  surface seemed to adhere stronger indicated by more spreading of cells with a larger cell area than on the GAGs-modified surfaces. Punctate actin structures were formed, especially at the periphery of macrophages. Further, larger focal adhesion plaques were lacking. Instead, rather clustered distribution of vinculin was found in the cells. This is also consistent with previous findings that podosome structures, but not focal contacts are the major adhesive structures present in macrophages adhering to surfaces (26). As expected, cell spreading on GAGs-modified surfaces was largely suppressed compared to  $\text{NH}_2$  surface, illustrated by the reduced actin and vinculin expression. Figure 5.4b shows the quantitative cell spreading area on various surfaces. The results revealed significantly lower spreading area of macrophages on all GAGs-modified surfaces in comparison to  $\text{NH}_2$  surface. Among the different GAGs, the highest extent in inhibiting cell spreading was found on HA-modified surfaces again. By contrast, adhesion (Figure 5.4a) and spreading (Figure 5.4b) were slightly increased on CS- and Hep-modified surfaces, but still significantly lower than on  $\text{NH}_2$  surface. The reason for the enhanced adhesion and spreading on CS- and Hep-modified surfaces might be due to the increased content of sulfate groups, which are reported to promote adhesion of several cell types (22, 27). Overall, immobilization of GAGs onto  $\text{NH}_2$  surface showed significant effects in reducing macrophage adhesion and spreading compared to the original  $\text{NH}_2$  SAM.

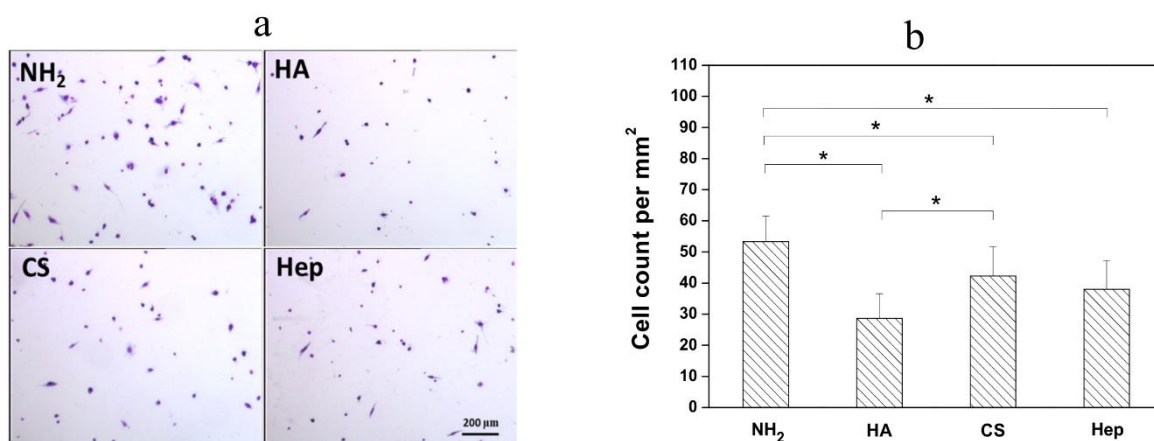


Figure 5.3. (a) Transmitted light microscopic images of adhering macrophages for 24 h incubation in serum-free RPMI medium and then stained with Giemsa on amino-terminated SAM (NH<sub>2</sub>) after immobilization of hyaluronic acid (HA), chondroitin sulfate (CS) and heparin (Hep) onto NH<sub>2</sub> surface. [Scale bar: 200 μm]. (b) Quantified macrophages per area adherent on NH<sub>2</sub>, HA, CS and Hep surfaces after 24 h incubation. Data represent mean ± SD, n = 4, \*p ≤ 0.05.



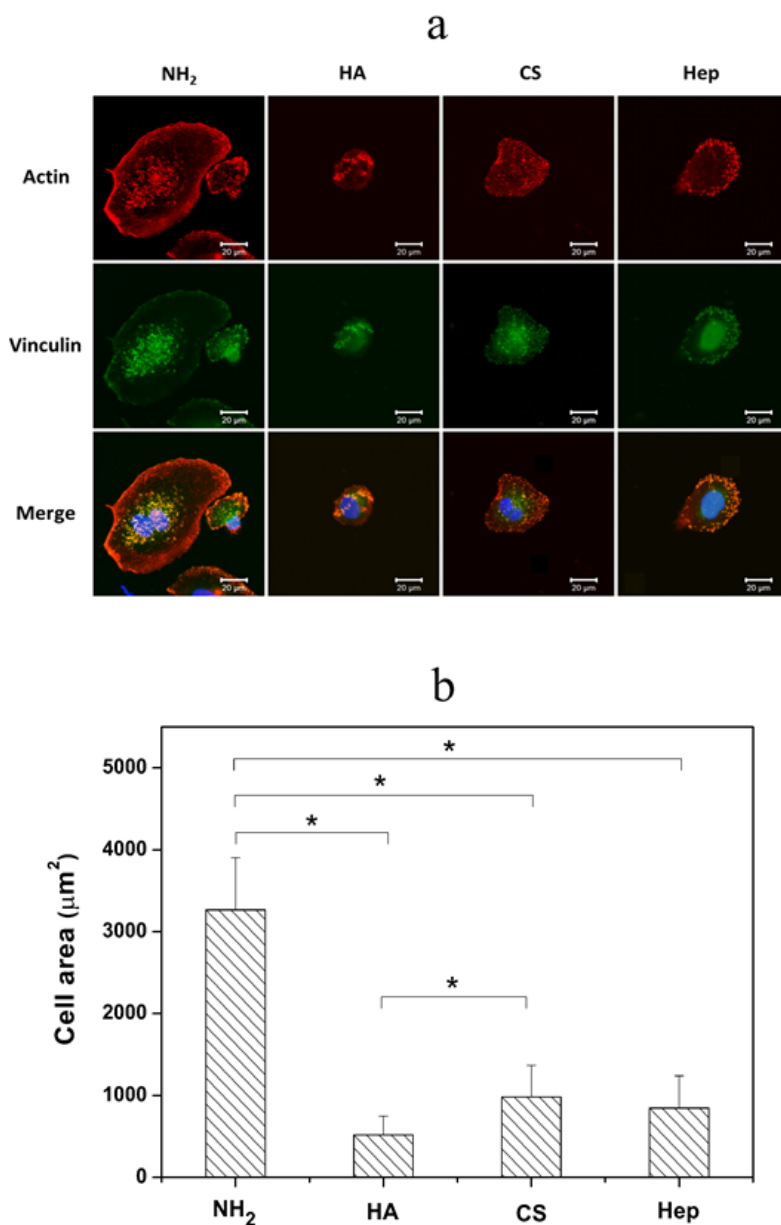


Figure 5.4. Representative confocal laser scanning microscopy (CLSM) images (a) and quantitative cell area (b) of macrophages after 24 h incubation in serum-free RPMI medium on amino-terminated SAM (NH<sub>2</sub>) and surfaces after immobilization of hyaluronic acid (HA), chondroitin sulfate (CS) and heparin (Hep) onto NH<sub>2</sub> SAM. The cells were stained for vinculin (green), actin (red), and nucleus (blue). [Scale bar: 20  $\mu\text{m}$ ].

Macrophages fusion into FBGCs is a hallmark of chronic inflammation (28). Moreover,  $\beta$ 1 integrin was reported to play a crucial role during macrophage fusion and FBGC formation (20). Furthermore, the extent of FBGC formation and  $\beta$ 1 integrin expression reflect the

proinflammatory potential of a biomaterial *in vitro* and *in vivo* (2, 29). Thereby, the macrophage fusion and  $\beta 1$  integrin expression in FBGCs were evaluated after 10 days incubation on GAGs-modified surfaces in comparison to  $\text{NH}_2$  surface (Figure 5.5 and Figure 5.6). Figure 5.5a shows that macrophage fusion was effectively inhibited on GAGs-modified surfaces in comparison to  $\text{NH}_2$  surface. Marked macrophage fusion was observed on  $\text{NH}_2$  surface in terms of more ( $n \geq 2$ ) nuclei accumulation within an extensively spread cell body. By contrast, less nuclei and reduced size of FBGCs were found on all GAGs-modified surfaces. Figure 5.5b depicts the area percentages of formed FBGCs on different surfaces, which confirms the findings in Figure 5.5a in a quantitative manner. Furthermore,  $\beta 1$  integrin expression on different surfaces (Figure 5.6) shows a similar trend with macrophage fusion data (Figure 5.5). Here, a significant reduction of  $\beta 1$  integrin expression (green staining) but also cell spreading was observed on GAGs-modified surfaces in comparison to  $\text{NH}_2$  surface. Also in these studies it was obvious that  $\text{NH}_2$  SAM promoted FBGC formation as cells there had more nuclei per cell body than on GAGs-modified surfaces. The highest extent of macrophage fusion on  $\text{NH}_2$  surface might be related to the highest macrophage number on this surface. This seems to increase probability of macrophage fusion, since the macrophage-macrophage fusion needs a certain cell adhesion density and spreading of the cells (30). Thereupon, a higher macrophage fusion extent is accompanied with a higher  $\beta 1$  integrin expression. In other words, the surfaces that did not support the initial macrophage adhesion and morphology development (cytoplasmic expansion) could not promote the ensuing macrophage fusion and  $\beta 1$  integrin expression (30). Consequently, the more hydrophilic and negatively charged GAGs-modified surfaces which reduced initial macrophage adhesion and spreading, limited macrophage fusion and  $\beta 1$  integrin expression significantly in comparison to  $\text{NH}_2$  SAM. However, besides cell number also release of cytokines has been identified as inducer of macrophage fusion, particularly IL-4 and IL-13 (31).

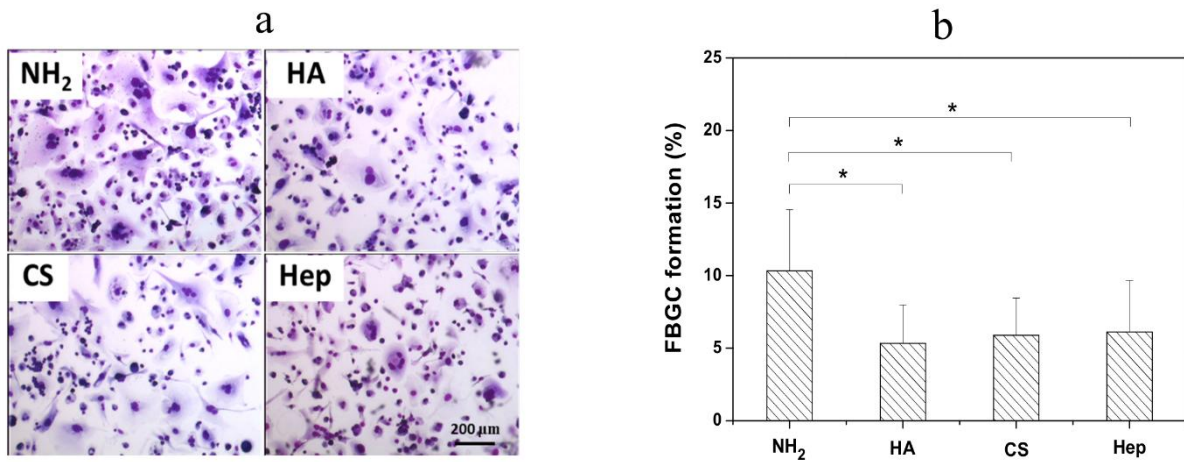


Figure 5.5. (a) Transmitted light microscopic images of Giemsa-stained foreign body giant cells (FBGCs) after 10 days incubation on amino-terminated SAM (NH<sub>2</sub>) and surfaces after immobilization of hyaluronic acid (HA), chondroitin sulfate (CS) and heparin (Hep) on NH<sub>2</sub> SAM [Scale bar: 200 μm]. (b) Quantified area percentage of FBGCs formed on NH<sub>2</sub>, HA, CS and Hep surfaces after 10 days incubation by quantitative evaluation of micrographs. Data represent mean ± SD, n = 10, \*p ≤ 0.05.

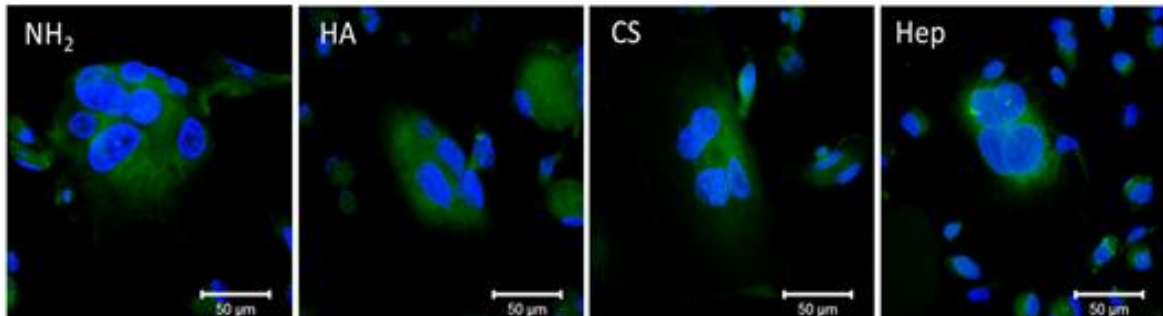


Figure 5.6. Expression of β1 integrin was determined on fusing macrophages/FBGCs after 10 days incubation on amino-terminated SAM (NH<sub>2</sub>) and surfaces after immobilization of hyaluronic acid (HA), chondroitin sulfate (CS) and heparin (Hep) on NH<sub>2</sub> SAM. Cells were fixed with 4% paraformaldehyde and stained for β1 integrin (green) and nuclei (blue) [Scale bar: 50 μm].

### 5.4.3 IL-1β cytokine production

During implant-associated inflammation, macrophages are activated and play important roles in modulating the inflammatory responses by secreting a variety of soluble signals such

as pro- or anti-inflammatory cytokines and chemokines (5). Besides, the production of proinflammatory cytokines, such as IL-1 $\beta$ , IL-6 and TNF- $\alpha$  in the cell cultures may reflect the potential of the biomaterial to induce inflammatory reactions (3, 29). Moreover, LPS is known as a strong stimulant for macrophage activation and can up-regulate the proinflammatory cytokine release (32). Since biomaterial implantation can be also accompanied sometimes by infection with gram negative bacteria, presence of endotoxin i.e. LPS is a possible complication. Therefore, the production of the proinflammatory cytokine IL-1 $\beta$  was studied here both presence and absence of LPS treatment to investigate the inflammatory potential of all surfaces.

Figure 5.7 shows the IL-1 $\beta$  production on different surfaces after 24 h incubation with (black bars) or without (white bars) LPS stimulation. It was found that the NH<sub>2</sub> surface (11 $\pm$ 3 pg/mL) causing strong spreading and fusion of macrophages produced here higher amounts of IL-1 $\beta$  than HA (7 $\pm$ 1 pg/mL) and CS (5 $\pm$ 0 pg/mL) modified surfaces in the absence of LPS stimulation. Likewise, the IL-1 $\beta$  production on HA (54 $\pm$ 6 pg/mL), CS (50 $\pm$ 5 pg/mL) and Hep (55 $\pm$ 5 pg/mL) modified surfaces were significantly reduced in comparison to the NH<sub>2</sub> surface (68 $\pm$ 10 pg/mL) in the presence of LPS stimulation. The data show also that IL-1 $\beta$  production by THP-1 derived macrophages was up-regulated on all surfaces after LPS treatment, which is well in line with previous findings demonstrating also the functionality of the cells (17, 33). The reduction of the proinflammatory cytokine IL-1 $\beta$  release by GAGs-modified surfaces is a further evidence for their potential to inhibit the inflammatory potential of biomaterials.

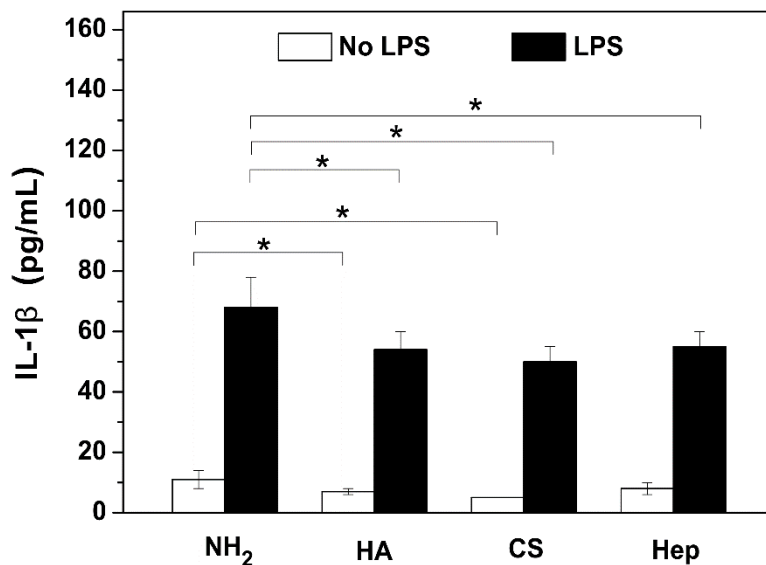


Figure 5.7. IL-1 $\beta$  production of macrophages after 24 h incubation in absence (white bars) and presence (black bars) of lipopolysaccharide (LPS) on amino-terminated SAM (NH<sub>2</sub>) and surfaces after immobilization of hyaluronic acid (HA), chondroitin sulfate (CS) and heparin (Hep) on NH<sub>2</sub> SAM. Data represent mean  $\pm$  SD, n = 6, \*p  $\leq$  0.05.

The anti-inflammatory effects observed here might be attributed partly to the physiochemical properties of the GAGs-modified surfaces. The immobilization of GAGs onto the NH<sub>2</sub> surface resulted in significant increase of wettability and negative charges, which are believed to reduce protein adsorption and cell adhesion (18, 22, 25) and further impair macrophage fusion and the ensuing inflammatory responses (17). It can be also assumed that both the physiochemical properties of the GAGs-modified surfaces as well as the physiologic roles of GAGs in regulation of inflammatory responses resulted in the remarkable anti-inflammatory effect compared to NH<sub>2</sub> surface (34, 35). Together, the present study and our previous work (17) demonstrate the remarkable inflammatory-inhibiting effects of GAGs. Here, we provided another way of immobilization of GAGs onto the surfaces, namely by covalent immobilization on biomaterial surfaces. An obvious advantage of the covalent immobilization is a more stable chemical bonding vs. adsorptive binding in the previous work (17) to be more suitable for long-term *in vivo* applications to reduce biomaterial-induced inflammatory responses.

## 5.5 Conclusions

In this study, different types of GAGs were covalently immobilized onto amino-terminated surfaces to evaluate their anti-inflammatory effects using a simple *in vitro* model. Static WCA and zeta potential measurements confirmed the successful immobilization of the GAGs resulting in more hydrophilic and negatively charged surfaces compared to the original substrate. The studies with THP-1 derived macrophages demonstrated that the GAGs-modified surfaces significantly reduced macrophage adhesion, spreading, FBGC formation,  $\beta 1$  integrin expression as well as pro-inflammatory cytokine IL-1 $\beta$  production compared to the amino-terminated surface. Among the GAGs, the HA-modified surface expressed a slightly higher reduction of initial macrophage adhesion and spreading compared to CS- and Hep-modified surfaces, possibly due to specific HA-CD44 interactions or steric effects of the larger HA molecules. Nevertheless, no significant differences were found regarding the other cellular responses among the different types of GAGs. Overall, the results suggest the great potential in reducing the inflammatory responses by covalent immobilization of GAGs onto NH<sub>2</sub>-terminated glass used as model surface. More importantly however is the wide applicability of this method to real biomaterial surfaces to improve the biocompatibility of implantable artificial organs, glucose-detecting biosensors, catheters, and tissue engineering scaffolds.

## 5.6 Acknowledgements

The assistance of Mrs. M. Porobin in zeta potential measurement is gratefully acknowledged.

## 5.7 Disclosures

Financial support: G. Zhou thanks the China Scholarship Council for offering the scholarship to work in Germany.

## 5.8 References

- [1] Martínez-Miguel P, de Sequera P, Albalade M, et al. Evaluation of a polynephron dialysis membrane considering new aspects of biocompatibility. *Int J Artif Organs*. 2015;38:45-53.
- [2] Anderson JM. Biological responses to materials. *Ann Rev Mater Res*. 2001;31:81-110.
- [3] Sun KN, Li YP, Lu ZD, Zhang L, Gao ZH, Jin QH. Suppression of titanium particle-induced TNF-alpha expression and apoptosis in human U937 macrophages by sirna silencing. *Int J Artif Organs*. 2013;36:522-7.
- [4] Wynn TA, Barron L. Macrophages: Master regulators of inflammation and fibrosis. *Seminars in Liver Disease*. 2010;30:245-57.
- [5] Anderson JM, Rodriguez A, Chang DT. Foreign body reaction to biomaterials. *Semin Immunol*. 2008;20:86-100.
- [6] Brodbeck WG, Nakayama Y, Matsuda T, Colton E, Ziats NP, Anderson JM. Biomaterial surface chemistry dictates adherent monocyte/macrophage cytokine expression in vitro. *Cytokine*. 2002;18:311-9.
- [7] Barron L, Wynn TA. Fibrosis is regulated by TH2 and TH17 responses and by dynamic interactions between fibroblasts and macrophages. *American Journal of Physiology-Gastrointestinal and Liver Physiology*. 2011;300:G723-G8.
- [8] Lourenco BN, Marchioli G, Song W, et al. Wettability influences cell behavior on superhydrophobic surfaces with different topographies. *Biointerphases*. 2012;7:46.
- [9] Llopis-Hernández V, Rico P, Ballester-Beltrán J, Moratal D, Salmerón-Sánchez M. Role of surface chemistry in protein remodeling at the cell-material interface. *Plos One*. 2011;6:e19610-e.
- [10] Franz S, Rammelt S, Scharnweber D, Simon JC. Immune responses to implants - a review of the implications for the design of immunomodulatory biomaterials. *Biomaterials*. 2011;32:6692-709.
- [11] Boontheekul T, Mooney DJ. Protein-based signaling systems in tissue engineering. *Current Opinion in Biotechnology*. 2003;14:559-65.
- [12] Severin IC, Soares A, Hantson J, et al. Glycosaminoglycan analogs as a novel anti-inflammatory strategy. *Frontiers in immunology*. 2012;3:293.

[13] Gandhi NS, Mancera RL. The structure of glycosaminoglycans and their interactions with proteins. *Chemical Biology & Drug Design*. 2008;72:455-82.

[14] Young E. The anti-inflammatory effects of heparin and related compounds. *Thrombosis Research*. 2008;122:743-52.

[15] Lovu M, Dumais G, du Souich P. Anti-inflammatory activity of chondroitin sulfate. *Osteoarthritis Cartilage*. 2008;16:S14-S8.

[16] Ruppert SM, Hawn TR, Arrigoni A, Wight TN, Bollyky PL. Tissue integrity signals communicated by high-molecular weight hyaluronan and the resolution of inflammation. *Immunologic Research*. 2014;58:186-92.

[17] Zhou GY, Niepel MS, Saretia S, Groth T. Reducing the inflammatory responses of biomaterials by surface modification with glycosaminoglycan multilayers. *J Biomed Mater Res Part A*. 2015; in press.

[18] Köewitsch A, Yang Y, Ma N, Kuntsche J, Maeder K, Groth T. Bioactivity of immobilized hyaluronic acid derivatives regarding protein adsorption and cell adhesion. *Biotechnology and Applied Biochemistry*. 2011;58:376-89.

[19] Park EK, Jung HS, Yang HI, Yoo MC, Kim C, Kim KS. Optimized THP-1 differentiation is required for the detection of responses to weak stimuli. *Inflammation Research*. 2007;56:45-50.

[20] McNally AK, Anderson JM. Beta 1 and beta 2 integrins mediate adhesion during macrophage fusion and multinucleated foreign body giant cell formation. *Am J Pathol*. 2002;160:621-30.

[21] Katzur V, Eichler M, Deigle E, et al. Surface-immobilized pamam-dendrimers modified with cationic or anionic terminal functions: Physicochemical surface properties and conformational changes after application of liquid interface stress. *J Colloid Interface Sci*. 2012;366:179-90.

[22] Yang Y, Köwitsch A, Ma N, et al. Functionality of surface-coupled oxidised glycosaminoglycans towards fibroblast adhesion. *Journal of Bioactive and Compatible Polymers: Biomedical Applications*. 2015:0883911515599999.

[23] Wang HM, Loganathan D, Linhardt RJ. Determination of the pKa of glucuronic acid and the carboxy groups of heparin by <sup>13</sup>C-nuclear-magnetic-resonance spectroscopy. *Biochemical Journal*. 1991;278:689-95.



[24] Shyue JJ, De Guire MR. Acid-base properties and zeta potentials of self-assembled monolayers obtained via in situ transformations. *Langmuir*. 2004;20:8693-8.

[25] Bacakova L, Filova E, Parizek M, Ruml T, Svorcik V. Modulation of cell adhesion, proliferation and differentiation on materials designed for body implants. *Biotechnology Advances*. 2011;29:739-67.

[26] DeFife KM, Jenney CR, Colton E, Anderson JM. Cytoskeletal and adhesive structural polarizations accompany IL-13-induced human macrophage fusion. *Journal of Histochemistry & Cytochemistry*. 1999;47:65-74.

[27] Amorim S, Pires RA, da Costa DS, Reis RL, Pashkuleva I. Interactions between exogenous FGF-2 and sulfonic groups: In situ characterization and impact on the morphology of human adipose-derived stem cells. *Langmuir*. 2013;29:7983-92.

[28] Kou PM, Babensee JE. Macrophage and dendritic cell phenotypic diversity in the context of biomaterials. *J Biomed Mater Res A*. 2011;96A:239-60.

[29] Anderson JM, Miller KM. Biomaterial biocompatibility and the macrophage. *Biomaterials*. 1984;5:5-10.

[30] McNally AK, Jones JA, MacEwan SR, Colton E, Anderson JM. Vitronectin is a critical protein adhesion substrate for IL-4-induced foreign body giant cell formation. *J Biomed Mater Res Part A*. 2008;86A:535-43.

[31] DeFife KM, Jenney CR, McNally AK, Colton E, Anderson JM. Interleukin-13 induces human monocyte/macrophage fusion and macrophage mannose receptor expression. *J Immunol*. 1997;158:3385-90.

[32] Loppnow H, Brade H, Durrbaum I, et al. IL-1 induction-capacity of defined lipopolysaccharide partial structures. *J Immunol*. 1989;142:3229-38.

[33] Zhou GY, Loppnow H, Groth T. A macrophage/fibroblast co-culture system using a cell migration chamber to study inflammatory effects of biomaterials. *Acta Biomaterialia*. 2015;26:54-63.

[34] Ruppert S, Hawn T, Arrigoni A, Wight T, Bollyky P. Tissue integrity signals communicated by high-molecular weight hyaluronan and the resolution of inflammation. *Immunologic Research*. 2014;58:186-92.

[35] Iovu M, Dumais G, Du Souich P. Anti-inflammatory activity of chondroitin sulfate. *Osteoarthritis Cartilage*. 2008;16:S14-S8.

## 6 Summary and outlook

This PhD thesis was aimed to advance the understanding of inflammatory and fibrotic responses on model biomaterials, as well as to develop anti-inflammatory strategies to avoid or minimize adverse biomaterial-induced inflammatory responses. Hence, first studies focused on development of a novel *in vitro* macrophage/fibroblast co-culture model based on a cell migration chamber that allowed a timely and locally controlled interaction of both cell types, to study the pro-inflammatory and pro-fibrotic potentials of model biomaterials. Using self-assembling monolayers (SAMs) with terminal methyl (CH<sub>3</sub>), amine (NH<sub>2</sub>), hydroxyl (OH) and carboxyl (COOH) groups as model surfaces, the results regarding both macrophage and fibroblast activities showed that the hydrophilic/anionic COOH SAMs possess the lowest potential of inducing both inflammatory and fibrotic responses. On the basis of these findings, the second part of the thesis aimed to develop anti-inflammatory strategies using glycosaminoclycans (GAGs), which are also hydrophilic and anionic macromolecules. Thereby, three kinds of GAGs - hyaluronic acid (HA), chondroitin sulfate (CS), and heparin (Hep) were immobilized on model substrata by two different immobilization approaches to reduce the inflammatory responses. In the first approach, GAGs were deposited alternatively together with chitosan (Chi) on glass substrata as multilayers through layer-by-layer (LBL) technique. In the other approach, GAGs were covalently immobilized onto amino-functionalized substrata by 1-ethyl-3-(3-dimethylaminopropyl) carbodiimide (EDC)/N-hydroxysuccinimide (NHS) crosslinking chemistry. It was shown that all the inflammatory responses in terms of macrophage activities were significantly reduced on each GAG-modified surface at both immobilization techniques. Moreover, it was found a pivotal role of the type of GAGs in modulating inflammatory responses in multilayers, with Hep-Chi system showing the highest anti-inflammatory potential. The physical adsorption of GAGs during LBL technique might allow the uptake of Hep molecules by macrophages, which could lead to a reduction of NF- $\kappa$ B nuclear translocation, and thus further lowered inflammatory responses.

A specific novelty of the study was the establishment of the macrophage/fibroblast co-culture model using the cell migration chamber, which can achieve mono-culture, separated and mixed co-cultures before and after removal of the fence chamber, to mimic autocrine, paracrine and juxtacrine signal exchange in one and the same system. In addition, it allowed the study of macrophage migration and fibroblast outgrowth in the presence of the

other cell type in a timely and locally controlled manner. Furthermore, the co-culture system possesses potent values to study the *in vitro* effects of additional factors like cytokines and other bioactive molecules on the interplay between the two cell types. In the second part of the thesis, we provided two different techniques for immobilization of GAGs on biomaterial surfaces to reduce the pro-inflammatory potential, which paved the way for the future design of anti-inflammatory coatings with improved biocompatibility used for various biomedical and tissue engineering applications. Since macrophages are the dominant cells in inflammatory reactions, the current studies focused only on the macrophage behavior in a mono-culture system, to learn about the initial anti-inflammatory effects of GAGs. Future studies will be performed with the fence chamber-generated macrophage/fibroblast co-culture system, together with the GAGs-modified surfaces, to gain more in depth information about the effect of GAGs on modulating inflammatory and fibrotic reactions, as well as the mechanism of action behind these effects. Furthermore, the incorporation of other anti-inflammatory reagents in addition to GAGs, or the combination with other inflammatory mediated factors such as topographical surface modification to integrate multiple anti-inflammatory strategies, might find synergies of the anti-inflammatory effects, and thus have more promising applications in clinical trials to treat various inflammatory related diseases.

## List of tables and figures

### Tables

Table 3.1. Surface chemistry differentially affects parameters of the inflammatory (dark grey color) and fibrotic responses (light grey color) on CH<sub>3</sub>, NH<sub>2</sub>, OH and COOH SAMs (+ weak, ++ strong, +++ very strong)..... 错误!未定义书签。

### Figures

Figure 1.1. Host responses to implanted biomaterials. Serum proteins adsorb onto the biomaterial surface immediately upon implantation. Leukocytes including neutrophils and monocytes are firstly recruited to the implant site, where monocytes differentiate into a “M1” phenotypic macrophages during acute inflammation. During the later chronic inflammatory stage, macrophages polarize towards the “M2” phenotype with pro-healing capacities, but also can fuse to form foreign body giant cells (FBGCs) in order to increase the phagocytic ability. Acting on the pro-fibrotic factors released from the “M2” macrophages and FBGCs, fibroblasts are activated to proliferate, as well as differentiated into myofibroblasts resulting in collagen deposition. Finally, a thick fibrotic capsule is formed around the biomaterial, leading to failure of implantation..... 15

Figure 1.2. Schematic representations of the four types of macrophage/fibroblast co-culture systems. (A) Mixed co-cultures with immediate cell-cell contact. (B) Conditioned medium from fibroblast culture was used to challenge macrophages, but signaling feedback between the two cell types was missed. (C) Membrane separated co-culture with signaling feedback but without cell-cell contact even at later stages. (D) Multifunctional co-culture system using cell migration fence chambers to mimic separated, paracrine and juxtacrine co-cultures in sequence within one and the same system [80]. ..... 20

Figure 1.3. Schematic representation of different anti-inflammatory strategies. (A) Physical and chemical modification of the biomaterials by alteration of surface topography, surface chemistry as well as anti-fouling coatings; (B) Incorporation of anti-inflammatory agents to biomaterials; (C) Immunomodulation approaches using bioactive molecules that can directly or indirectly modulate the host immune system. PEG - polyethylene glycol; DEX - dexamethasone; α-MSH - alpha

	melanocyte-stimulating hormone; IL-1Ra - interleukin-1 receptor antagonists; GAGs - glycosaminoglycans. ....	21
Figure 1.4.	Schematic diagrams of anti-inflammatory mechanisms of (A) Heparin (HEP), (B) Chondroitin sulfate (CS) and (C) Hyaluronic acid (HA). HSPG - heparan sulfate proteoglycan; NF- $\kappa$ B - nuclear factor- $\kappa$ B; HMW-HA - high molecular weight HA; LMW-HA - low molecular weight HA; Hyals – hyaluronidases; ROS - reactive oxygen species; TLRs - toll-like receptors (Adapted from [130, 131] )......	25
Figure 2.1.	Schematic overview of the used SAM surfaces. Four different surfaces (A – D) were prepared. A) ODS, chlorodimethyloctadecylsilane, determined CH <sub>3</sub> in the paper. B) APTES, 3-aminopropyltriethoxysilane, determined NH <sub>2</sub> in the paper. C) GPTMS, glycidoxypopyl trimethoxysilane, determined OH in the paper. D) TESPSA, triethoxysilylpropyl succinic anhydride, determined COOH in the paper. RT, room temperature. ....	48
Figure 2.2.	Schematic description of the establishment of the macrophage/fibroblast co-culture model using the cell migration fence chamber. ....	50
Figure 2.3.	Results of dynamic water contact angle measurements of self-assembled monolayers with different terminal groups. The wetting properties were characterised by measuring advancing (white bars) and receding (black bars) water contact angles using the sessile drop method. Data represent mean $\pm$ SD, n = 6.....	54
Figure 2.4.	The zeta potentials of the SAMs with different terminating groups and glass. Zeta potentials were measured in the pH range 3–10. ....	55
Figure 2.5.	(A) Transmitted light microscopic images of macrophage adhesion on different surfaces. THP-1 cells were differentiated into macrophage cells by incubation with 200 nM PMA for 48 h. The THP-1-derived macrophage cells were then detached and seeded on SAMs for 24 h in serum-containing RPMI medium. The attached macrophages on different surfaces were stained by 10% (v/v) Giemsa solution [scale bar: 100 $\mu$ m]. The red arrows show the initial fusion of macrophages and the yellow arrows show the spreading cells. (B) Cell numbers of adhering macrophages per area on different SAM surfaces were determined after 24 h incubation in serum-containing medium. Data represent mean $\pm$ SD, n = 4, *p < 0.05.....	56
Figure 2.6.	Transmitted light microscopic images of Giemsa staining of FBGC in macrophage mono-culture (upper row) and macrophage/fibroblast co-cultures (lower row) on	

CH <sub>3</sub> , NH <sub>2</sub> , OH and COOH surfaces for 10 days after removal of fence chambers. The red arrow shows the FBGCs. Bar = 200 μm. ....	57
Figure 2.7. The area percentage of FBGCs on SAM surfaces was determined 10 days after removal of fence chambers in macrophage mono-cultures (white bars) and macrophage/fibroblast co-cultures (black bars) by quantitative evaluation of micrographs. Data represent mean ± SD, n ≥ 10, *p < 0.05. ....	58
Figure 2.8. Expression of β1 integrin was determined on fusing macrophages/FBGCs in macrophage mono-cultures (upper row) and macrophage/fibroblast co-cultures (lower row) on CH <sub>3</sub> , NH <sub>2</sub> , OH and COOH surfaces 10 days after removal of the fence chambers. Cells were fixed with 4% paraformaldehyde and stained for β1 integrin (green) and nuclei (To-pro-3, blue). Bar in all figures = 50 μm. ....	59
Figure 2.9. IL-6 (A) and TNF-α (B) production of macrophage mono-cultures (Mac mono), fibroblast mono-cultures (HF mono) and macrophage/ fibroblast co-cultures (Co-culture) was measured after additional 24 h of incubation with (+ LPS) or without 1 μg/mL LPS (-LPS) after removal of the fence chamber. Data represent mean ± SD, n = 6, *p < 0.05. ....	60
Figure 2.10. The IL-6 (A) and TNF-α (B) production on SAM surfaces in macrophage/ fibroblast co-cultures at day 0, 1 and 10 days after removal of the fence chamber was determined. Data represent mean ± SD, n = 6, *p < 0.05. ....	62
Figure 2.11. (A) The accumulated distance of macrophage migration on different SAM surfaces within a 24 h migration period in macrophage mono-cultures (grey bars) and macrophage/fibroblast co-cultures (white bars). Box-whisker diagrams indicate the 25th and 75th percentile, the median (dash) and mean (black square) values, respectively, n ≥ 30, *p < 0.05. (B) The percentage of macrophages that migrate to the direction of the gap generated by the removal of the fence chambers within a 24 h migration period in macrophage mono-cultures (grey bars) and macrophage/fibroblast co-cultures (white bars). Data represent mean ± SD, n ≥ 3, *p < 0.05. ....	64
Figure 3.1. Schematic description for establishment of the fibroblast/macrophage co-culture model using the cell migration fence chamber. ....	78
Figure 3.2. Physical characterization of the SAM surfaces. (A) Static water contact angle (WCA) measurement of CH <sub>3</sub> , NH <sub>2</sub> , epoxy, OH and COOH SAMs. Results are the means ± SD of two independent experiments, each performed in triplicate. (B) Zeta potential measurements of the SAMs with different terminating groups	

- compared with bare glass. Zeta potentials were measured in the pH range 3–10.  
 .....82
- Figure 3.3. Adhesion, spreading and proliferation of human fibroblasts (HFs) on CH<sub>3</sub>, NH<sub>2</sub>, OH and COOH SAMs. Representative CLSM images (A) of HFs after 4 h incubation with immune fluorescence staining of vinculin (green), actin (red) and nuclei (blue). Bar = 20 μm. Quantitative cell adhesion number (B) and spreading area (C) of HFs adhesion on different SAMs after 4 h incubation in serum-containing medium. Data represent mean ± SD, n = 4, \*p < 0.05. (D) HFs proliferation after 24 h and 72 h culture on CH<sub>3</sub>, NH<sub>2</sub>, OH and COOH SAMs in serum-containing medium. Data represent mean ± SD, n = 4, \*p < 0.05.....85
- Figure 3.4. Representative crystal violet staining images (A) and quantitative outgrowth distances (B) of HF outgrowth in HF monocultures (HF mono, white bars) and fibroblast/macrophage co-cultures (Co-culture, black bars) on CH<sub>3</sub>, NH<sub>2</sub>, OH and COOH SAMs. The cells were seeded and cultured for 24 h before removal of the fence chambers. The fibroblasts were then left to grow for 3 days in both mono- and co-cultures. Afterwards, the cells were fixed and stained by 0.5% (w/v) crystal violet in methanol. Bar = 2000 μm. Data represent mean ± SD, n = 6, \*p < 0.05. ..  
 .....87
- Figure 3.5. Foreign body giant cells (FBGCs) formation on CH<sub>3</sub>, NH<sub>2</sub>, OH and COOH SAMs in the macrophage region of co-cultures after 3 days of HF outgrowth. Afterwards, the cells were fixed and stained by 0.5% (w/v) crystal violet in methanol. The red arrows show the FBGCs. Bar = 200 μm. ....88
- Figure 3.6. IL-6 (A) and IL-10 (B) release in human fibroblast monocultures (HF mono, white bars) and fibroblast/macrophage co-cultures (Co-culture, black bars) on CH<sub>3</sub>, NH<sub>2</sub>, OH and COOH SAMs after 3 days of incubation with 10 ng mL<sup>-1</sup> TGF-β1. Data represent mean ± SD, n = 6, \*p < 0.05. ....89
- Figure 3.7. Immunofluorescence staining of (A) ED-A FN (green), (B) α-SMA (red) and nuclei (blue) after 3 day incubation with 10ng mL<sup>-1</sup> TGF-β in HF mono-cultures (HF mono) and fibroblast/macrophage co-cultures (Co-culture) on CH<sub>3</sub>, NH<sub>2</sub>, OH and COOH SAMs. Bar = 100 μm.....91
- Figure 3.8. Surface chemistry-dependent differences in α-SMA expression after 3 day incubation in the presence of 10 ng mL<sup>-1</sup> TGF-β. Aspect ratio (A) and percentage (B) of α-SMA positively stained cells on CH<sub>3</sub>, NH<sub>2</sub>, OH and COOH SAMs in both HF mono-cultures (HF mono) and fibroblast/macrophage co-cultures (Co-culture). Data represent mean ± SD, n ≥ 20, \*p < 0.05.....92

- Figure 4.1. Multilayer mass calculated from angle shifts obtained with surface plasmon resonance (SPR). Up to nine layers were adsorbed on the primary PEI layer and abbreviated as follows: (HA-Chi)HA (■), (CS-Chi)CS (●), and (Hep-Chi)Hep (▲). Odd layers: GAGs - hyaluronic acid (HA), chondroitin sulfate (CS), and heparin (Hep). Even layers: chitosan (Chi). Results are means  $\pm$  SD of two independent experiments. .... 109
- Figure 4.2. Static water contact angles (WCA) for up to nine layers on top of PEI abbreviated as (HA-Chi)HA (■), (CS-Chi)CS (●), and (Hep-Chi)Hep (▲). Odd layers: GAGs - hyaluronic acid (HA), chondroitin sulfate (CS), and heparin (Hep). Even layers: chitosan (Chi). Results are means  $\pm$  SD of two independent experiments and triplicate samples for each condition..... 110
- Figure 4.3. Zeta potential measurements of the initial PEI layer (○) and multilayers abbreviated as (HA-Chi)<sub>4</sub>HA (■), (CS-Chi)<sub>4</sub>CS (●), and (Hep-Chi)<sub>4</sub>Hep (▲)... 111
- Figure 4.4. (a) Transmitted light microscopic images of macrophage adhesion on the primary PEI layer and terminal layer of (HA-Chi)<sub>4</sub>HA, (CS-Chi)<sub>4</sub>CS, and (Hep-Chi)<sub>4</sub>Hep. THP-1 cells were differentiated by incubation with 200 nM PMA for 48 h. The resulting macrophage cells were collected and cultured for additional 24 h in serum-free RPMI medium as well as stained with 10% (v/v) Giemsa solution [Scale bar: 200  $\mu$ m]. (b) Quantified macrophages per area adherent on PEI and different terminal GAG layers after 24 h. Data represent mean  $\pm$  SD, n = 4, \*p  $\leq$  0.05..... 112
- Figure 4.5. Representative confocal laser scanning microscopy (CLSM) images of macrophages after 24 h incubation in serum-free RPMI medium on the initial PEI layer and terminal layers of (HA-Chi)<sub>4</sub>HA, (CS-Chi)<sub>4</sub>CS, and (Hep-Chi)<sub>4</sub>Hep. The cells were stained for vinculin (green), actin (red), and nucleus (blue). [63-fold oil immersion objective, scale: 20  $\mu$ m]. .... 113
- Figure 4.6. Transmitted light microscopic images of Giemsa-stained foreign body giant cells (FBGCs) after 10 days incubation in absence (upper row) and presence (lower row) of lipopolysaccharide (LPS) on the initial PEI layer and terminal layers of (HA-Chi)<sub>4</sub>HA, (CS-Chi)<sub>4</sub>CS, and (Hep-Chi)<sub>4</sub>Hep [Scale: 200  $\mu$ m]..... 114
- Figure 4.7. The area percentage of FBGCs adherent on the initial PEI layer as well as terminal GAG layers of (HA-Chi)<sub>4</sub>HA, (CS-Chi)<sub>4</sub>CS, and (Hep-Chi)<sub>4</sub>Hep was determined after 10 days incubation in absence (white bars) and presence (black



- bars) of lipopolysaccharide (LPS) by quantitative evaluation of micrographs. Data represent mean  $\pm$  SD, n = 10, \*p  $\leq$  0.05. ....115
- Figure 4.8. Expression of  $\beta$ 1 integrin was determined on fusing macrophages/FBGCs after 10 days incubation in absence (upper row) and presence (lower row) of lipopolysaccharide (LPS) on the initial PEI layer and the terminal GAG layer of (HA-Chi)<sub>4</sub>HA, (CS-Chi)<sub>4</sub>CS, and (Hep-Chi)<sub>4</sub>Hep. Cells were fixed with 4% paraformaldehyde and stained for  $\beta$ 1 integrin (green) and nuclei (blue) [Scale: 50  $\mu$ m]. ....116
- Figure 4.9. IL-1 $\beta$  production of macrophages after 24 h incubation in absence (white bars) and presence (black bars) of lipopolysaccharide (LPS) on the initial PEI layer and the terminal layer of (HA-Chi)<sub>4</sub>HA, (CS-Chi)<sub>4</sub>CS, and (Hep-Chi)<sub>4</sub>Hep. Data represent mean  $\pm$  SD, n = 6, \*p  $\leq$  0.05. ....117
- Figure 5.1. Static water contact angle (WCA) measurements for amino-terminated SAM (NH<sub>2</sub>) and surfaces after immobilization of hyaluronic acid (HA), chondroitin sulfate (CS) and heparin (Hep) onto NH<sub>2</sub> SAM. Results are means  $\pm$  SD of two independent experiments and triplicate samples for each condition, \*p  $\leq$  0.05. ....132
- Figure 5.2. Zeta potential measurements of amino-terminated SAM (NH<sub>2</sub>, ■) and surfaces after immobilization of hyaluronic acid (HA, ●), chondroitin sulfate (CS, ▲) and heparin (Hep, ▼) onto NH<sub>2</sub> SAM. ....133
- Figure 5.3. (a) Transmitted light microscopic images of adhering macrophages for 24 h incubation in serum-free RPMI medium and then stained with Giemsa on amino-terminated SAM (NH<sub>2</sub>) after immobilization of hyaluronic acid (HA), chondroitin sulfate (CS) and heparin (Hep) onto NH<sub>2</sub> surface. [Scale bar: 200  $\mu$ m]. (b) Quantified macrophages per area adherent on NH<sub>2</sub>, HA, CS and Hep surfaces after 24 h incubation. Data represent mean  $\pm$  SD, n = 4, \*p  $\leq$  0.05. ....135
- Figure 5.4. Representative confocal laser scanning microscopy (CLSM) images (a) and quantitative cell area (b) of macrophages after 24 h incubation in serum-free RPMI medium on amino-terminated SAM (NH<sub>2</sub>) and surfaces after immobilization of hyaluronic acid (HA), chondroitin sulfate (CS) and heparin (Hep) onto NH<sub>2</sub> SAM. The cells were stained for vinculin (green), actin (red), and nucleus (blue). [Scale bar: 20  $\mu$ m]. ....136
- Figure 5.5. (a) Transmitted light microscopic images of Giemsa-stained foreign body giant cells (FBGCs) after 10 days incubation on amino-terminated SAM (NH<sub>2</sub>) and surfaces after immobilization of hyaluronic acid (HA), chondroitin sulfate (CS) and

---

heparin (Hep) on NH<sub>2</sub> SAM [Scale bar: 200 μm]. (b) Quantified area percentage of FBGCs formed on NH<sub>2</sub>, HA, CS and Hep surfaces after 10 days incubation by quantitative evaluation of micrographs. Data represent mean ± SD, n = 10, \*p ≤ 0.05.....138

Figure 5.6. Expression of β1 integrin was determined on fusing macrophages/FBGCs after 10 days incubation on amino-terminated SAM (NH<sub>2</sub>) and surfaces after immobilization of hyaluronic acid (HA), chondroitin sulfate (CS) and heparin (Hep) on NH<sub>2</sub> SAM. Cells were fixed with 4% paraformaldehyde and stained for β1 integrin (green) and nuclei (blue) [Scale bar: 50 μm]. .....138

Figure 5.7. IL-1β production of macrophages after 24 h incubation in absence (white bars) and presence (black bars) of lipopolysaccharide (LPS) on amino-terminated SAM (NH<sub>2</sub>) and surfaces after immobilization of hyaluronic acid (HA), chondroitin sulfate (CS) and heparin (Hep) on NH<sub>2</sub> SAM. Data represent mean ± SD, n = 6, \*p ≤ 0.05.....140

## Acknowledgment

During the PhD studies, many people have supported and helped me, without whom the thesis would not have been completed successfully. I would like to convey my deepest gratitude to all of them as following.

Firstly, I would like to express my most sincere gratitude to my supervisor Prof. Dr. Thomas Groth for providing me with the opportunity to work on this interesting research topic, as well as the continuous help, advice, guidance and encouragement to complete my PhD thesis. I have gained a lot from his vast knowledge, as well as the competent advice and valuable comments. Furthermore, I am deeply grateful to him for not only in the scientific aspect, but also on a personal level throughout the period of my PhD.

I would also like to thank Prof. Dr. Harald Loppnow from the Department of Internal Medicine III of Martin Luther University Halle-Wittenberg for his support with Elisa measurements, as well as the fruitful discussions on data analysis and paper writing.

I want to thank Prof. Dr. Viktoria Weber from Danube University Krems and Prof. Dr. Lea Ann Dailey from Martin Luther University Halle-Wittenberg for taking the time to review and evaluate the thesis.

Sincere thanks go to all previous and current members of biomedical materials group for a warm, collaborative and supportive working atmosphere. Many thanks to Mrs. Marlis Porobin for the help with zeta potential measurements and official documents. Special thanks go to Dr. Ing. Marcus Niepel and Alex Köwitsch for numerous inspiring discussions concerning experimental issues and their kind help with “German related stuff”. I would also like to express my sincere gratitude to my former supervised diploma and master students Hala Al-khoury and Shivam Saretia for their good job in experimental work and the productive research outcome. In addition, I would like to render my deepest heartfelt thanks to Hala Al-khoury for all her kind care to me, like my younger sister, during my thesis writing and pregnancy. I enjoy the time and experiences together with her and I cherish very much the precious friendship with her.

I would also like to thank all my friends for their kind supports to make me a pleasant stay in Halle during the entire PhD studies.

Finally, I want to express my deepest gratitude to my parents and my husband for all their supports, encouragement, love and sacrifice, even though no words can describe all my

gratitude. Last but not least, I would like to dedicate the thesis to my coming baby Kexin, who gave me infinite energies and spirits to finish my PhD thesis. I am looking forward to a more beautiful future together with my lovely family.

## Publication list with declaration of self-contribution to research articles

1. **G. Zhou** and T. Groth

Host responses to implants and the design of anti-inflammatory biomaterials – a short review. To be submitted to Journal of bioactive and compatible polymers .

My contribution was about 90%. I wrote the whole review paper and Prof. Dr. T. Groth helped me planning and revising the manuscript.

2. **G. Zhou**, H. Loppnow and T. Groth

A macrophage/fibroblast co-culture system using a cell migration chamber to study inflammatory effects of biomaterials. *Acta Biomaterialia*. 2015;26:54-63.

My contribution was about 85%. I performed all the experiments, analysed all the experimental data and wrote the full paper. Prof. Dr. H. Loppnow supported me with the Elisa measurements and he was also involved in the manuscript revision. Prof. Dr. T. Groth helped me in planning the experiments and manuscript revision.

3. **G. Zhou** and T. Groth

In vitro study of the host responses to model biomaterials via a fibroblast/macrophage co-culture system. Submitted to *Biomaterials Science*, under revision.

My contribution was about 90%. I conducted all the experiments, analysed all the experimental data and wrote the full paper. Prof. Dr. T. Groth supported me with planning of experiments and contributed during the revision of the manuscript.

4. **G. Zhou**, M. S. Niepel, S. Saretia and T. Groth

Reducing the inflammatory responses of biomaterials by surface modification with glycosaminoglycan multilayers. *J Biomed Mater Res Part A*. 2016;104, 493-502.

My contribution was about 70%. I conducted most of the experiments except the multilayer formation, macrophage adhesion and fusion experiments which were done by S. Saretia under my supervision. I also wrote most parts of the manuscripts while M. S. Niepel contributed to the writing of surface characterisation and cell adhesion sections. Prof. Dr. T. Groth supported the planning of experiments and also contributed during the revision of the manuscript.

5. **G. Zhou**, H. Al-khoury and T. Groth

Covalent immobilization of glycosaminoglycans to reduce the inflammatory effects of biomaterials. *Int J Artif Organs*. 2016;39, 37-44.

My contribution was about 80%. I wrote the whole manuscript with the help of Prof. Dr. T. Groth who helped me planning the experiments and revising the manuscript. I performed most of the experiments except for the surface preparation, macrophage adhesion and fusion experiments which were done by H. Al-khoury under my supervision.

**Other publications that are not involved in this thesis**

1. Z. Li, A. Kowitsch, **G. Zhou**, T. Groth, B. Fuhrmann, M. Niepel, E. Amado and J. Kressler

Enantiopure chiral poly(glycerol methacrylate) self-assembled monolayers knock down protein adsorption and cell adhesion. *Adv Healthc Mater*. 2013;2, 1377-87.

2. A. Kowitsch, **G. Zhou** and T. Groth.

Medical Application of Glycosaminoglycans - A Review. *Journal of Tissue Engineering and Regenerative Medicine*, under revision.

### **Published Abstracts**

1. **G. Zhou**, H. Loppnow and T. Groth. Characterization of inflammatory potential of biomaterials by using a novel macrophage/fibroblast co-culture system. The International Journal of Artificial Organs, 37 (8), 2014, p. 616.
2. **G. Zhou**, M. Jurado, A. Köwitsch, S. Schlenker, B. Fuhrmann and T. Groth. Development of an in vitro inflammation model by patterned co-cultures of macrophages and human fibroblasts. BioNanomat, 13(1-4), 2012, p. 216.
3. Z. Li, A. Kowitsch, **G. Zhou**, T. Groth, B. Fuhrmann, M. Niepel, E. Amado and J. Kressler. Chirality of poly(glycerol methacrylate) brushes affects protein adsorption and cell adhesion. Abstr Pap Am Chem Soc. 2013, 245, 523.

### **Oral presentations**

1. **G. Zhou**, S. Saretia, H. Al-Khoury, T. Groth. Glycosaminoglycans as efficient tool to reduce inflammatory response to biomaterials for anti-inflammation targeting. 7th International Congress BioNanoMed 2016 – Nanotechnology enables Personalized Medicine, 6th – 8th April, 2016, Krems, Austria.
2. **G. Zhou**, H. Al-Khoury, S. Saretia, T. Groth. Immobilization strategies for glycosaminoglycans on biomaterials for anti-inflammatory purposes. XLIII Annual Congress of the European Society for Artificial Organs. 14th – 17th September, 2016, Warsaw, Poland.

### **Posters**

1. **G. Zhou**, H. Al-Khoury, S. Saretia, T. Groth. Reduced inflammatory response to biomaterials after glycosaminoglycan immobilization. Summer school on Biomaterials and Regenerative Medicine. 4th – 9th July, 2016, Riva del Garda, Trentino Region, Italy.
2. **G. Zhou**, H. Loppnow and T. Groth. Characterization of inflammatory potential of

biomaterials by using a novel macrophage / fibroblast co-culture system. 41st Congress of European Society for Artificial Organs, 17th - 20th September, 2014, Rome, Italy.

3. **G. Zhou**, S. Schlenker, B. Fuhrmann, H. Loppnow and T. Groth. Development of a Macrophage/Fibroblast Co-culture System for Characterization of Inflammatory Potential of Biomaterials. Advanced summer school: inflammation/repair interface, 25th – 28th June, 2013, Porto, Portugal.
4. **G. Zhou**, M. Jurado, A. Köwitsch, S. Schlenker, B. Fuhrmann and T. Groth. Development of an in vitro inflammation model by patterned co-cultures of macrophages and human fibroblasts. Annual Meeting of the German Society for Biomaterials, 1st – 3rd November, 2012, Hamburg, German.



## Curriculum vitae

### Personal data

---

Name: Guoying Zhou  
Address: Brandbergweg 35, 06120, Halle (Saale), Germany  
Date of birth: 19. January 1987 in Shandong, China  
Academic degree: Master of Science

### Education

---

2011.09-present Biomedical Materials in Institute of Pharmacy, Martin Luther University Halle-Wittenberg, Halle (Saale), Germany (**PhD Candidate**)  
PhD topic: In vitro studies on inflammatory potential of biomaterials with development of anti-inflammatory strategies

2008.09-2011.07 Polymer Chemistry and Physics, University of Science & Technology of China, Hefei, P. R. China (**Master of Science**)  
Master topic: Synthesis of poly(ethylene glycol) containing copolymers and study of their protein resistance properties  
Grade: First Class

2004.09-2008.07 Department of polymer material and engineering, University of Jinan, Jinan, P. R. China. (**Bachelor of Science**)  
Grade: First Class

### Awards / Grants

---

10/2016-03/2017 Doctoral award scholarship for young foreign scientists  
10/2015-11/2015 Scholarship from DAAD

Halle (Saale), 11. August 2016

Guoying Zhou

## Selbstständigkeitserklärung

Hiermit erkläre ich gemäß § 5 der Promotionsordnung der Naturwissenschaftlichen Fakultät I der Martin-Luther-Universität Halle-Wittenberg, dass ich die Ergebnisse der vorliegenden kumulativen Dissertationsarbeit

*In vitro studies on inflammatory potential of biomaterials  
with development of anti-inflammatory strategies*

am Institut für Pharmazie in der Arbeitsgruppe Biomedizinische Materialien unter Anleitung von Prof. Dr. rer. nat. habil. Thomas Groth selbständig erarbeitet und die Dissertation ohne fremde Hilfe verfasst habe.

Weiterhin erkläre ich, dass ich keine anderen als die von mir angegebenen Quellen und Hilfsmittel zur Erstellung meiner Dissertation verwendet habe. Den benutzten Werken wörtlich oder inhaltlich entnommene Stellen sind als solche gekennzeichnet.

Ferner erkläre ich, dass ich mich mit der vorliegenden Dissertationsarbeit erstmals um die Erlangung eines Doktorgrades bewerbe.

Halle (Saale), den 11. August 2016

Guoying Zhou